

Ph.D. Course on
“*Vorticity, Vortical Flows and Vortex-Induced Vibrations*”
26-30 August 2019, Technical University of Denmark

Lecture 4

Long- and short-wave instabilities

Thomas Leweke

IRPHE, CNRS, Marseille, France



irphé

Institut de Recherche sur les
Phénomènes Hors Equilibre



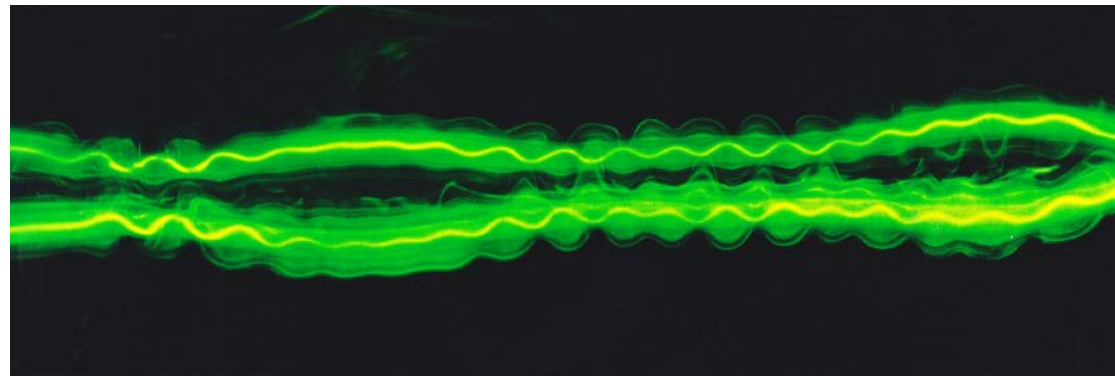
Long-wave instabilities of a vortex / system

- displacement / deformation of the vortex shape
- description by a filament approach

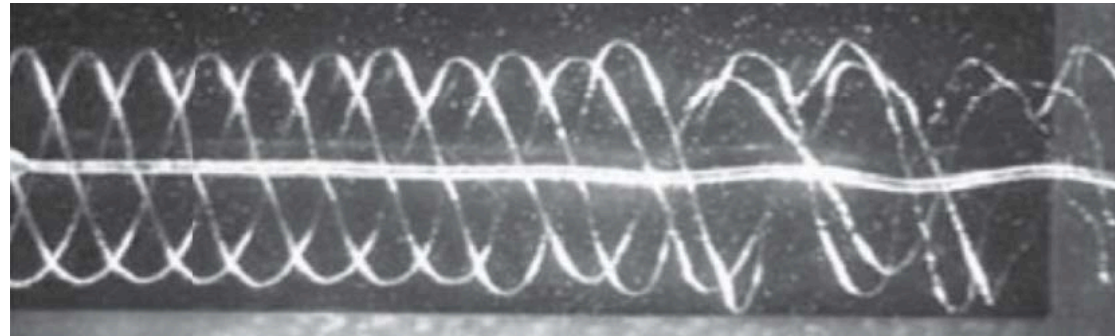
Short-wave instabilities

- internal deformations of the vortex core
- interaction of vortex Kelvin modes

Vortex pairs



Helical vortices



Long-wave instability
Vortex pairs

Crow instability

Visualisations of aircraft trailing wakes



Photo Copyright Josef P. Willems

AIRLINERS.NET



© Erwin van Dijck Fotografie





Photo Copyright Josef P. Willems



win van Dijck Fotografie

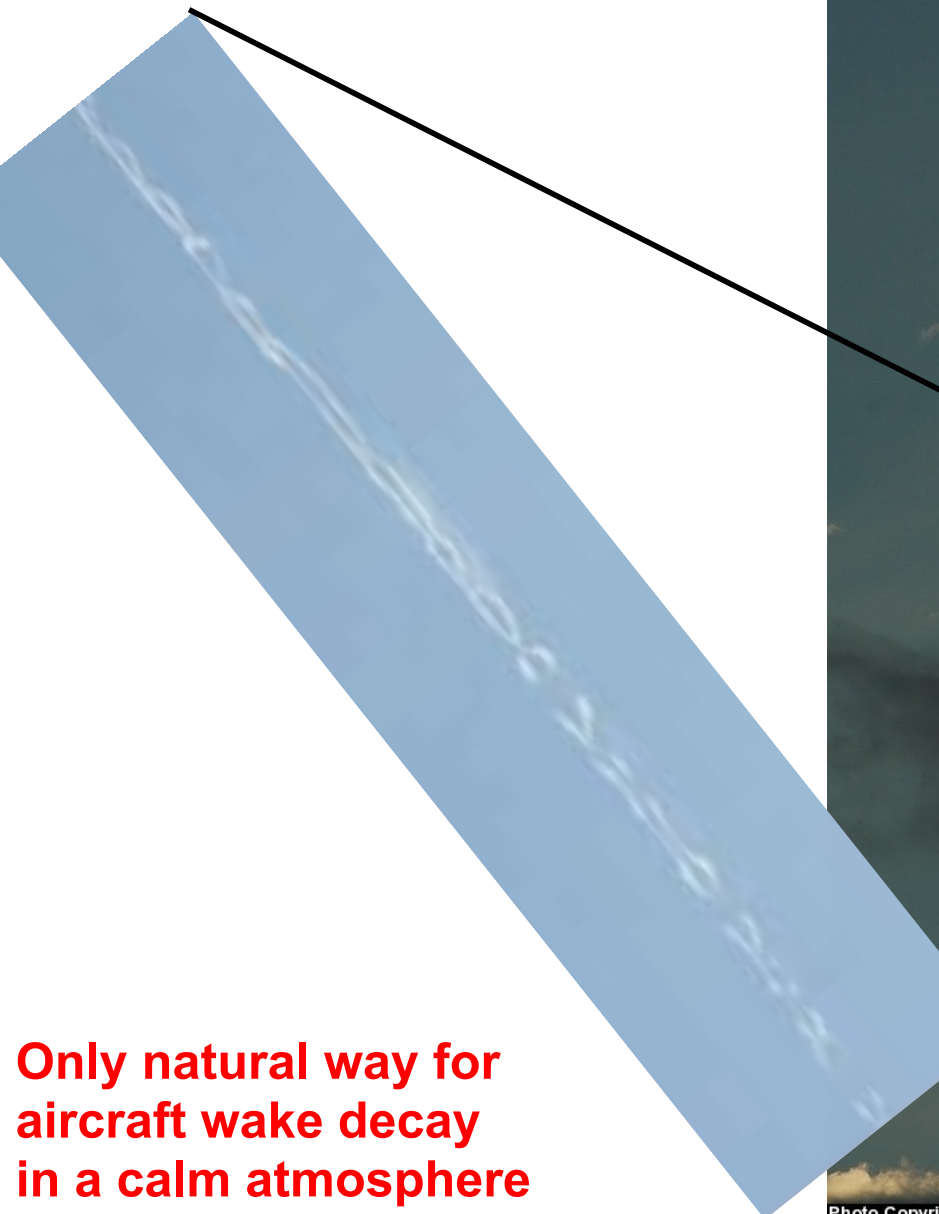
SEMPRE A BORDO. SEMPRE REFRESCANTE.

Long-wavelength Crow instability



© 2011 H. Raab

Crow instability



Only natural way for
aircraft wake decay
in a calm atmosphere

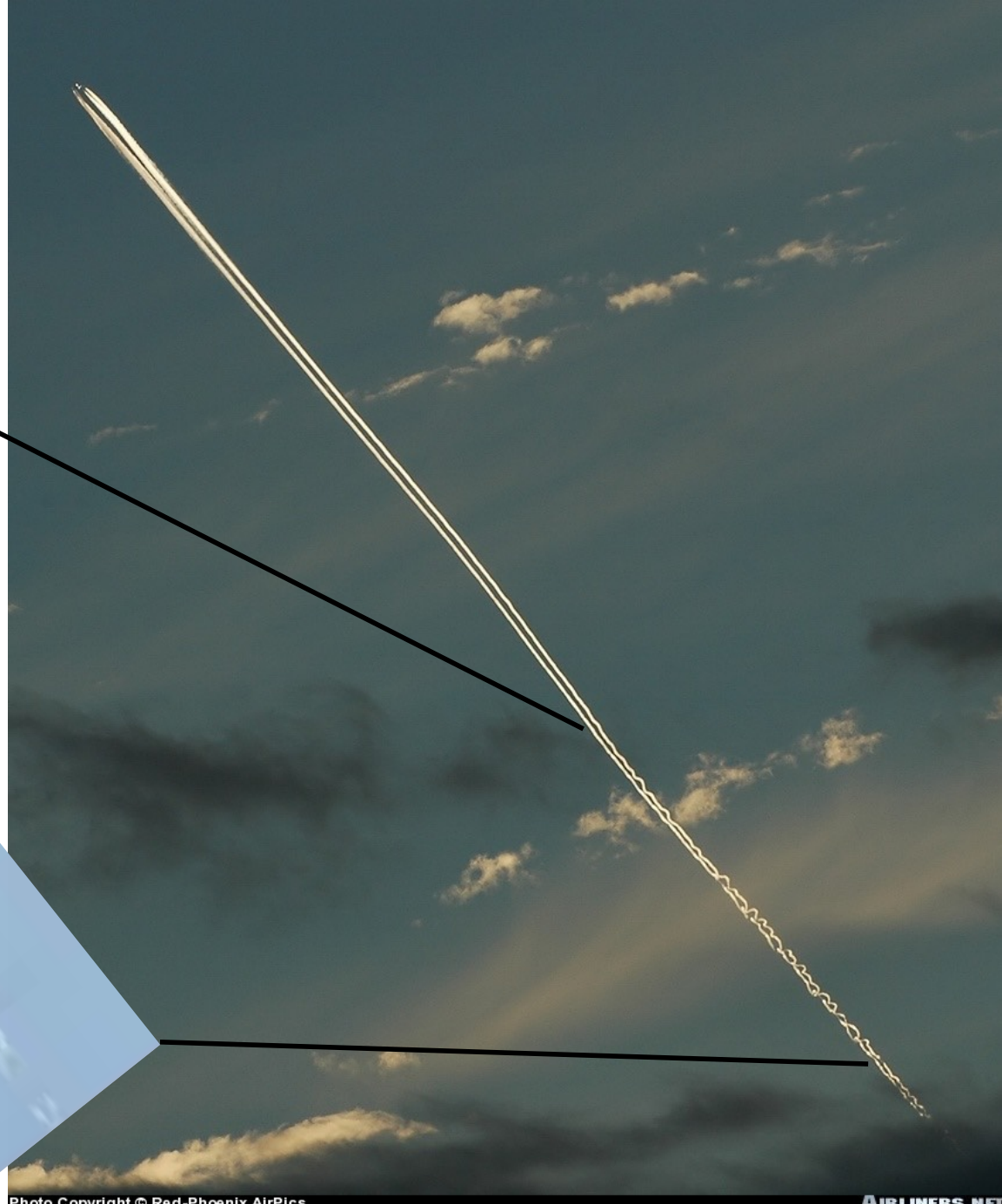
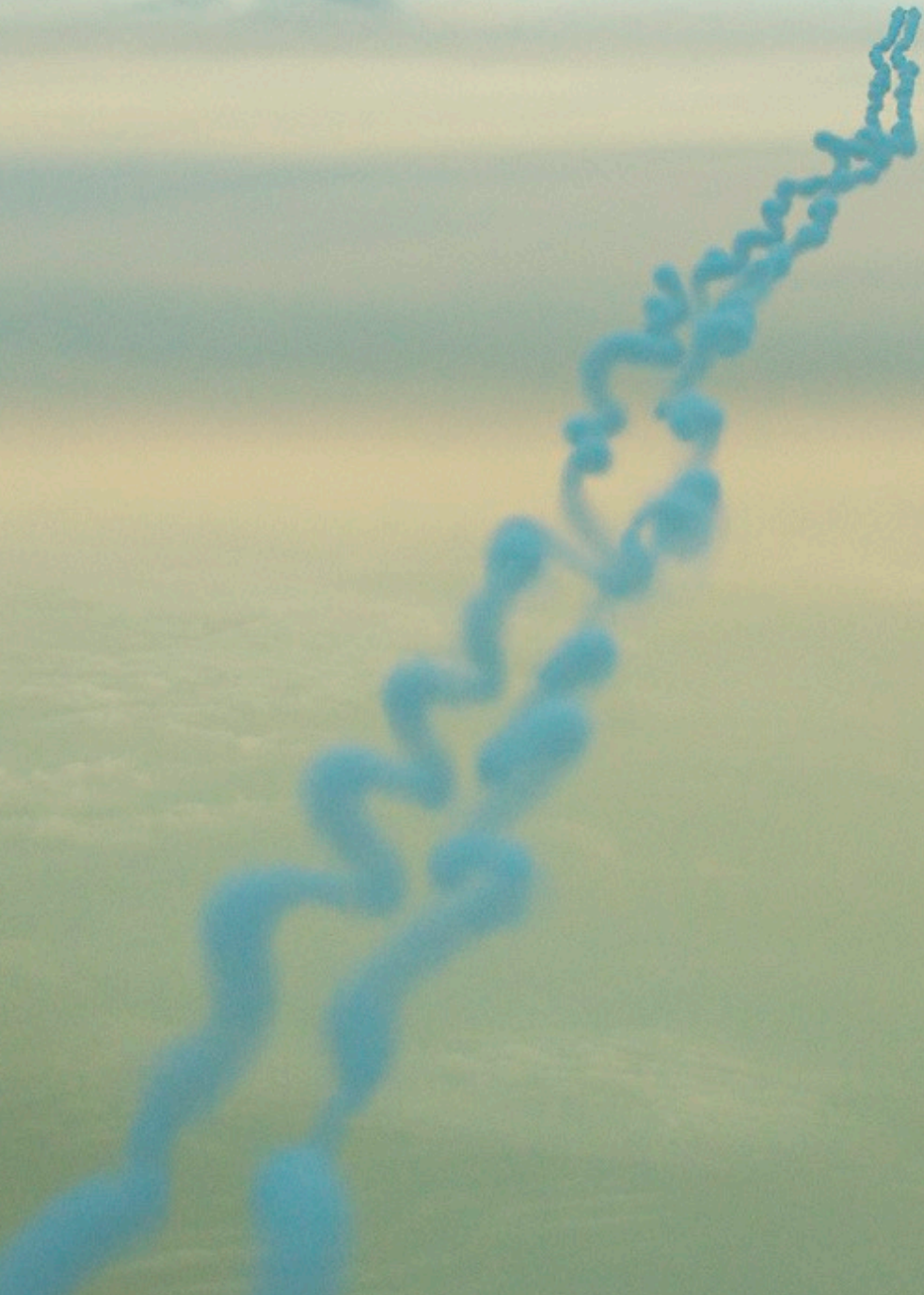


Photo Copyright © Red-Phoenix AirPics

AIRLINERS.NET





*NASA Langley Research Center
Wake Vortex Experiments*



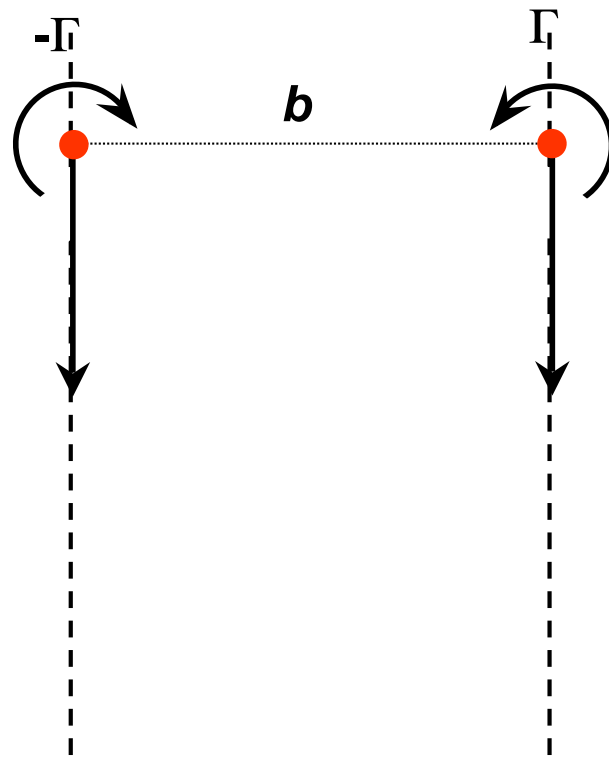
*NASA Langley Research Center
Wake Vortex Experiments*



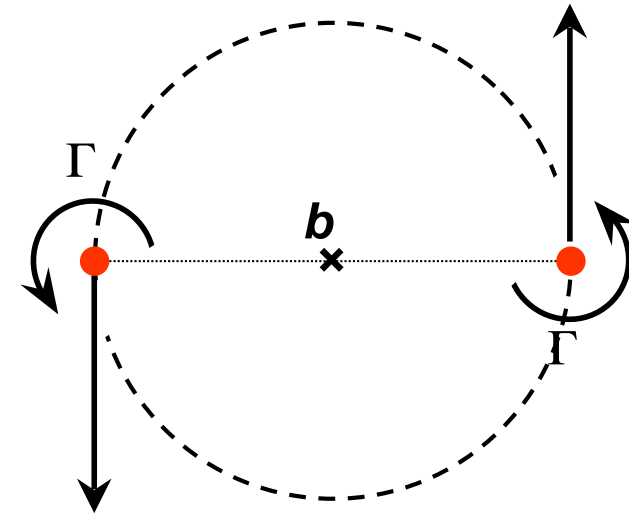
Dynamics of two point vortices

- same circulation -

counter-rotating



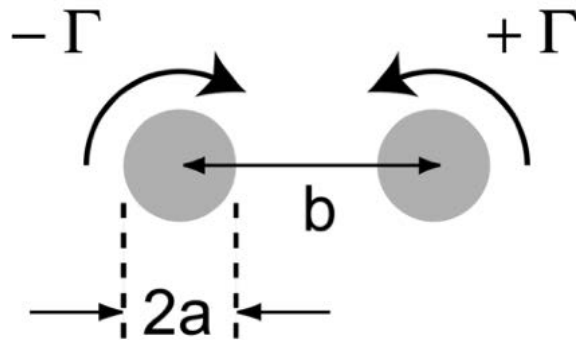
co-rotating



mutually induced velocity:
 $|V| = \Gamma / 2\pi b$

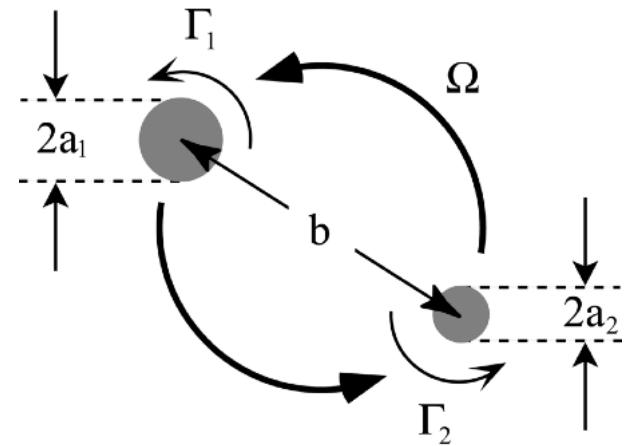
Vortex pair parameters

counter-rotating



- vortex separation b
- descent speed $V = \Gamma / 2\pi b$
- non-dim. time $t^* = t V / b$

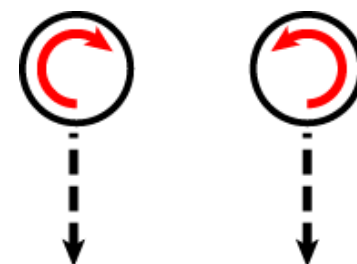
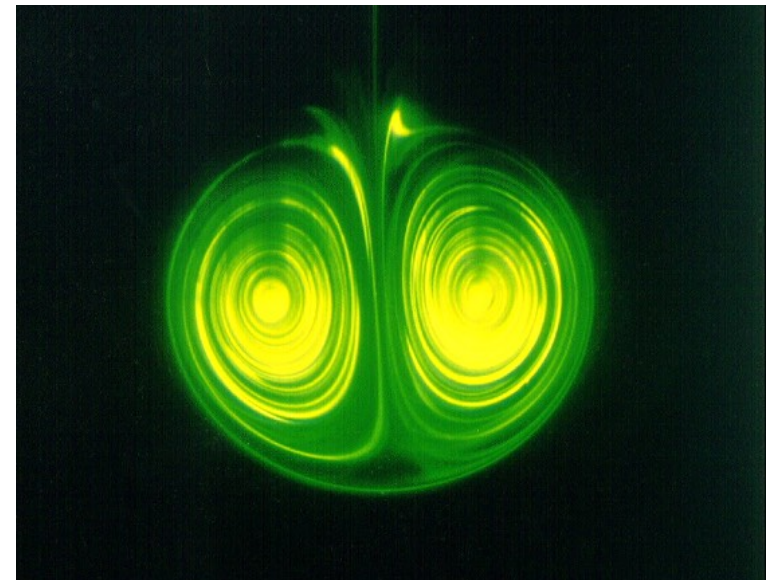
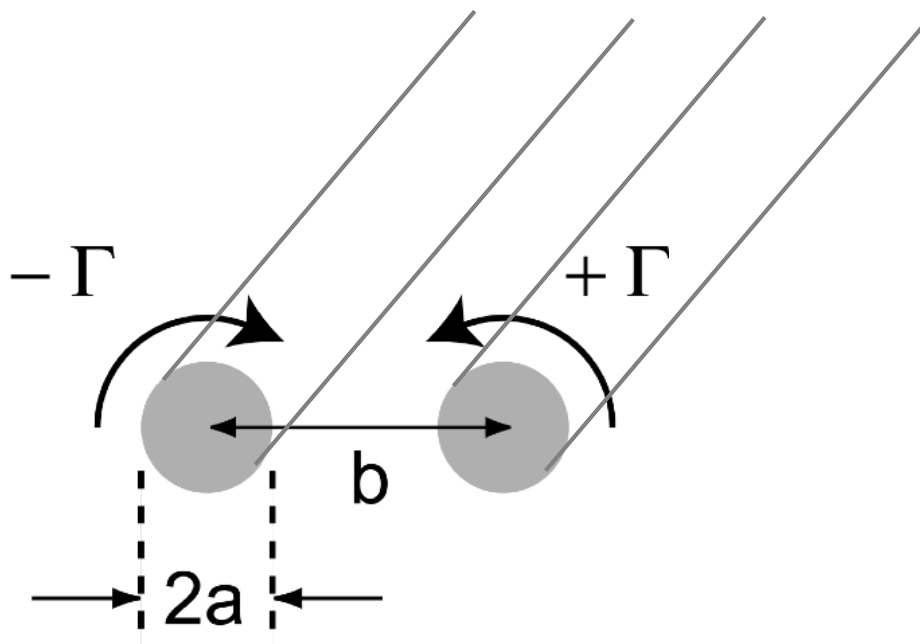
co-rotating



- vortex separation b
- angular freq. $\Omega = (\Gamma_1 + \Gamma_2) / 2\pi b^2$
- non-dim. time $t^* = t \Omega / 2\pi$

rate of strain induced by one vortex on the other: $\varepsilon = \Gamma / 2\pi b^2$

Counter-rotating vortex pair



Basic state:
vertical translation
with speed $V = \Gamma / 2\pi b$

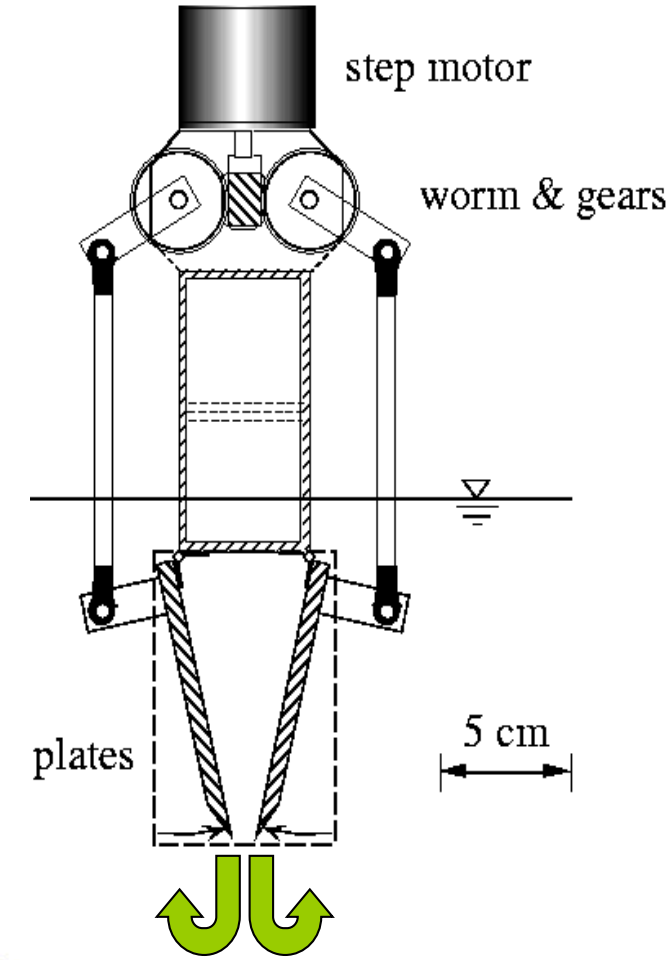
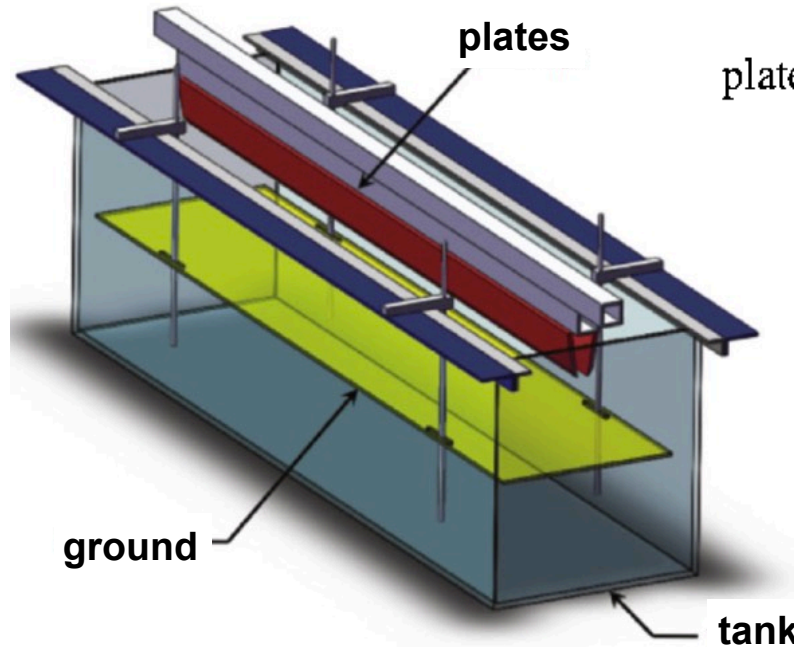
Counter-rotating vortex pairs

Experimental set-up

- water tank ($180 \times 45 \times 60 \text{ cm}^3$)
- starting vortices generated by impulsively rotated plates
- computer-controlled plate motion

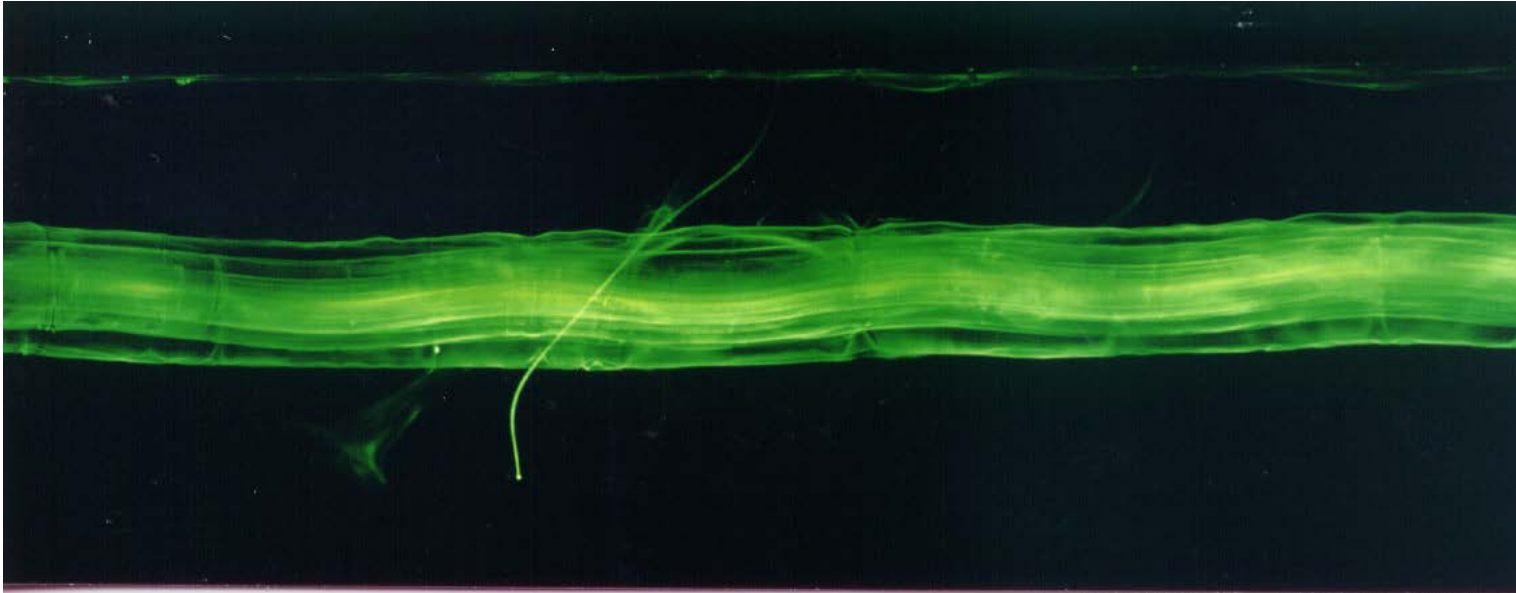
methods:

- visualisation
- image analysis
- Particle Image Velocimetry (PIV)

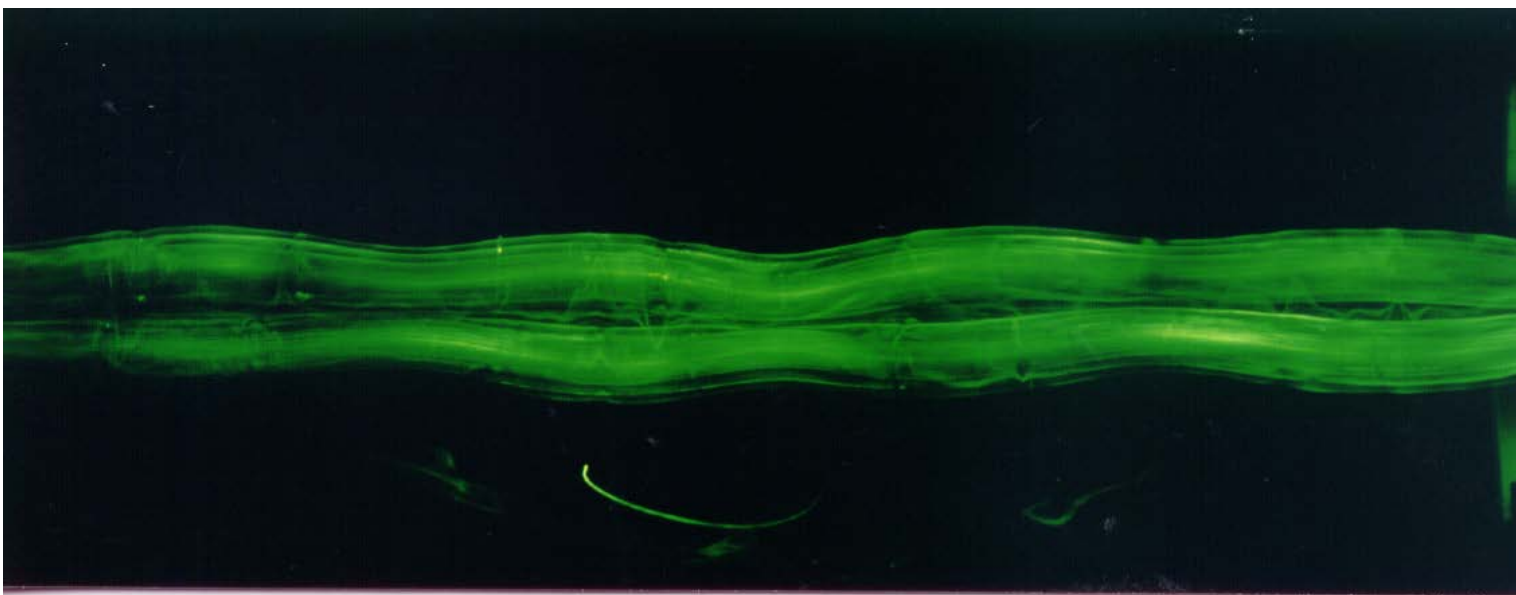


length: 170 cm

Crow instability ($Re = 1500\text{--}2500$, $a/b \approx 0.2$)

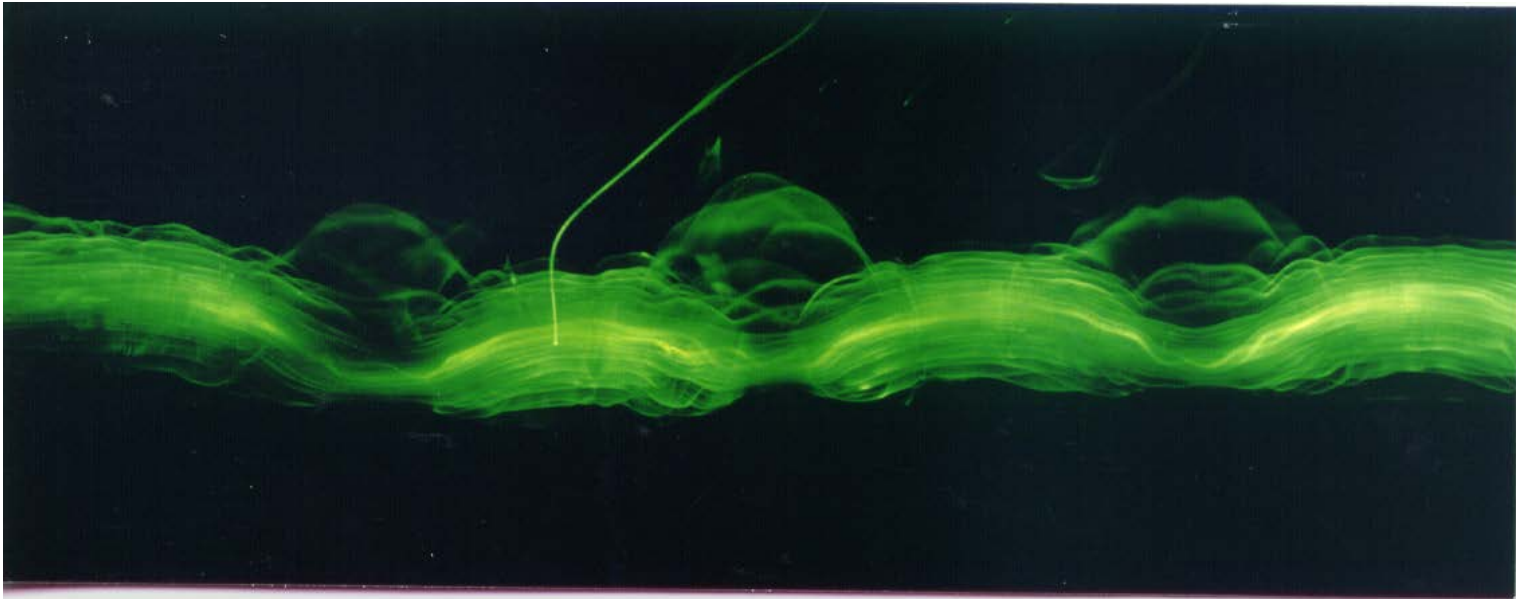


side
view

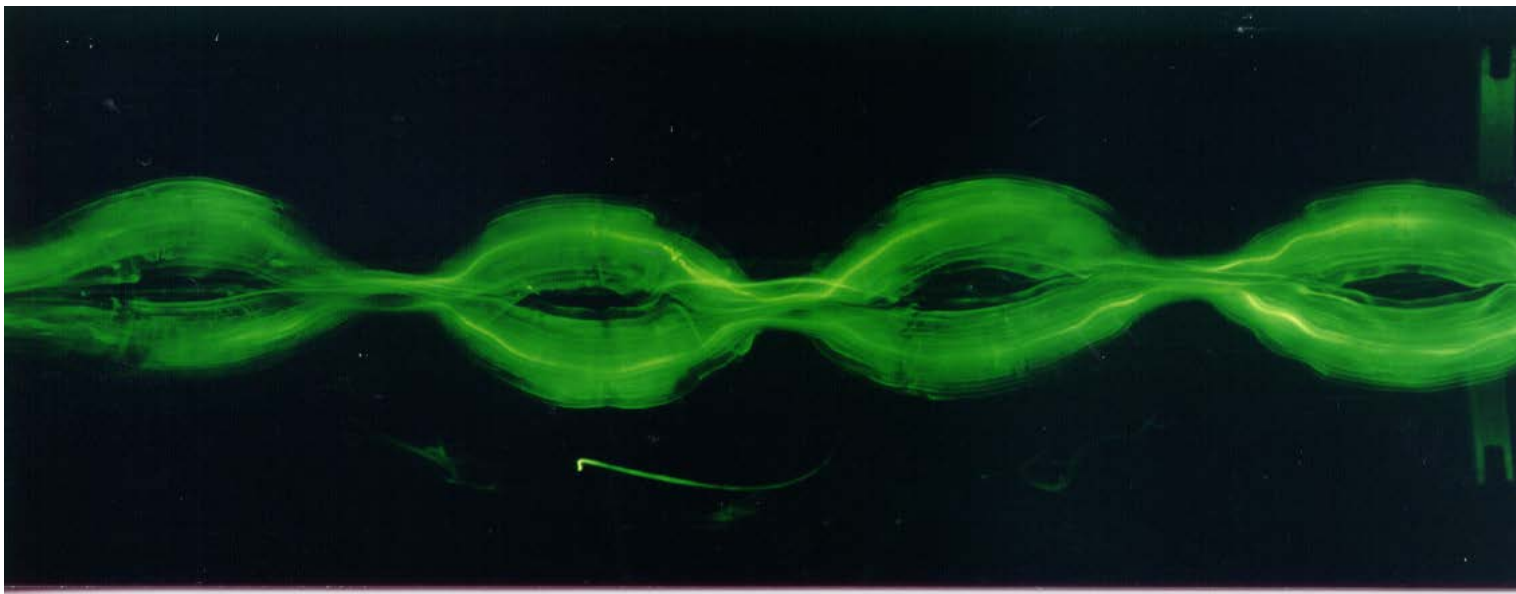


bottom
view

Crow instability ($Re = 1500\text{--}2500$, $a/b \approx 0.2$)

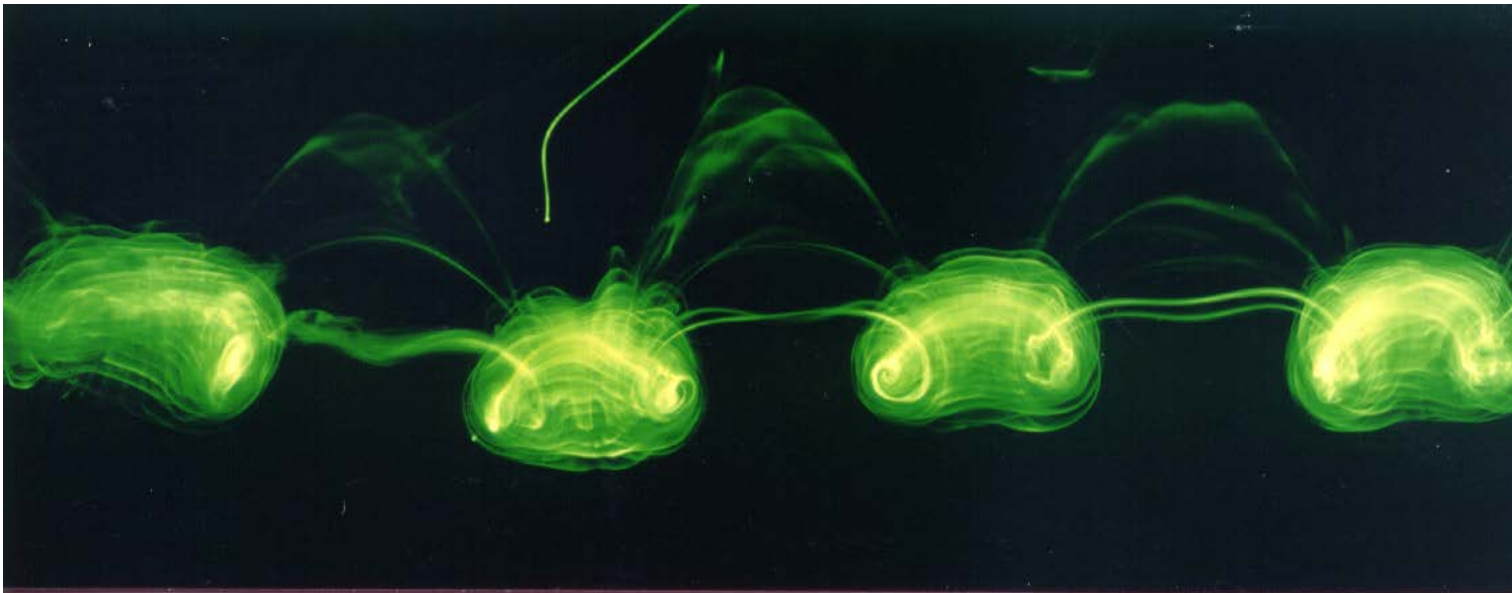


side
view

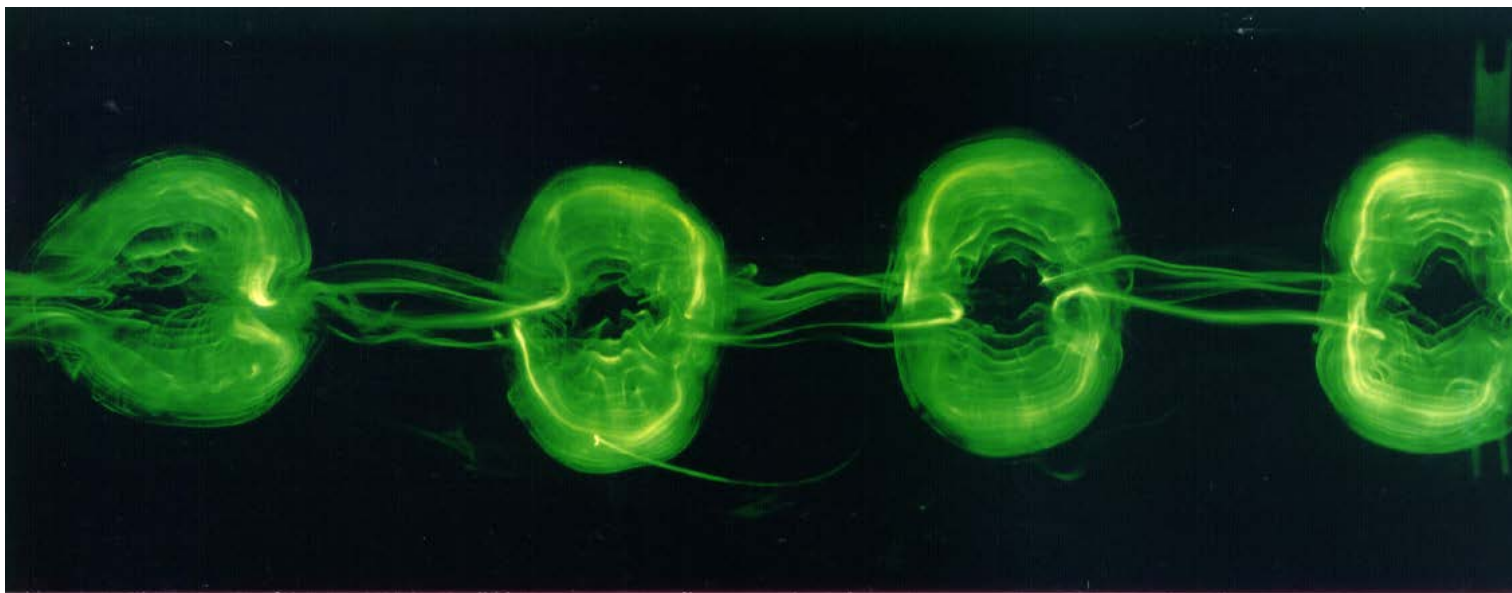


bottom
view

Crow instability ($Re = 1500\text{--}2500$, $a/b \approx 0.2$)

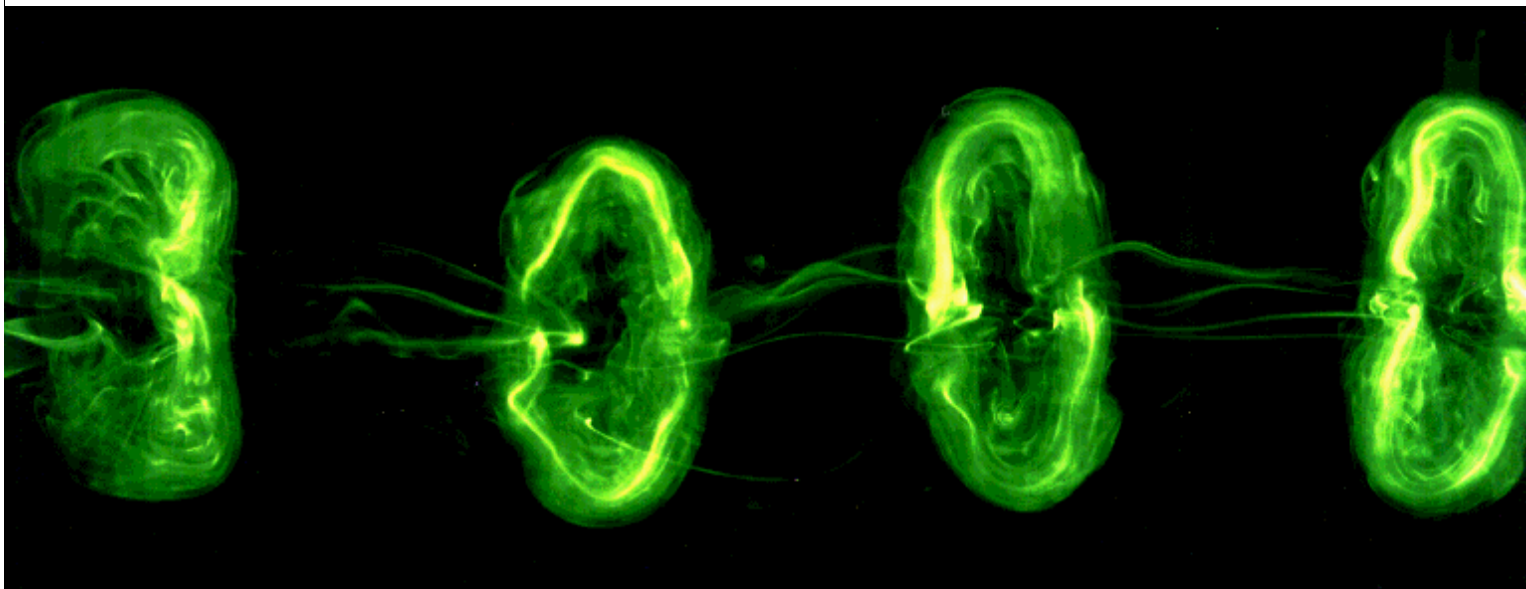
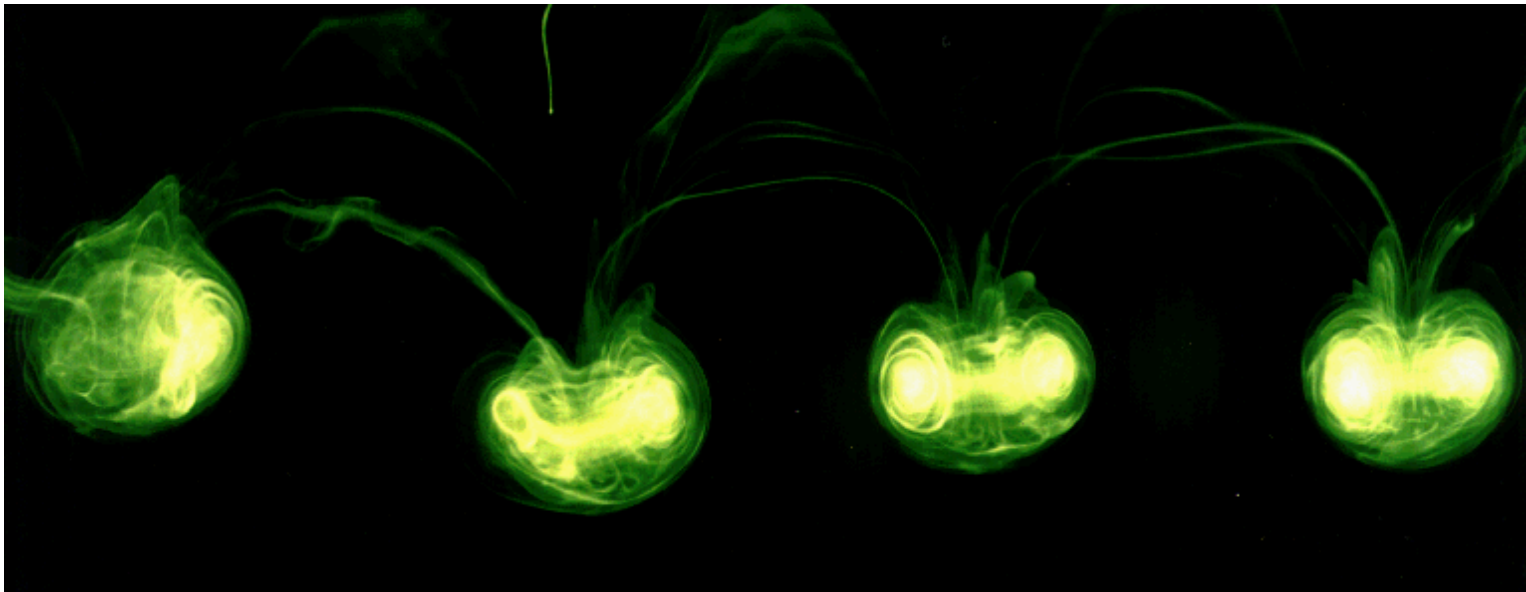


side
view



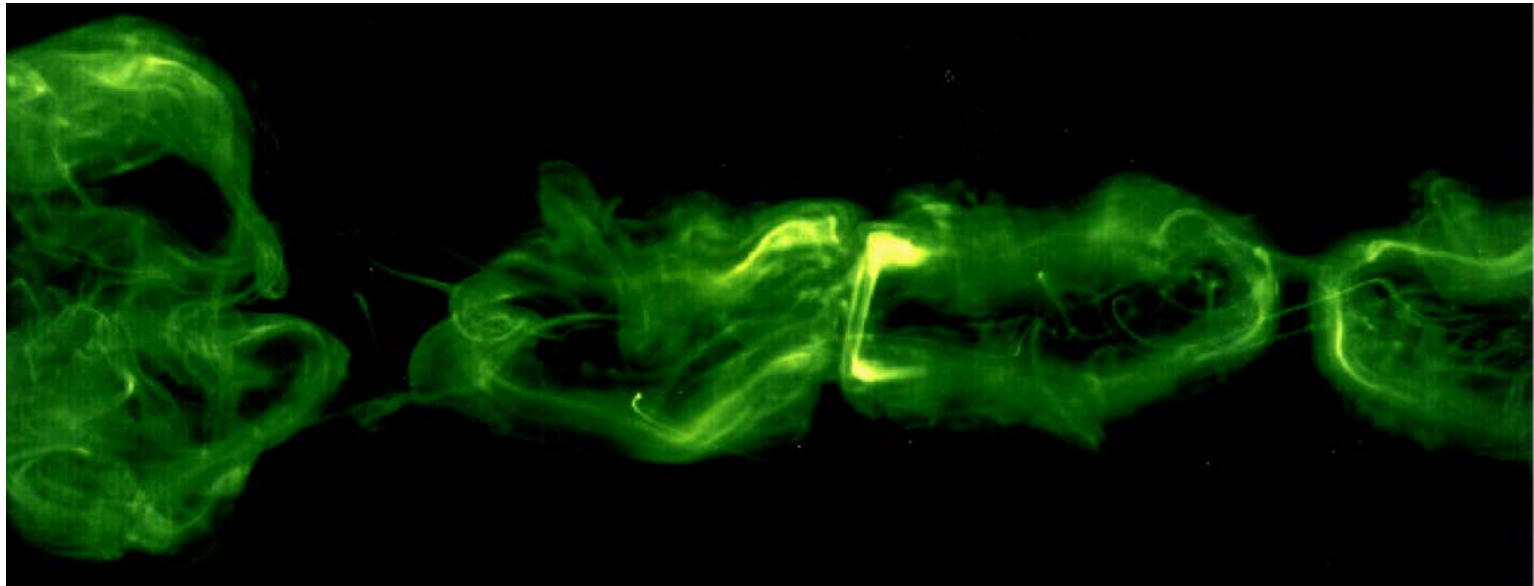
bottom
view

Crow instability ($Re = 1500\text{--}2500$, $a/b \approx 0.2$)



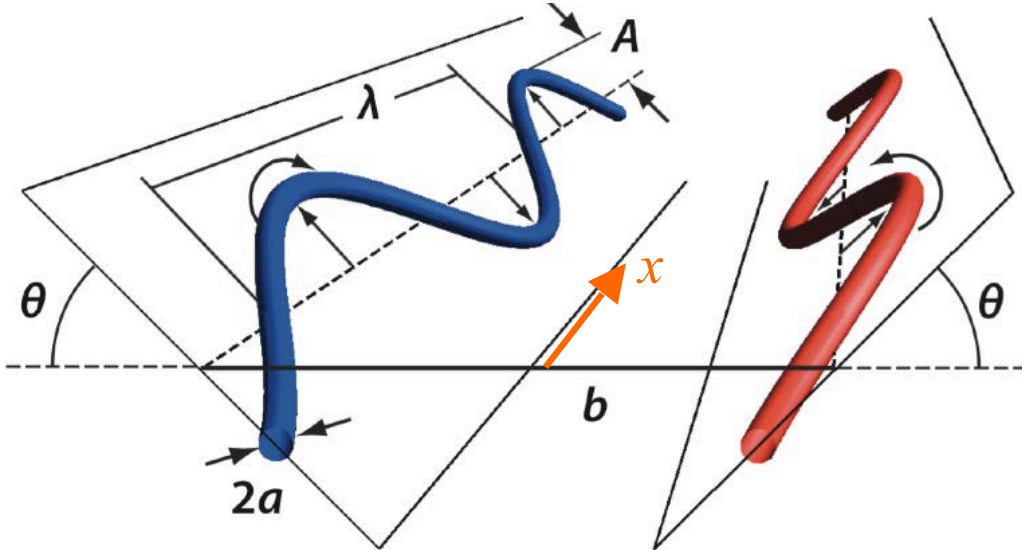
Crow instability ($Re = 1500\text{--}2500$, $a/b \approx 0.2$)

side
view



bottom
view

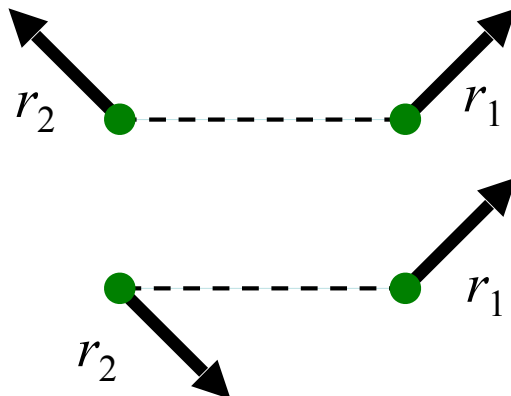
Crow instability mechanism



Consider:

- two vortex filaments (core size a , separation b)
- plane sinusoidal displacement perturbations (wavelength λ , orientation θ)

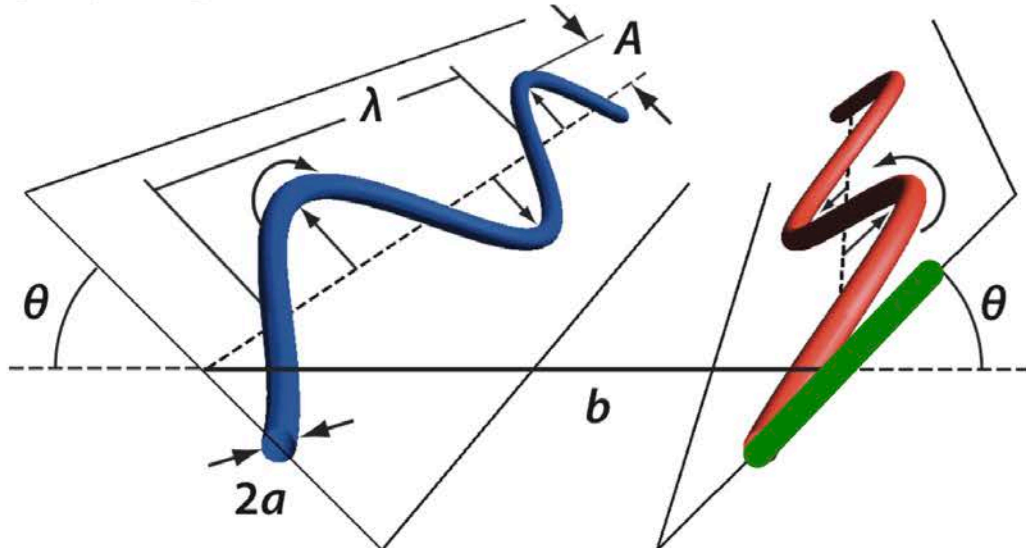
Symmetric modes



Anti-symmetric modes

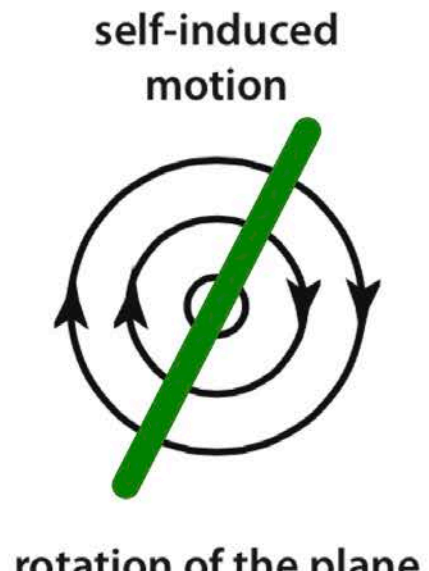
$$r_1 = \hat{r}_1 \sin\left(\frac{2\pi x}{\lambda}\right) \exp(\alpha t)$$

Crow instability mechanism



Evolution of perturbation

(example: **right** vortex):

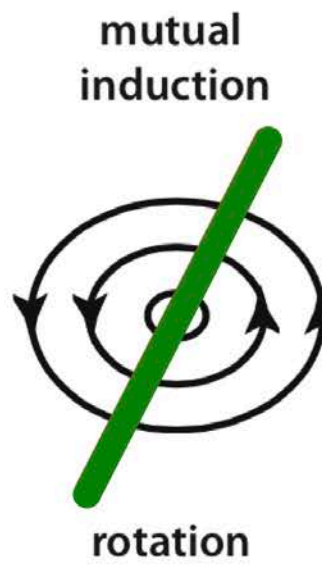


rotation of the plane



rotation
+ stretching

$$f(a, \lambda)$$



rotation
+ stretching

$$f(\theta, \lambda)$$

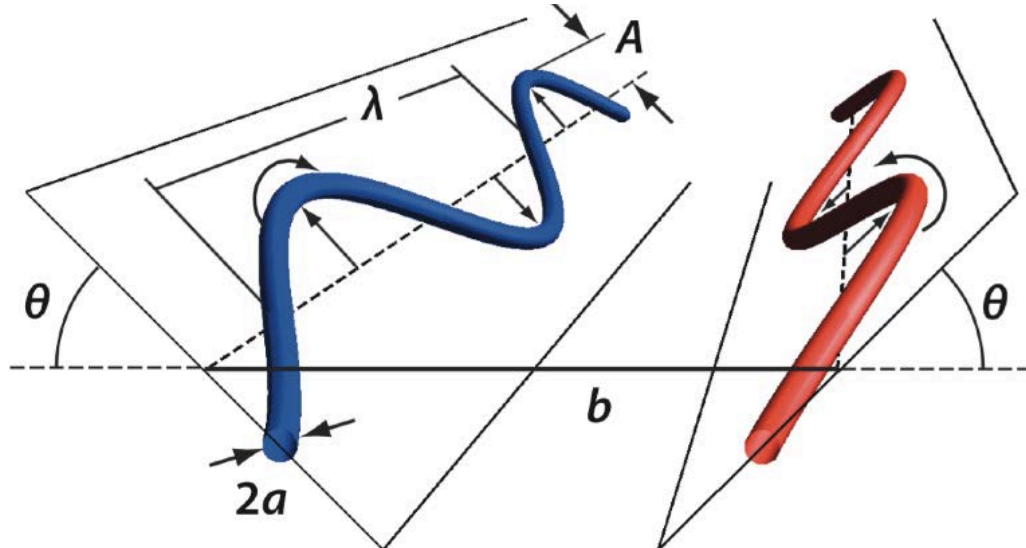
IF

- total rotation = 0
- total stretching > 0

↓

Instability

Crow instability mechanism



Find α :

- Biot-Savart line integrals
- cut-off method for self-induction
- linearisation

$$(\alpha^*)^2 = \left[1 - (kb_o)^2 K_o(kb_o) - kb K_1(kb_o) - \frac{\sigma}{(a_e/b_o)^2} \right] \left[1 + kb_o K_1(kb_o) + \frac{\sigma}{(a_e/b_o)^2} \right]$$

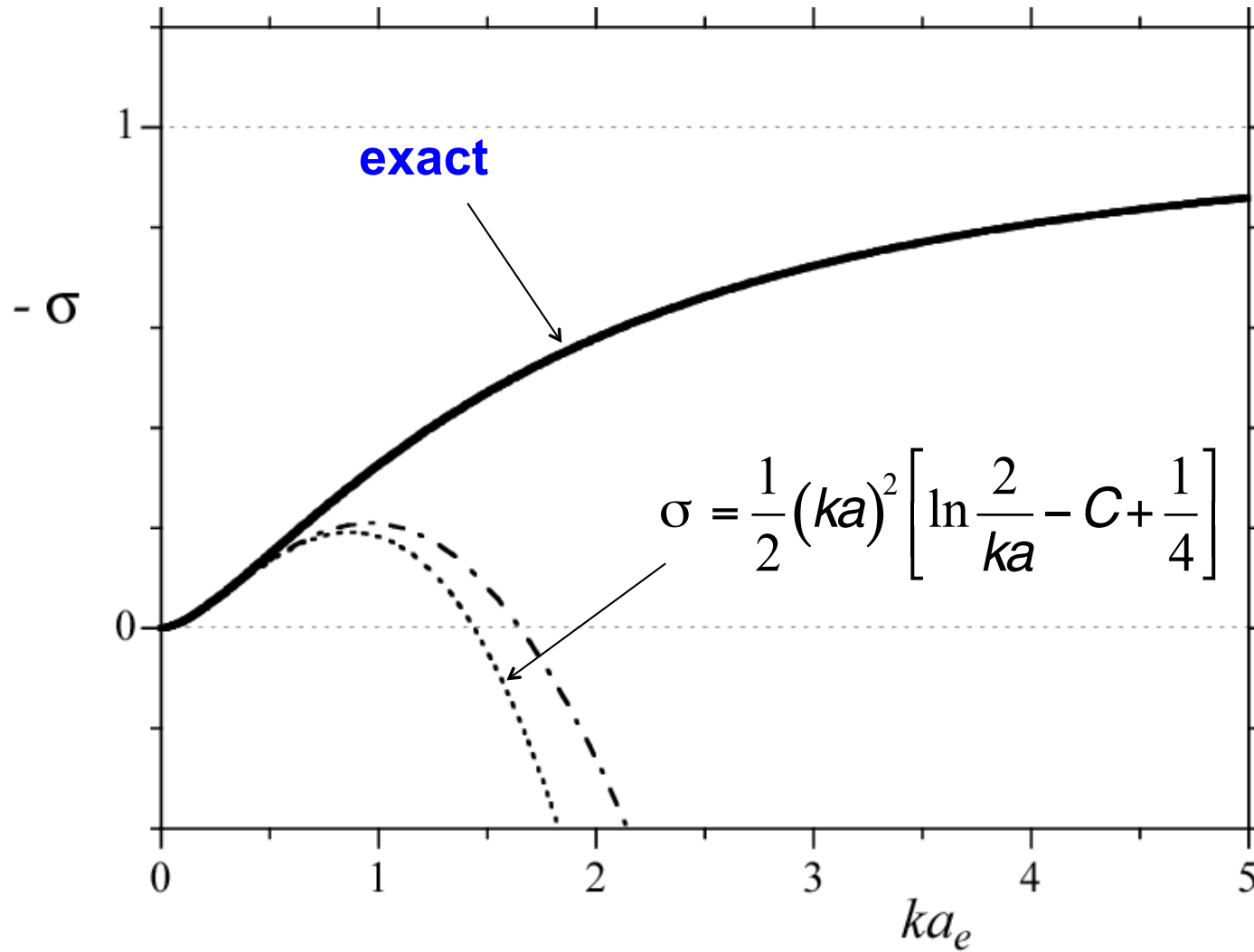
$$\alpha^* = \alpha (2\pi b^2/\Gamma)$$

$$k = 2\pi/\lambda$$

σ : self-induced rotation rate

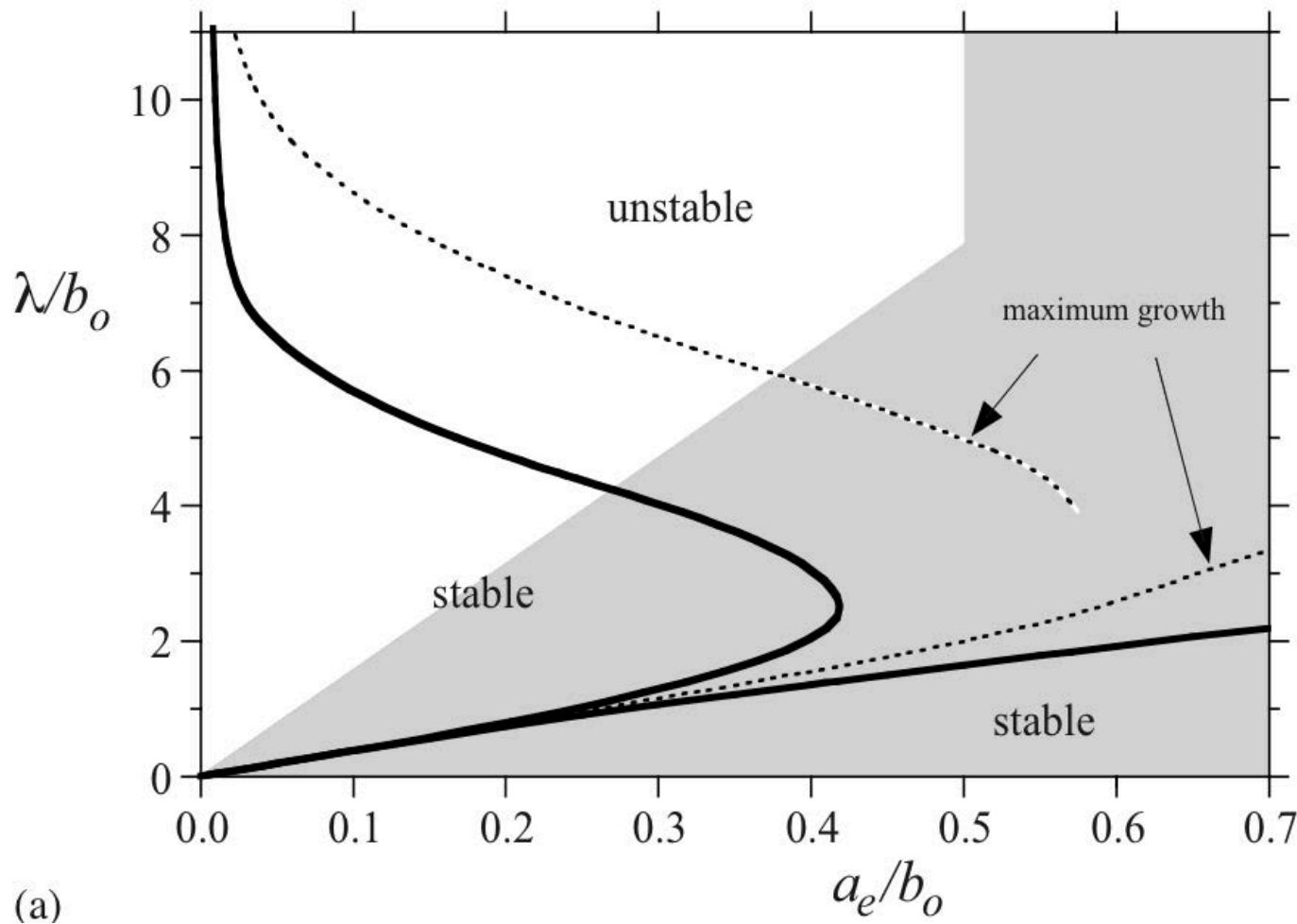
Self-induced rotation of a sinusoidal vortex filament

(Rankine vortex, Kelvin 1880)



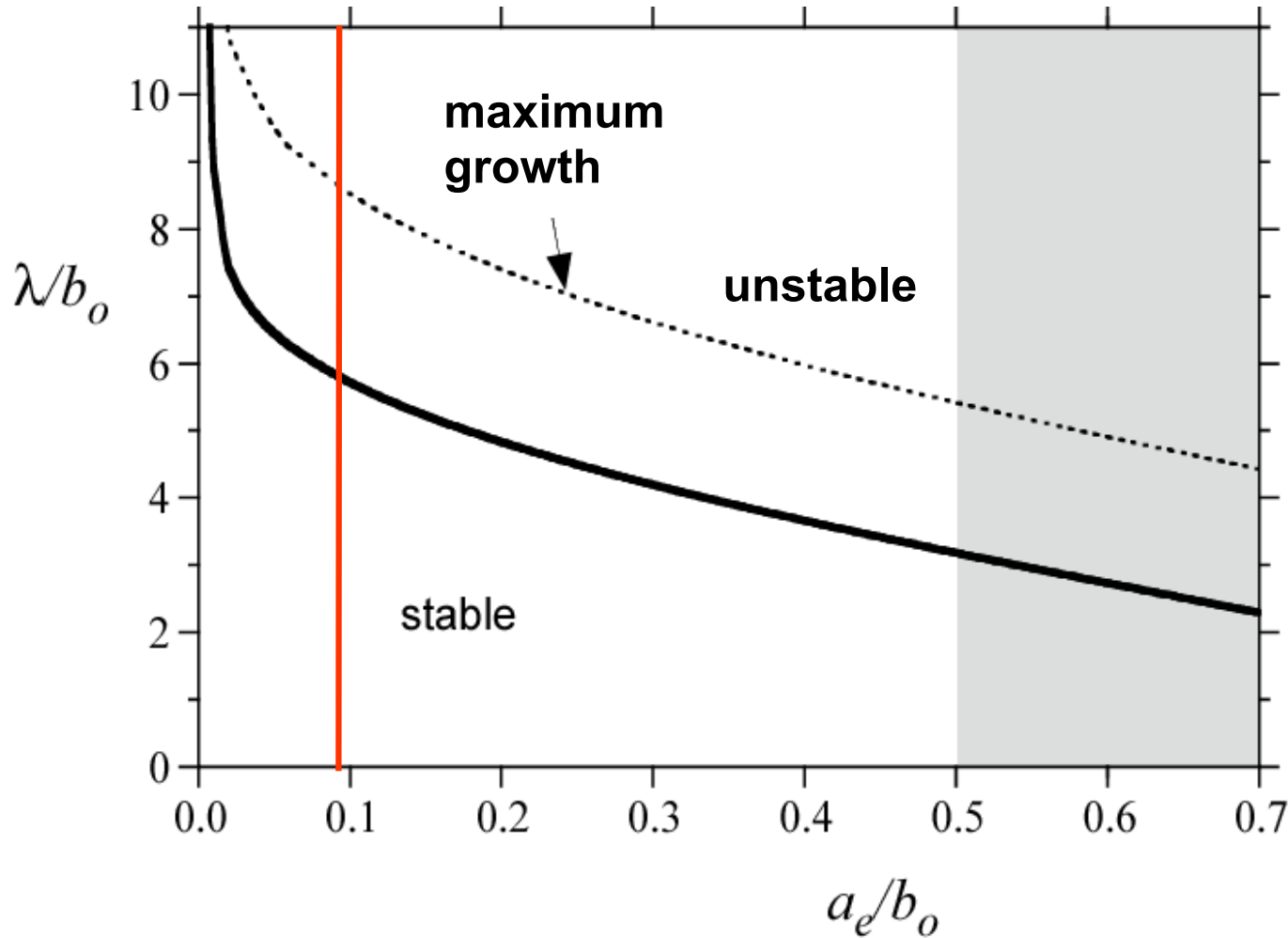
Stability diagram for a pair of counter-rotating vortices

(symmetric mode)



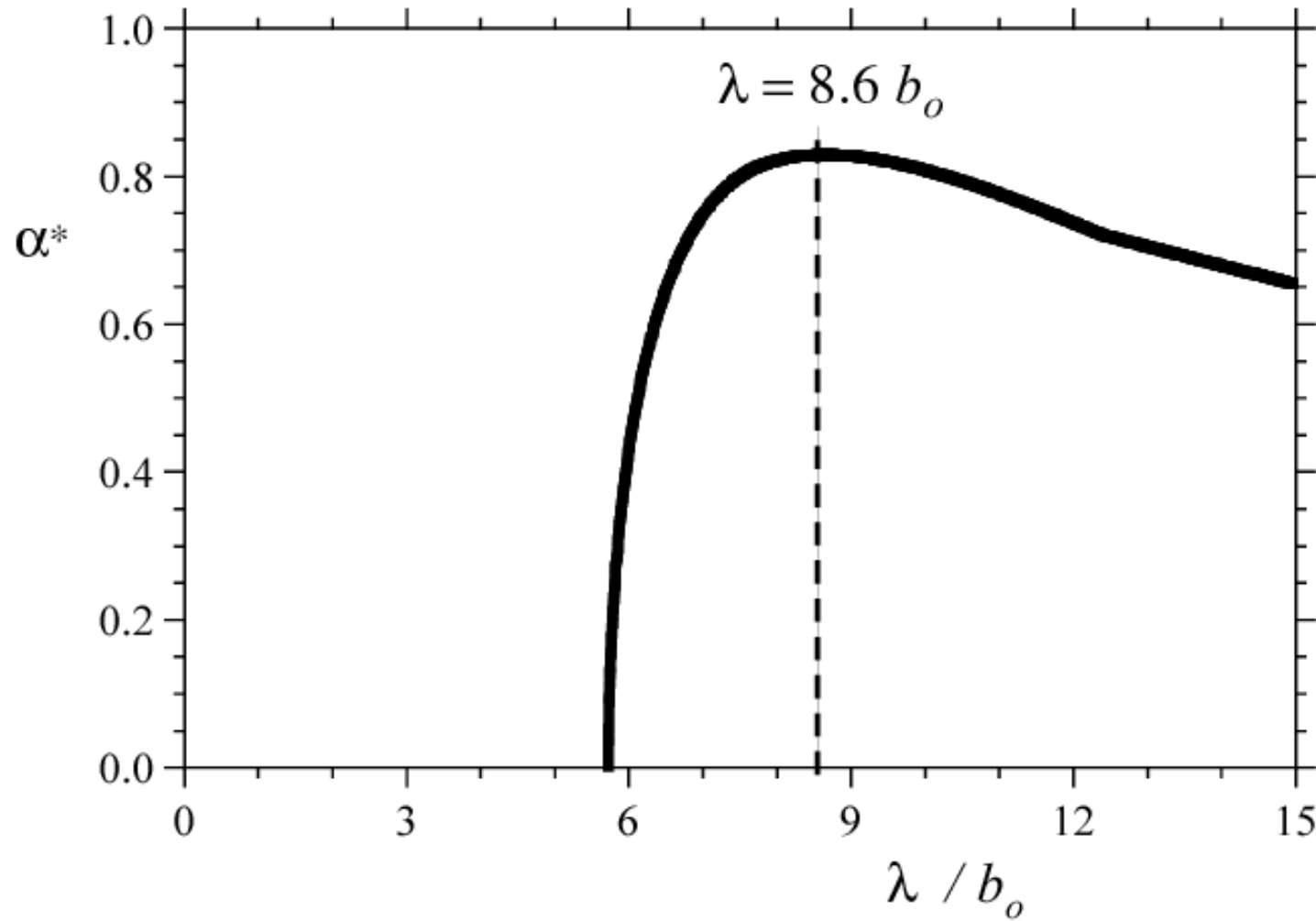
Stability diagram for a pair of counter-rotating vortices

(symmetric mode)



Growth rate of the Crow instability

$(a/b = 0.0985)$



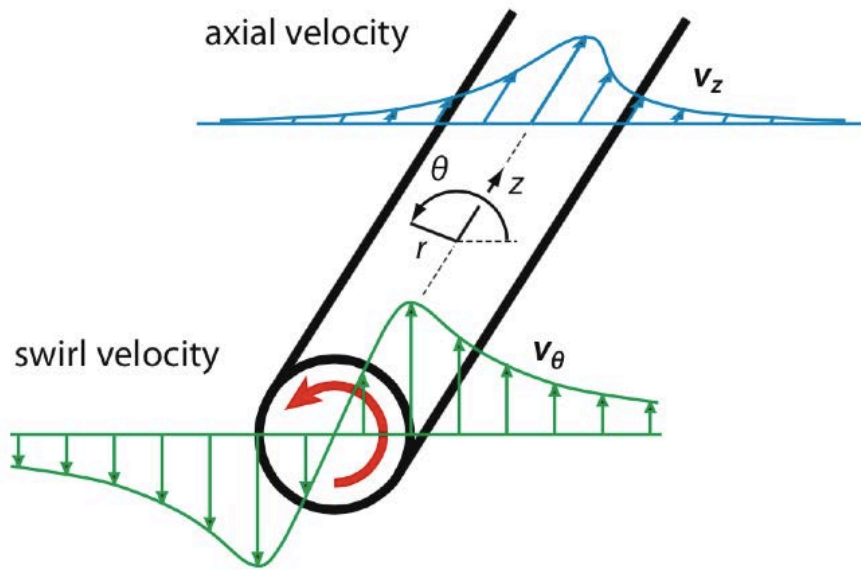
Generalization to vortices other than Rankine

Equivalent core size
(Widnall et al. 1971)

$$a_e = a \cdot \exp \left[\frac{1}{4} - A + C \right]$$

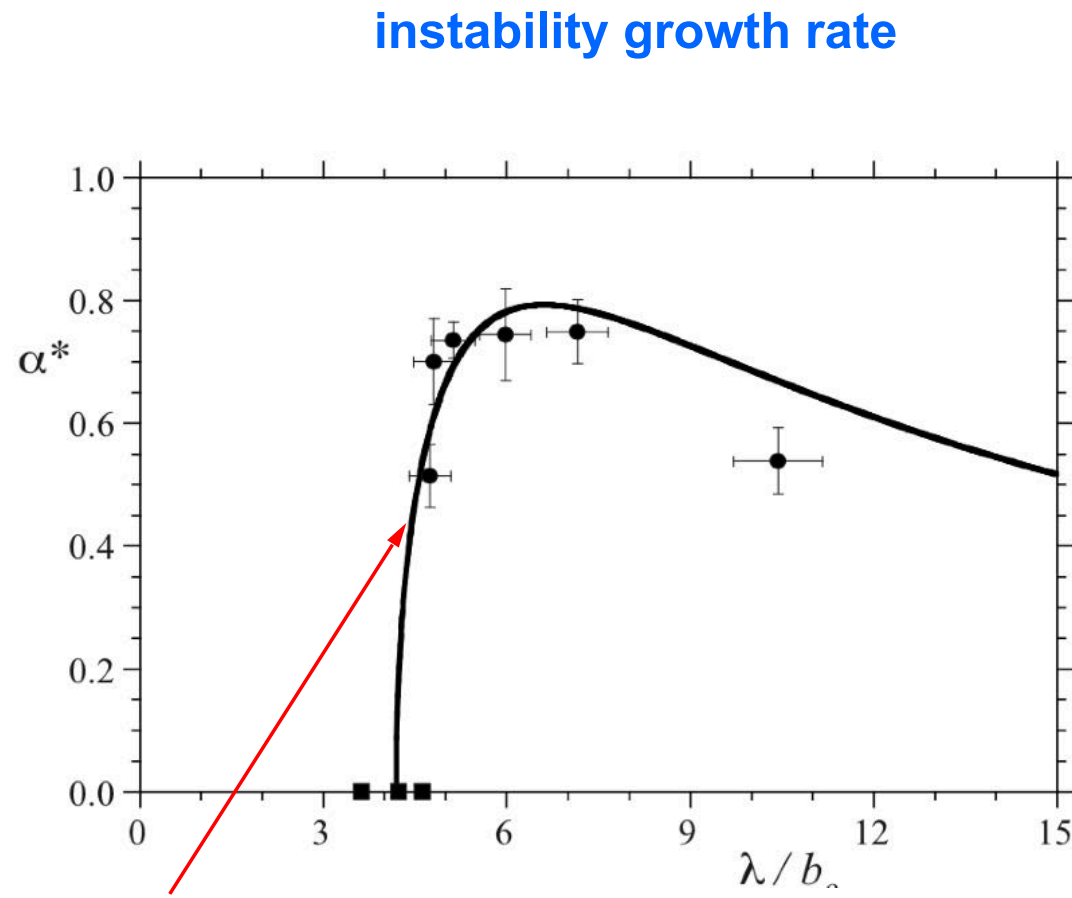
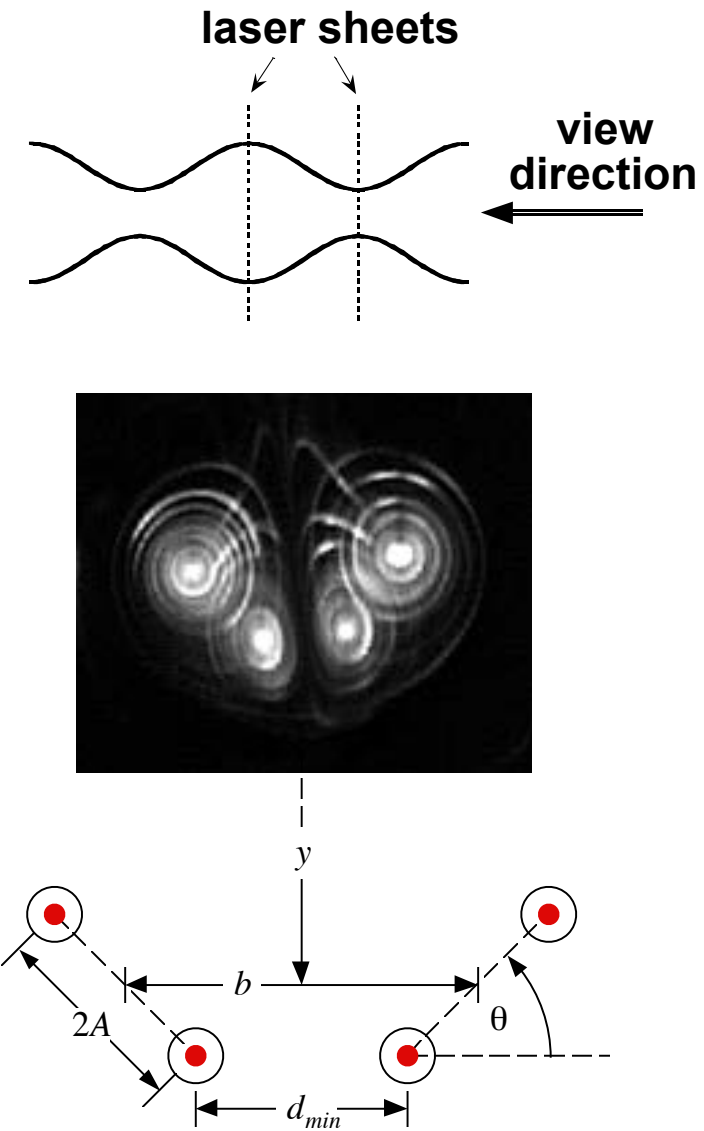
$$A = \lim_{r \rightarrow \infty} \left[\frac{4\pi^2}{\Gamma^2} \int_0^r \bar{r} v_\phi^2(\bar{r}) d\bar{r} - \ln \frac{r}{a} \right]$$

$$C = \frac{8\pi^2}{\Gamma^2} \int_0^\infty \bar{r} v_z^2(\bar{r}) d\bar{r}$$



valid for $\lambda \gtrsim 15 a$

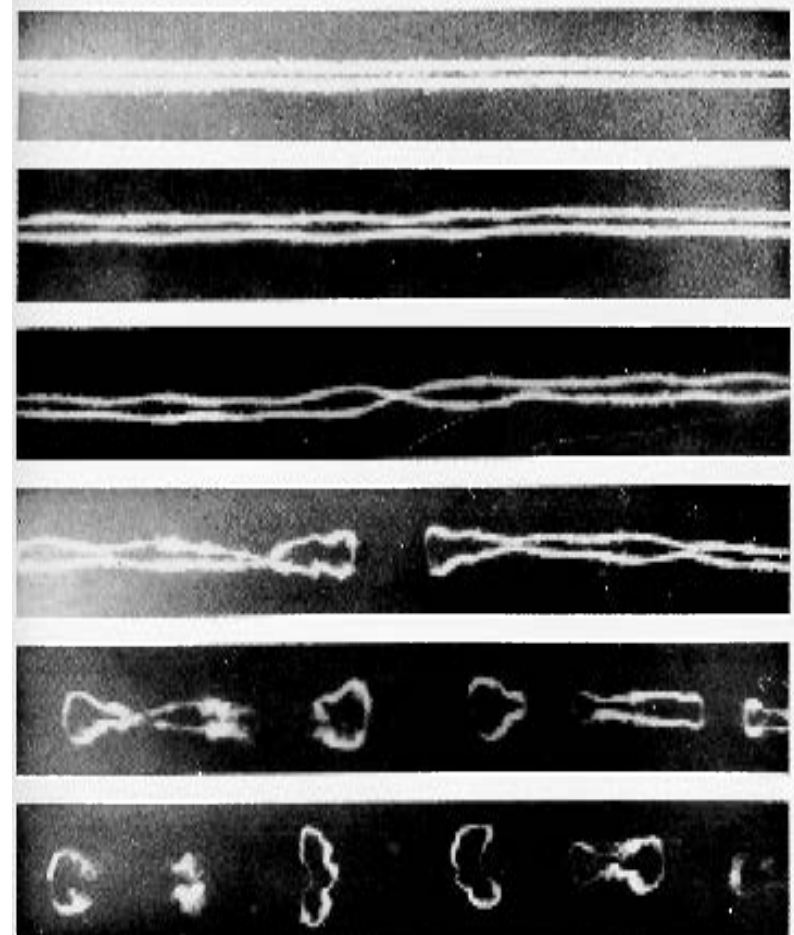
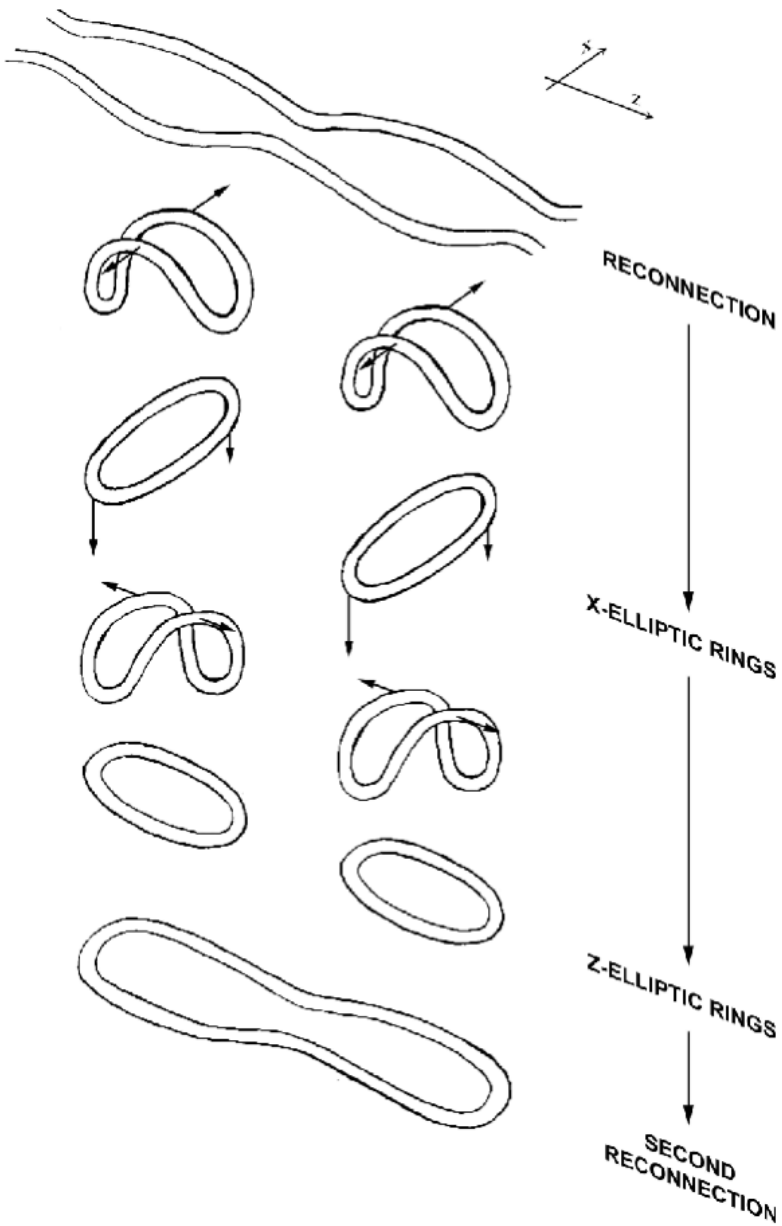
Crow instability (measurements)



theoretical prediction

- uses a/b_0 and vortex **velocity profile**
(Crow 1970, Widnall *et al.* 1971)

Crow instability (long-term evolution)



Photographs of aircraft wake (Crow 1970)

Tip vortices of a Hawker Sea Fury

AIR14 air show at Payerne Switzerland, 7 September 2014

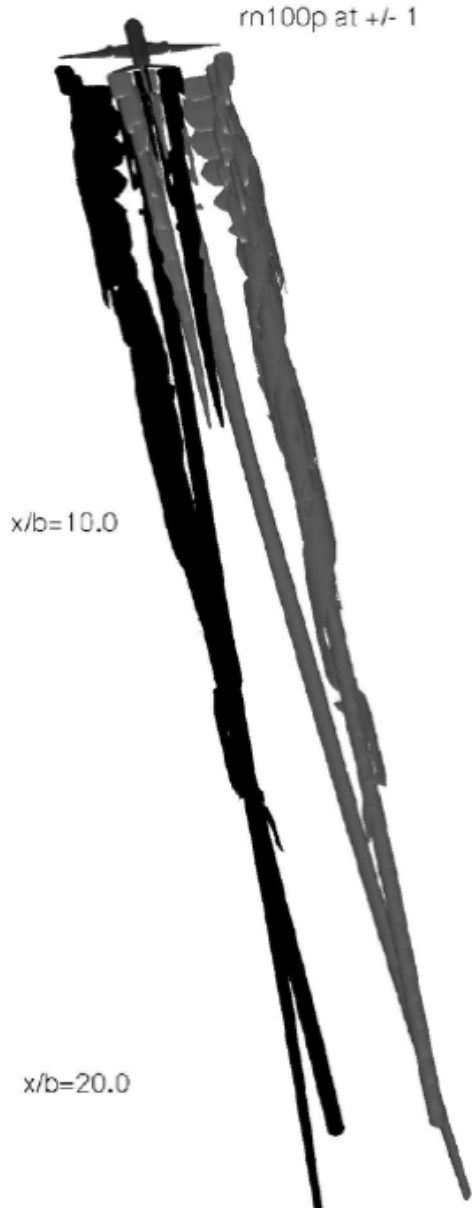
(video by G. Balestra)



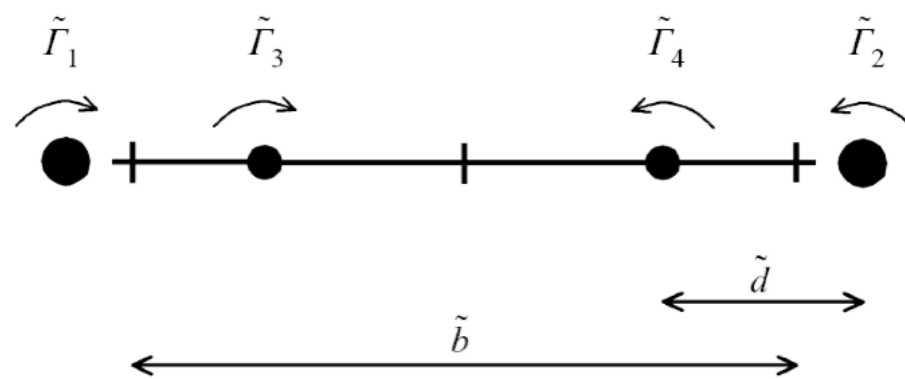
Long-wave instability

Vortex pairs

**“Crow” instability
of 4-vortex systems**

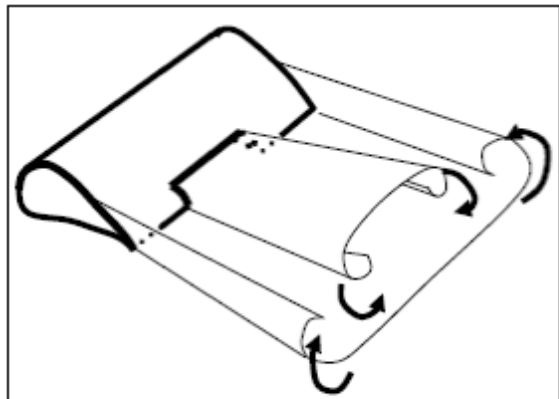


Co-rotating 4-vortex system (Crouch, Boeing)

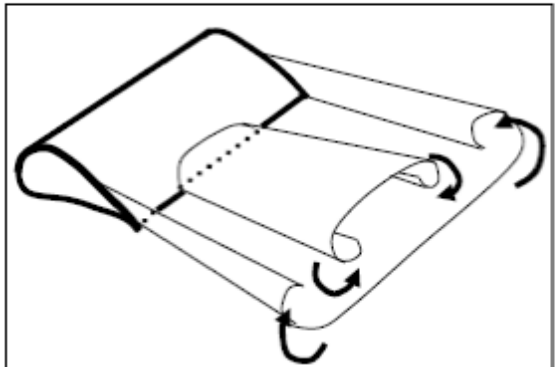


Counter-rotating 4-vortex system

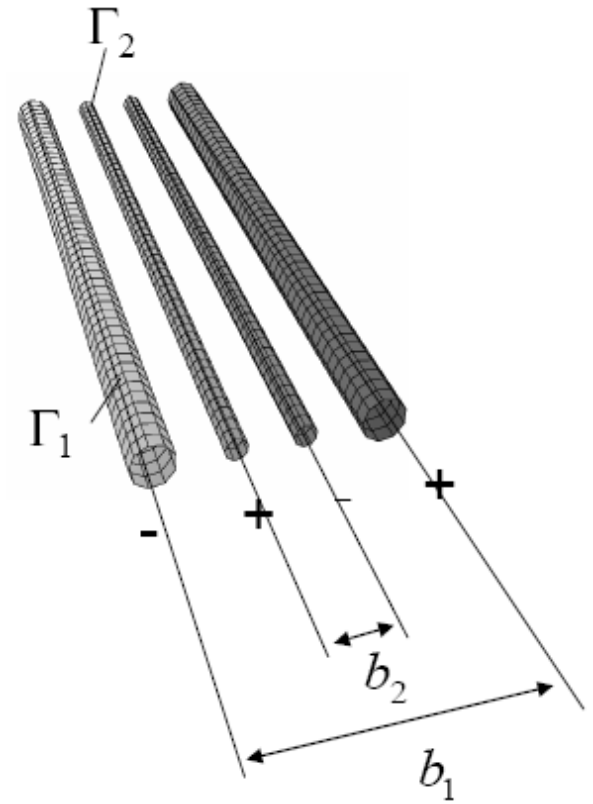
(Jacquin et al., ONERA)



- outboard flaps
- horizontal tail plane

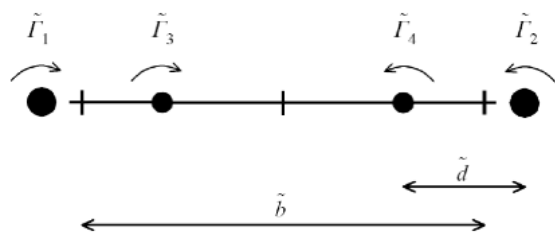


- $C_{z\max}$: separation !

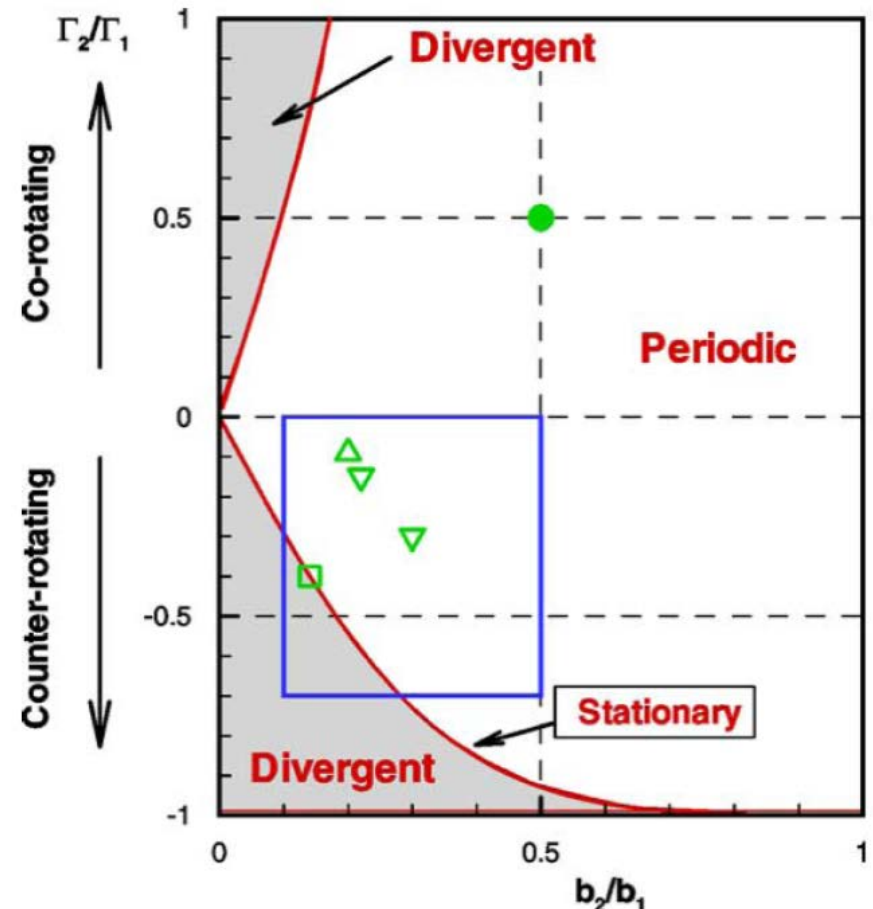
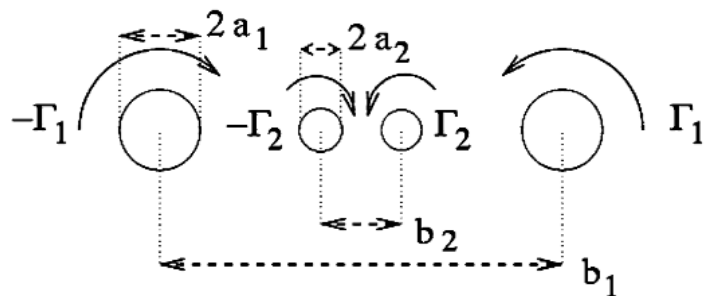


Four-vortex systems

- two co-cotating pairs



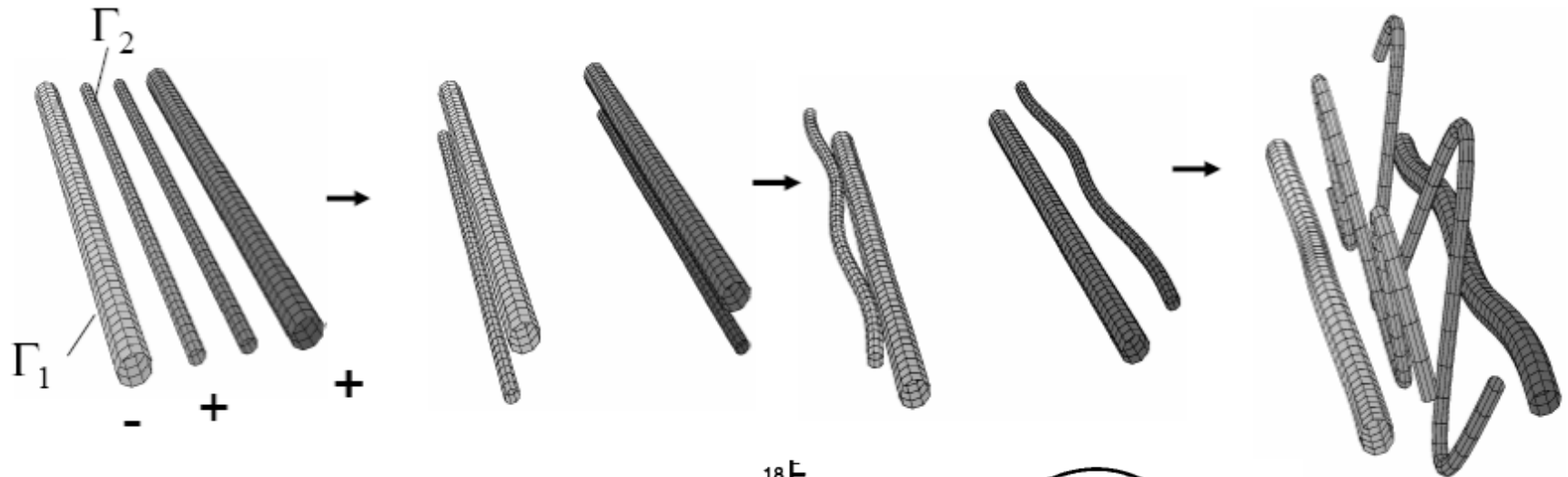
- two counter-cotating pairs



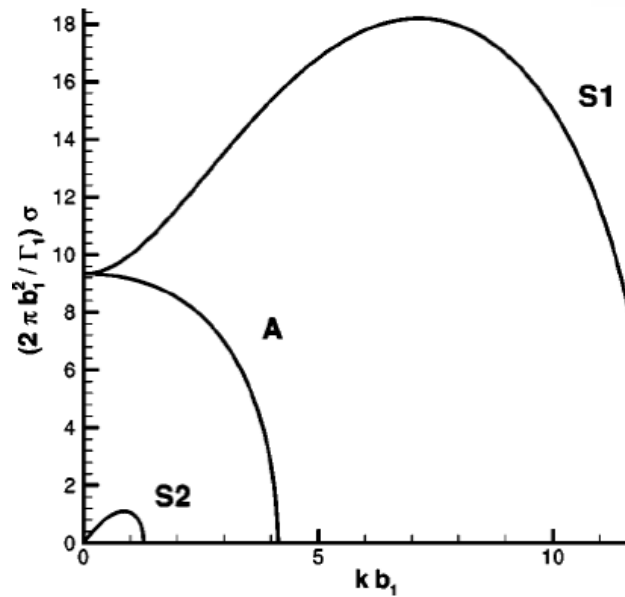
classification chart
(Fabre et al. 2002)

Counter-rotating 4-vortex system

(Jacquin et al., ONERA)



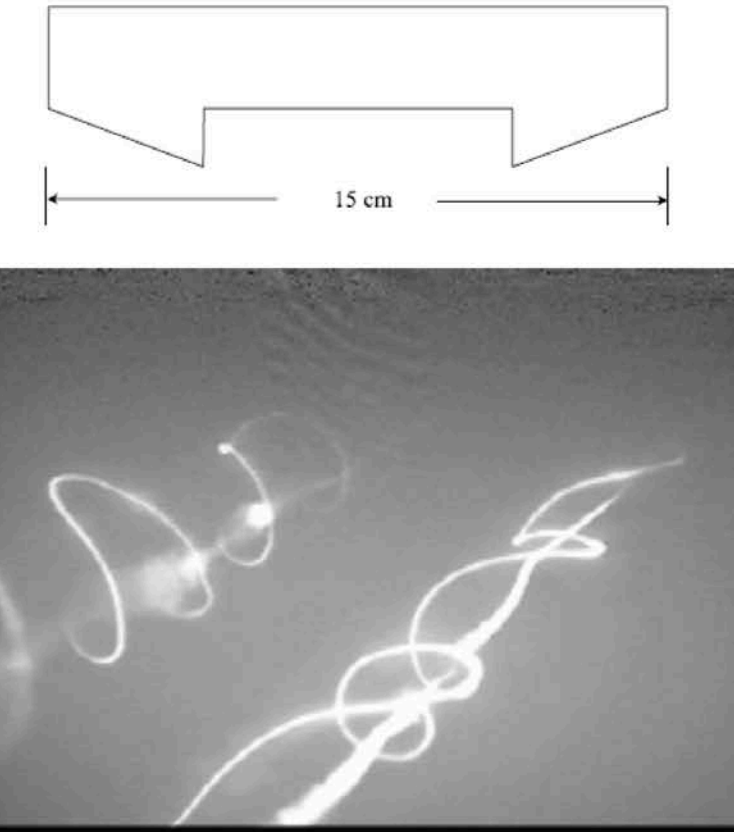
- deformations of inner vortices
- large growth rate
- $\lambda/b_1 = O(1)$



Counter-rotating 4-vortex system

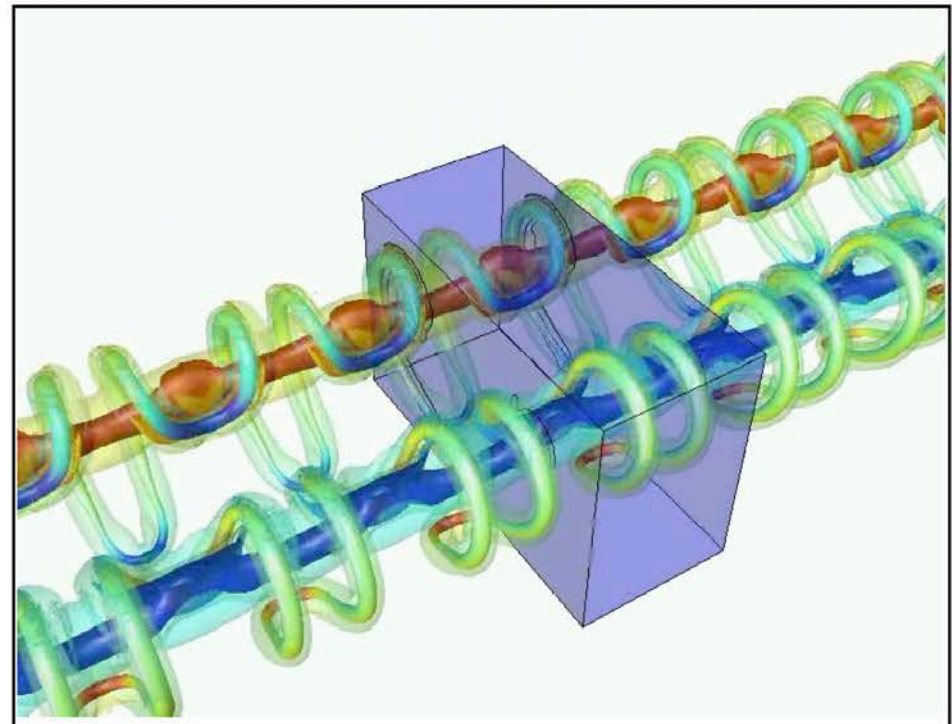
Towing tank **experiment**

Ortega, Savas (Berkeley)



Numerical **simulation**

Winckelmans (UCL)

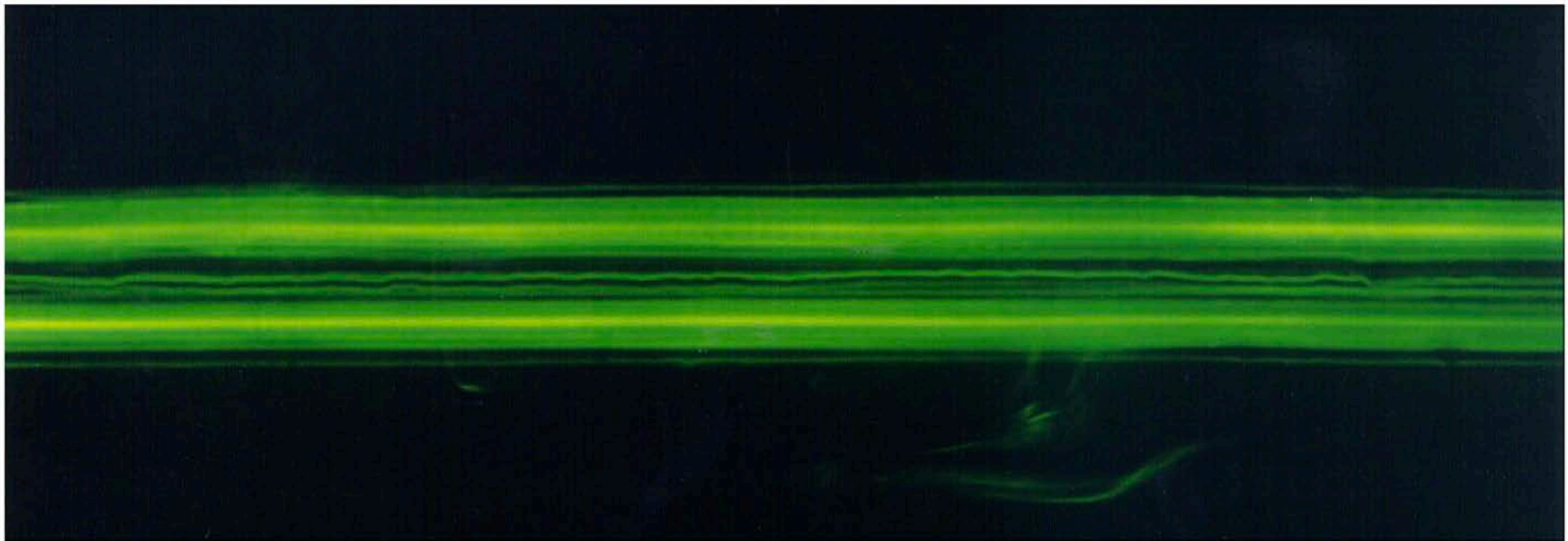


Short-wave instability
Vortex pairs

Elliptic instability

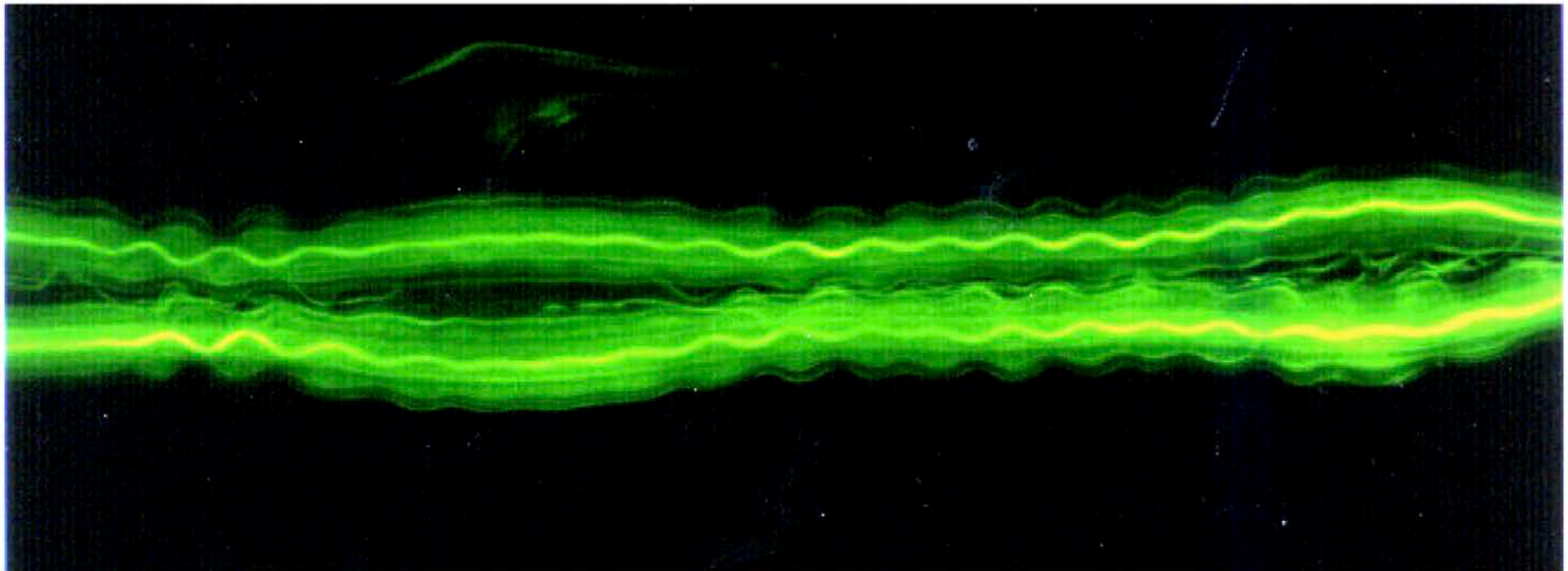
Short-wave instability ($Re = 2500\text{--}4000$, $a/b \approx 0.2$)

initial condition



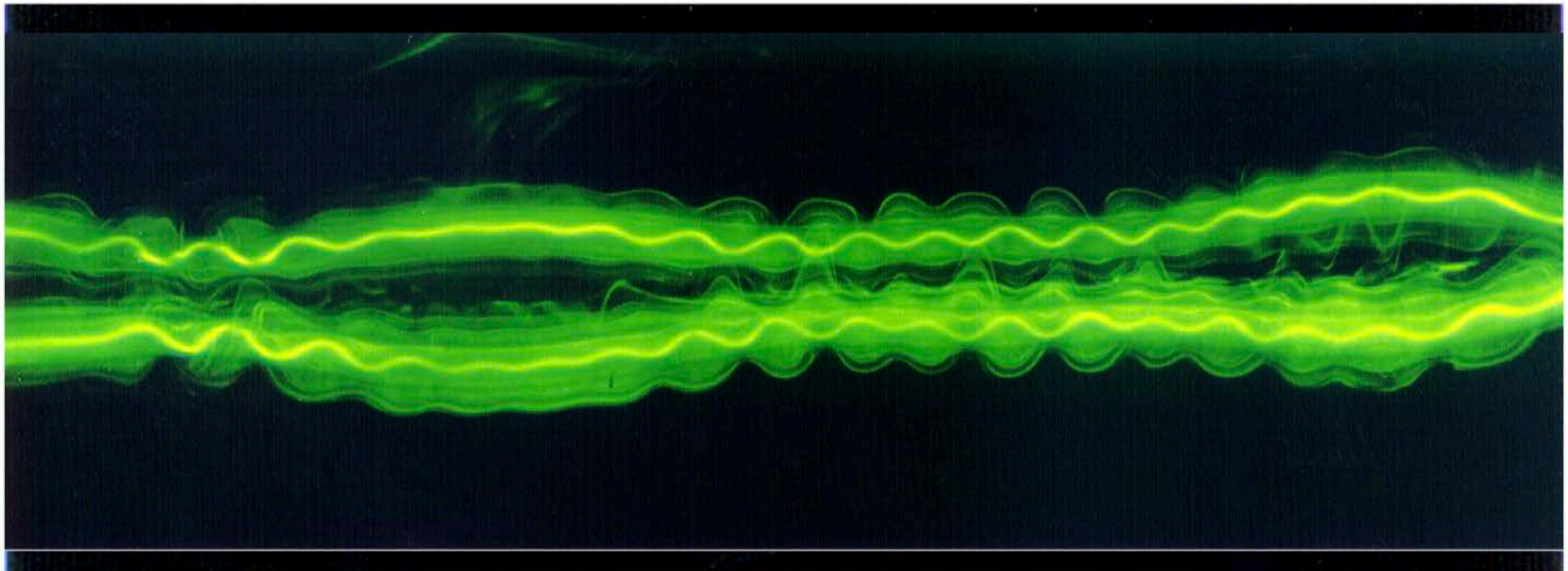
bottom view

***Short-wave instability* ($Re = 2500\text{--}4000$, $a/b \approx 0.2$)**



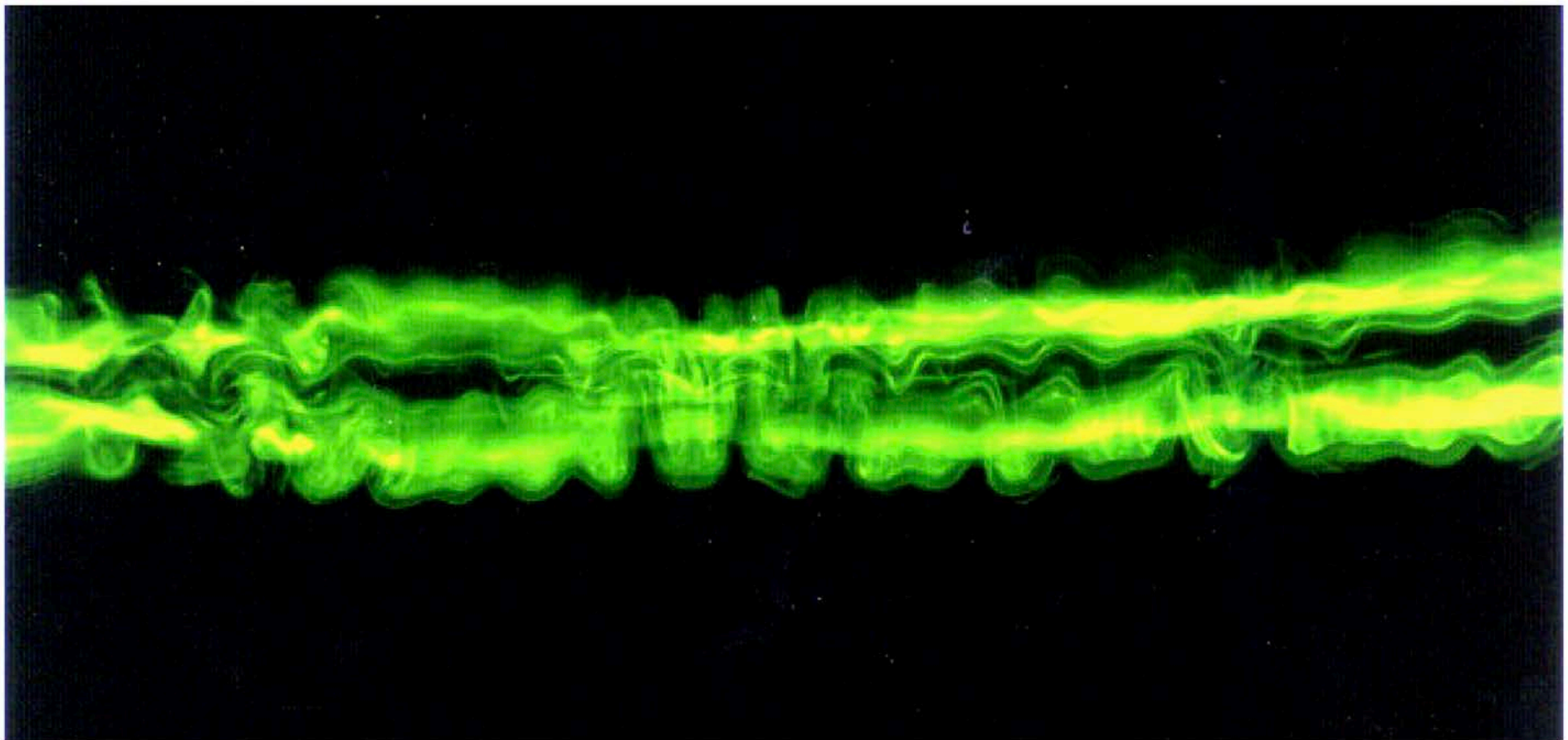
bottom view

***Short-wave instability* ($Re = 2500\text{--}4000$, $a/b \approx 0.2$)**



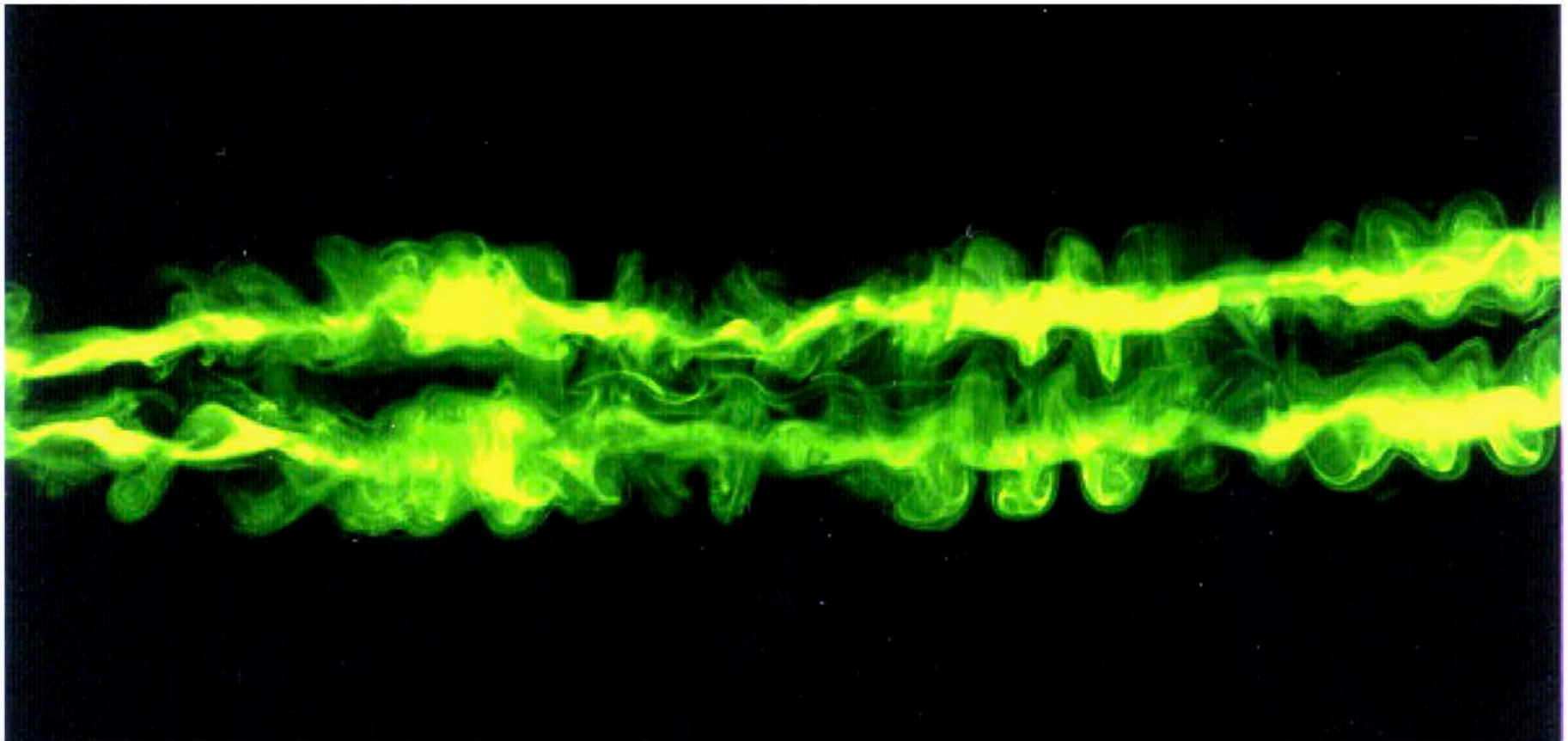
bottom view

***Short-wave instability* ($Re = 2500\text{--}4000$, $a/b \approx 0.2$)**



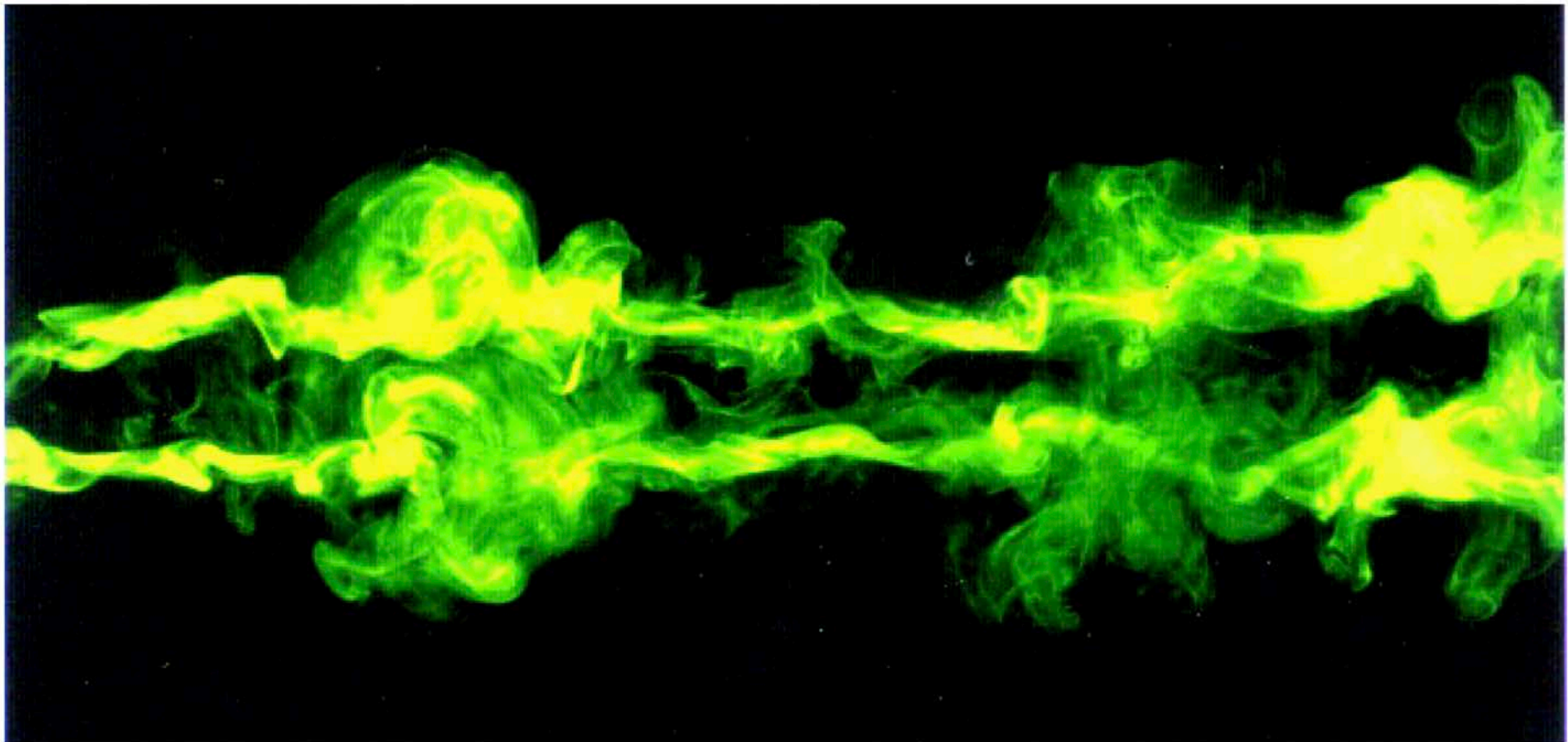
bottom view

***Short-wave instability* ($Re = 2500\text{--}4000$, $a/b \approx 0.2$)**



bottom view

***Short-wave instability* ($Re = 2500\text{--}4000$, $a/b \approx 0.2$)**



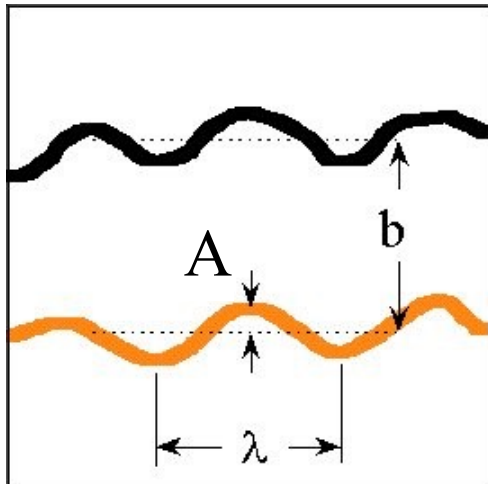
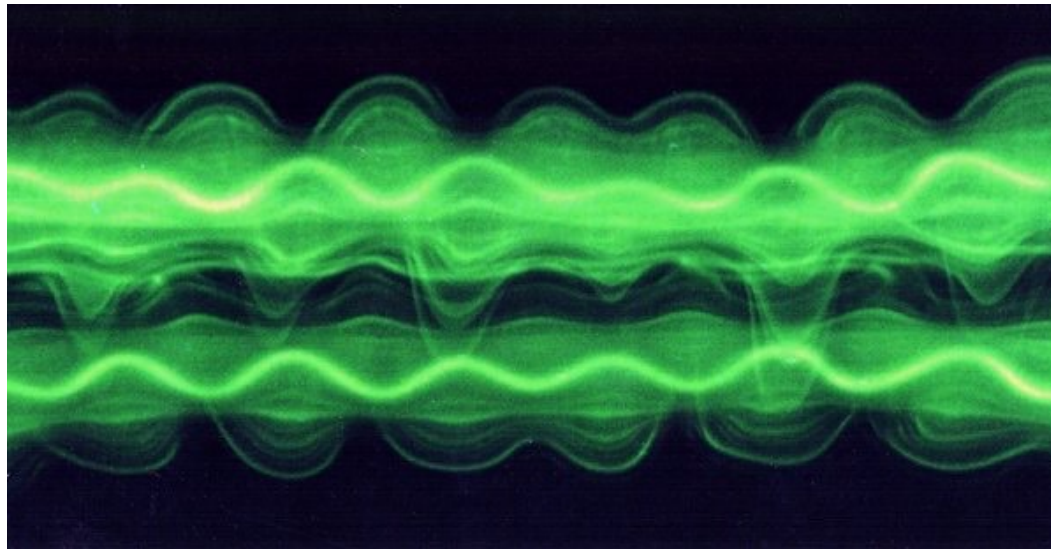
bottom view

Short-wave instability ($Re = 2500\text{--}4000$, $a/b \approx 0.2$)

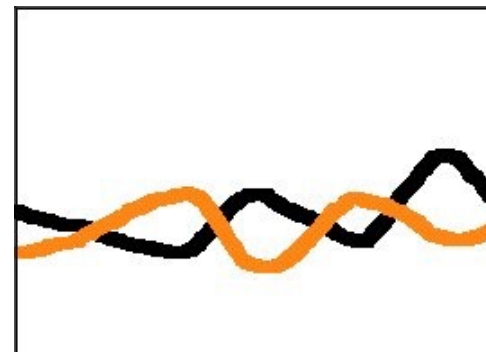


side view

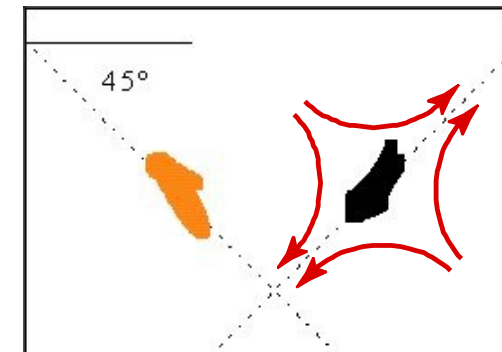
Short-wave instability (spatial structure & symmetry)



bottom view



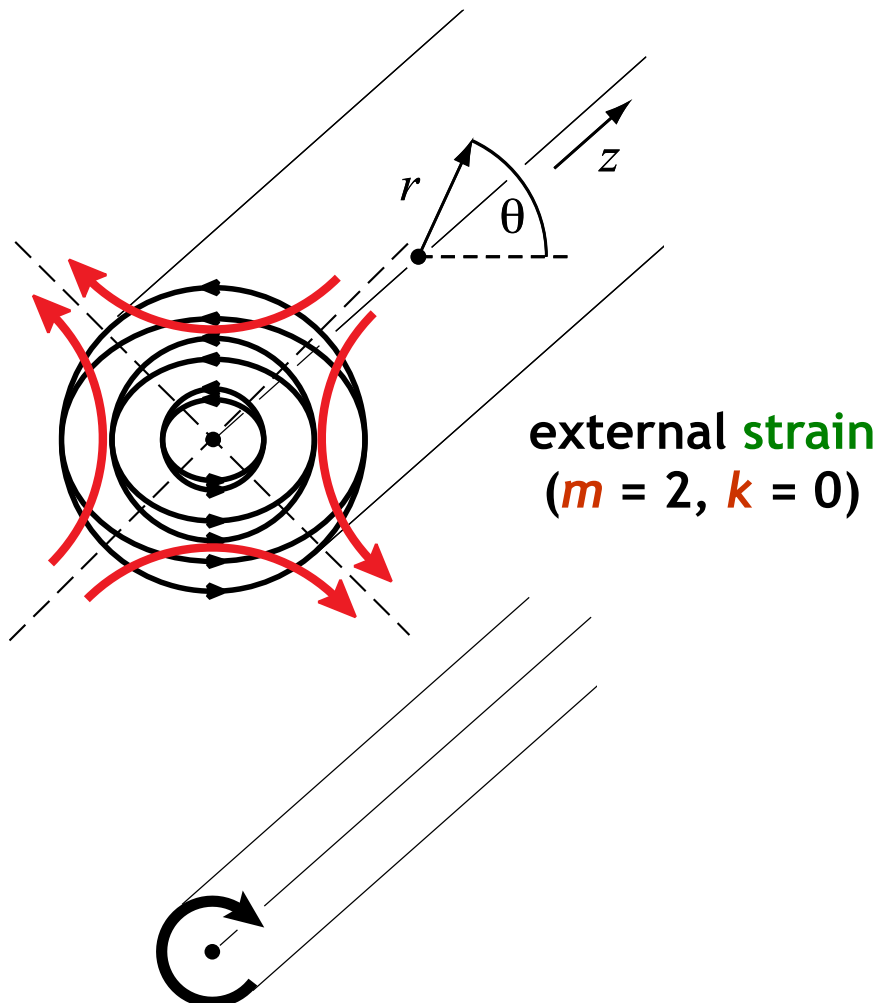
side view



axial view

Short-wave instability mechanism

example: vortex in a strain - elliptic instability



Perturbations of a vortex
("Kelvin modes")

$$u(r) \cdot \exp[i(kz + m\theta + \omega t)]$$

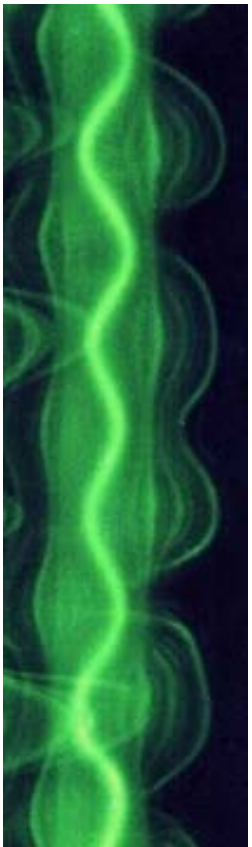
Resonance between two modes
(m_1, k_1, ω_1) and (m_2, k_2, ω_2) and
a strain field is possible if

$$\begin{aligned} |m_1 - m_2| &= 2 \\ k_1 - k_2 &= 0 \\ \omega_1 - \omega_2 &= 0 \end{aligned}$$

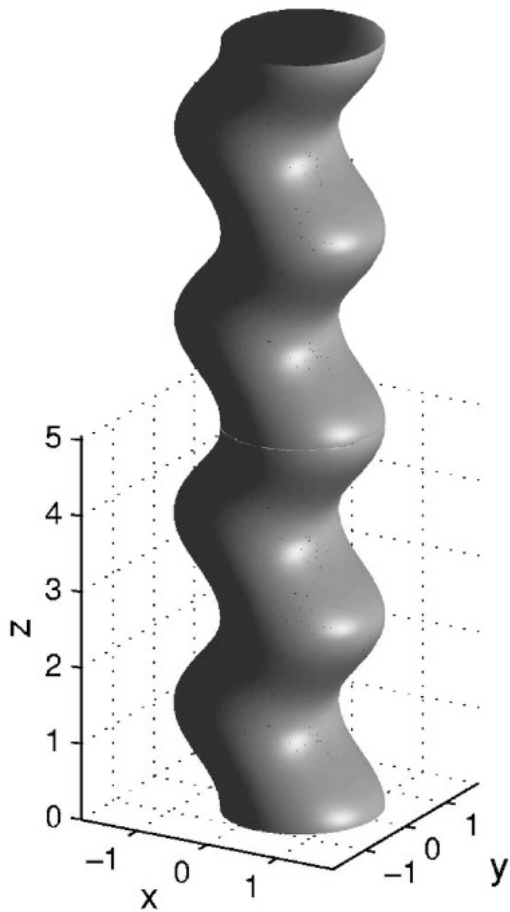
Amplification of perturbations
→ Instability

Short-wave instability mechanism

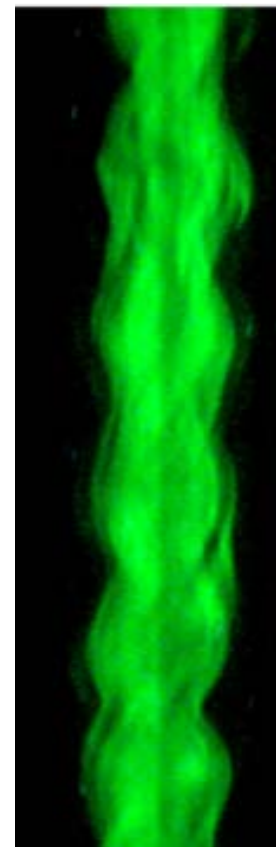
example: vortex in a strain - elliptic instability



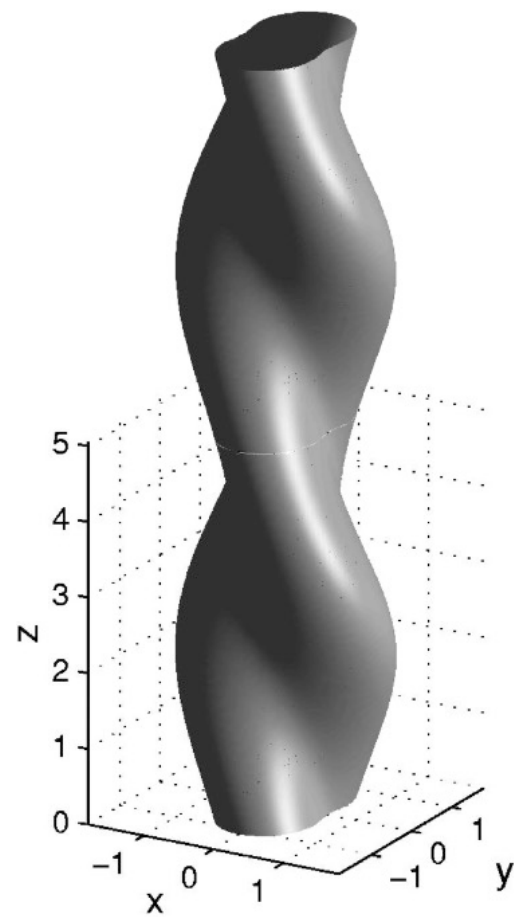
Experiment
vortex pair



Theory
 $m_1 = -1, m_2 = 1$



Experiment
vortex pair
with axial flow



Theory
 $m_1 = 2, m_2 = 0$

Short-wave instability in the wake of a Boeing 747

31 March 2004 – flying from Marseille to Frankfurt

(courtesy of Charles Williamson, Cornell)



Short-wave instability in the wake of a Boeing 747

**31 March 2004 – flying from Marseille to Frankfurt
(courtesy of Charles Williamson, Cornell)**



Long-wave instability
Helical vortices

Pairing instability

Helical vortices

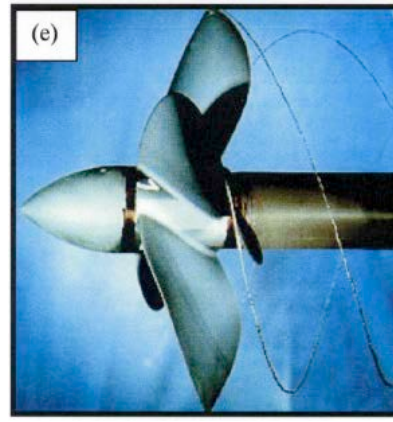
– Applications –



- helicopters
- propellers
- wind turbines



Hand *et al.* (2001)



Senocak *et al.* (2002)

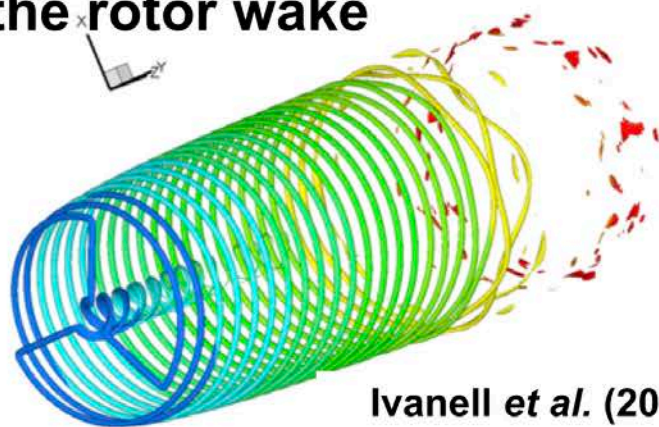


Helical vortices

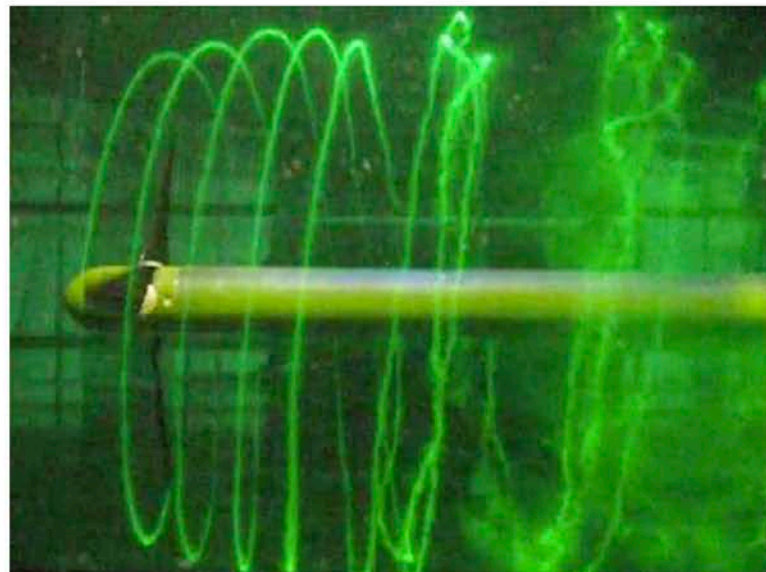
– Applications –

Wind turbines

- Downstream evolution of the rotor wake



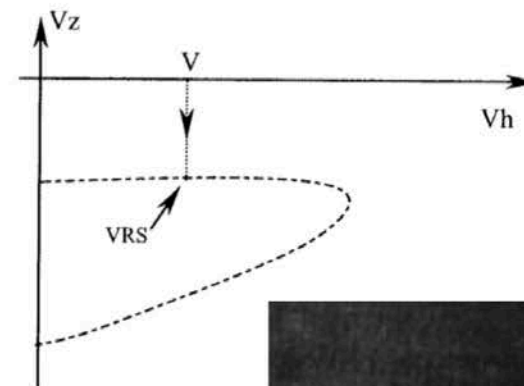
Ivanell et al. (2010)



Mikkelsen
(2010, priv. comm.)

Helicopters

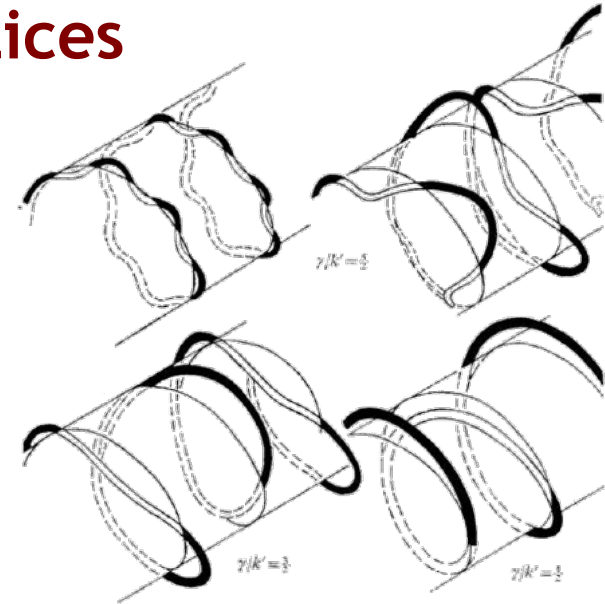
- transition from helical wake to Vortex Ring State (VRS)



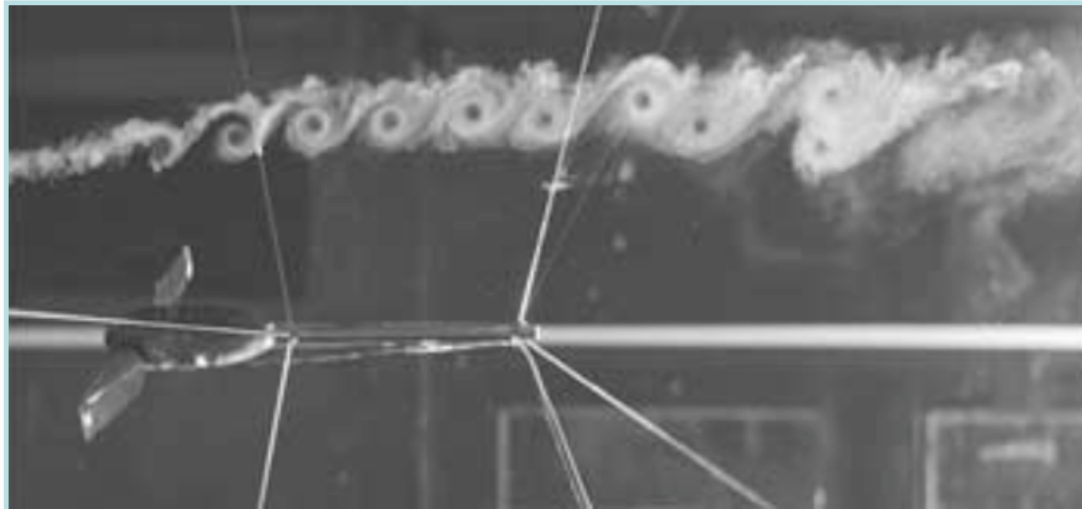
Meijer Drees & Hendal (1950)

Instabilities of helical vortices

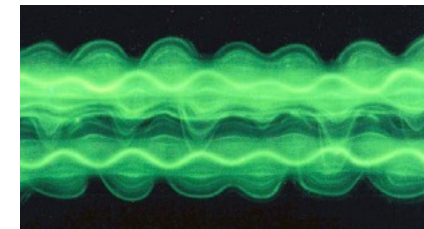
- Long-wave displacement instabilities (filaments)
- Short-wave core instabilities (elliptic, curvature)
- Swirling jet instability (vortex breakdown)



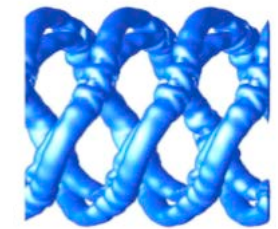
Widnall (1972)



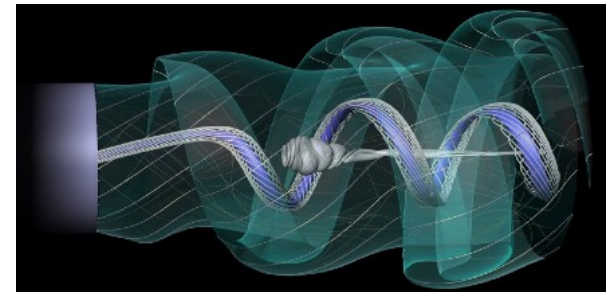
Alfredsson & Dahlberg (1979)



Leweke & Williamson (1998)

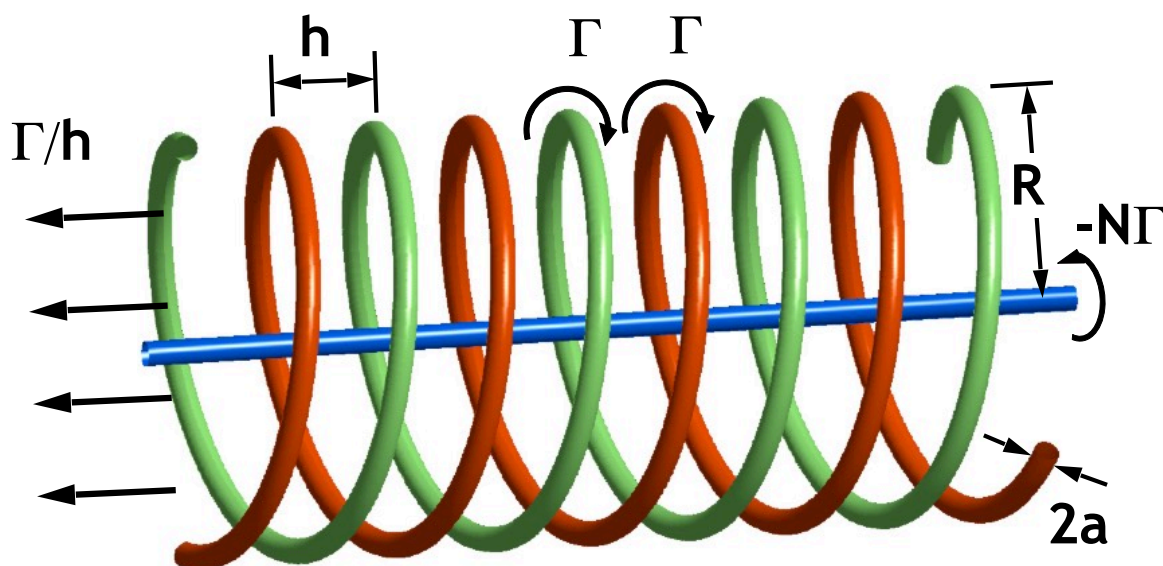
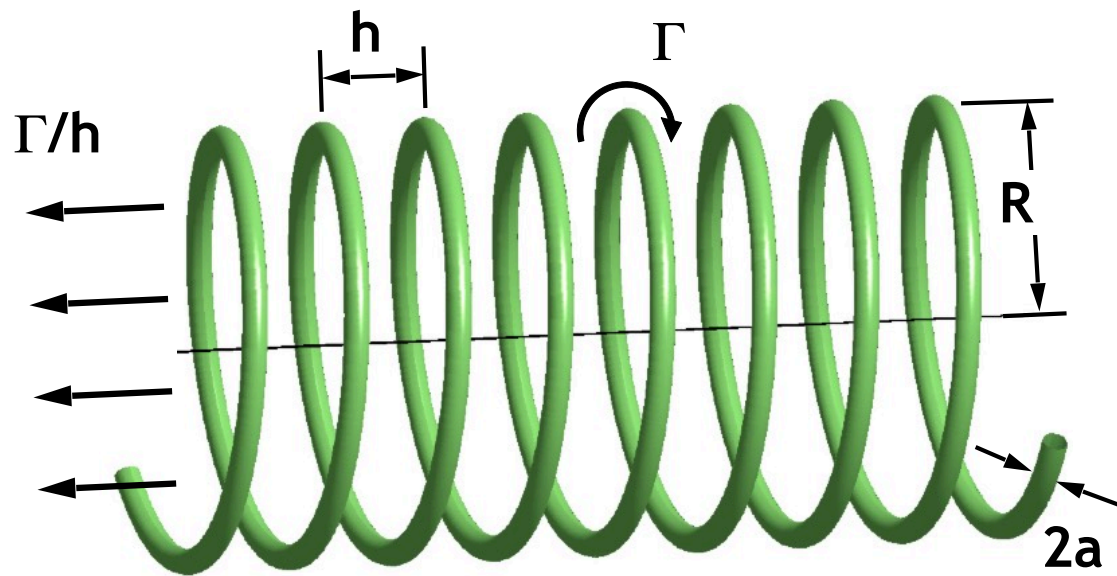


Walther et al. (2007)



Petz et al. (2011)

Configuration



infinite helical vortices

- circulation Γ
- radius R , pitch h ($\times N$)
- core radius a

parameters: $R/a, h/a, Re = \Gamma/\nu$
 $\sim 40, \sim 20, \sim 10^4$

characteristic scales

- advection velocity : $\sim \Gamma/2h$
 - length scale : h
 - time scale : $2h^2/\Gamma$
- $\rightarrow \sigma^* = \sigma \cdot (2h^2/\Gamma)$

Experimental study

Water channel:

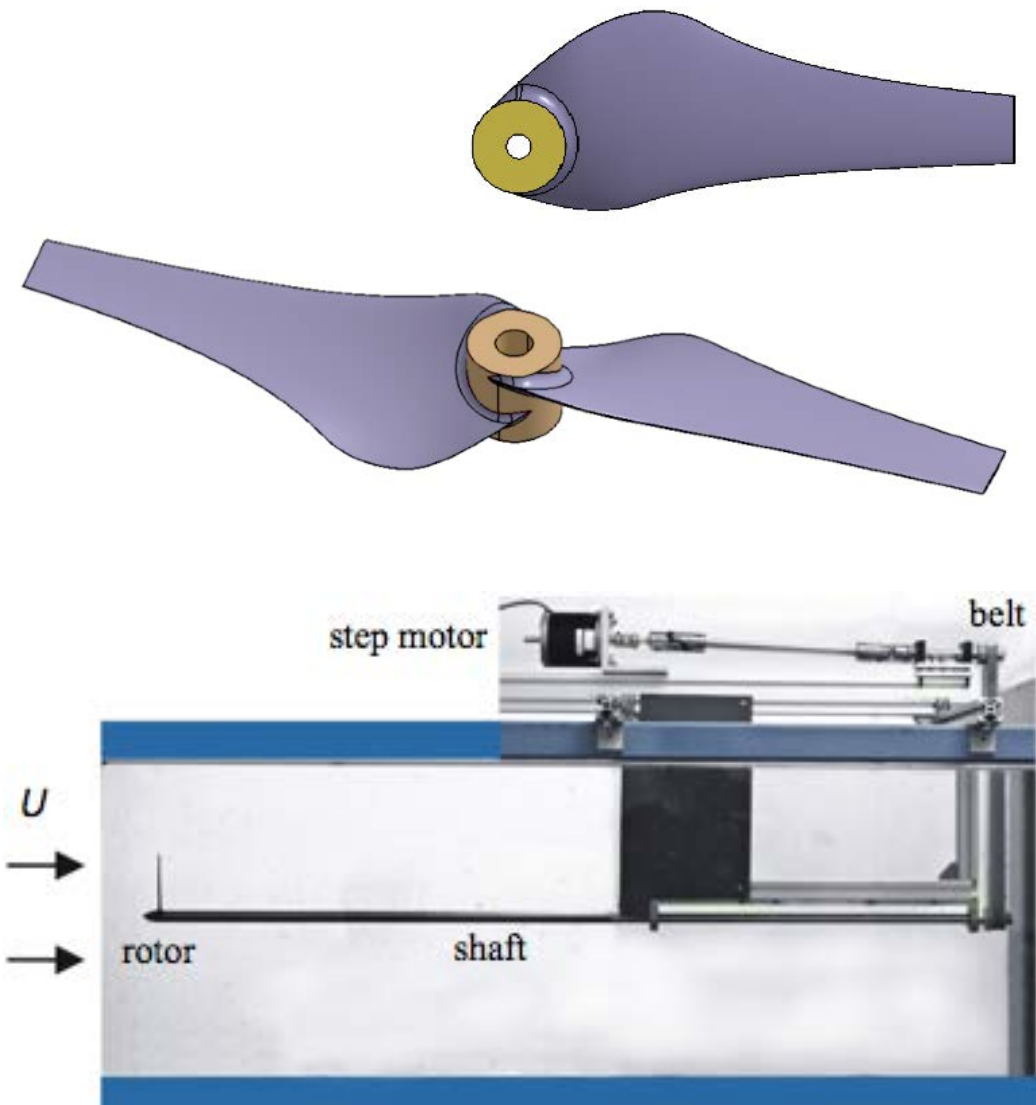
- recirculating, free surface
- test section 37 cm × 50 cm × 150 cm
- free stream velocity $U = 35\text{-}45 \text{ cm/s}$

Rotors:

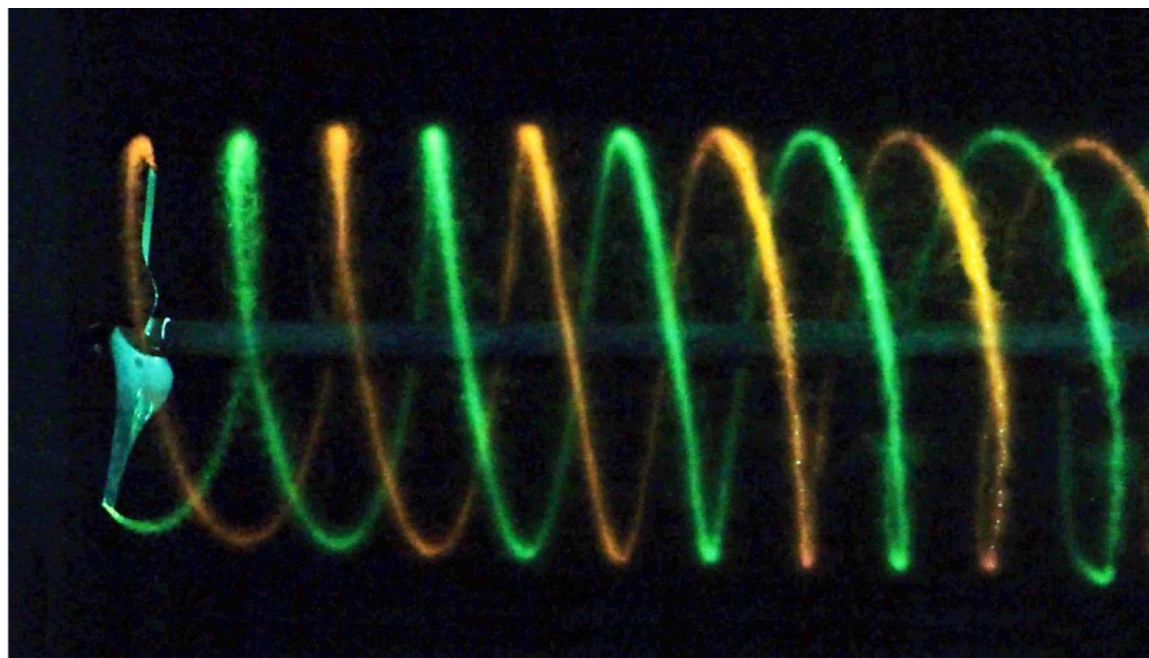
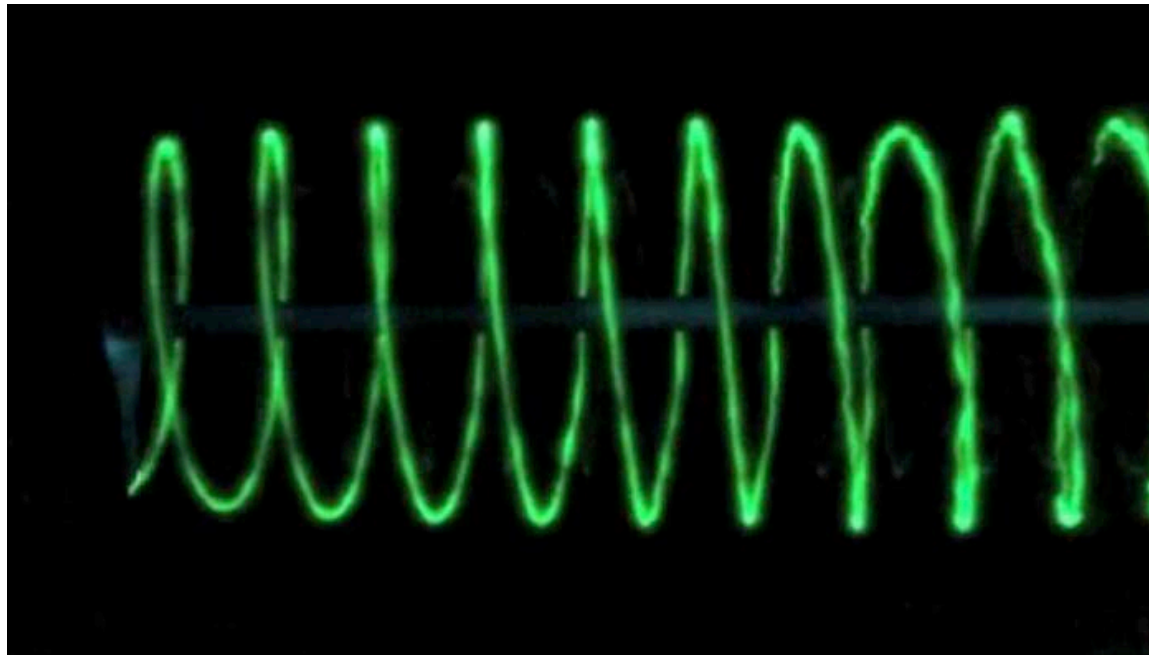
- one or two blades
- low-Re airfoil (A18 - M.S. Selig, UIUC)
- tip chord $c = 11 \text{ mm}$ - $\text{Re}_c = 30000$
- radius: 80 mm
- constant circulation
- $\Omega = 3\text{-}6 \text{ rps}$ tip speed ratio $\lambda = 5\text{-}9$

Methods:

- dye visualisations
- Particle Image Velocimetry (2C & 3C)
- high-speed video & PIV



Experimental study



Long-wave instability - theoretical results

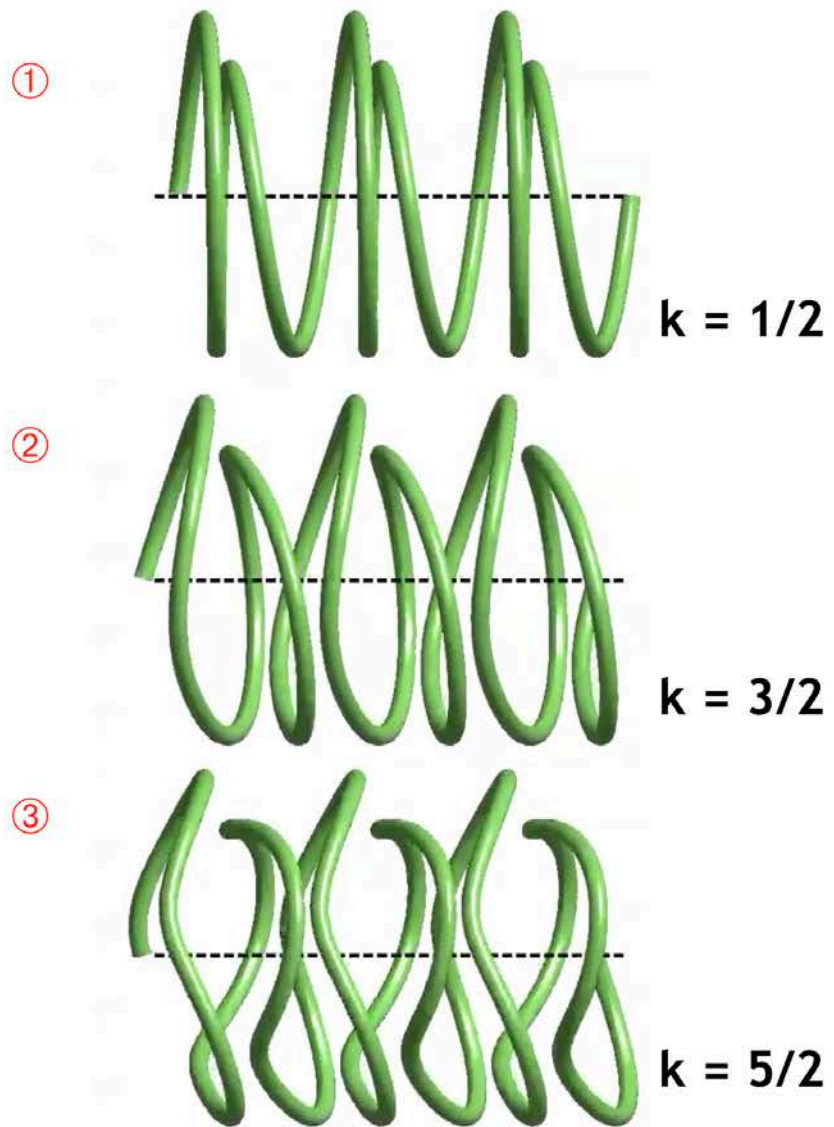
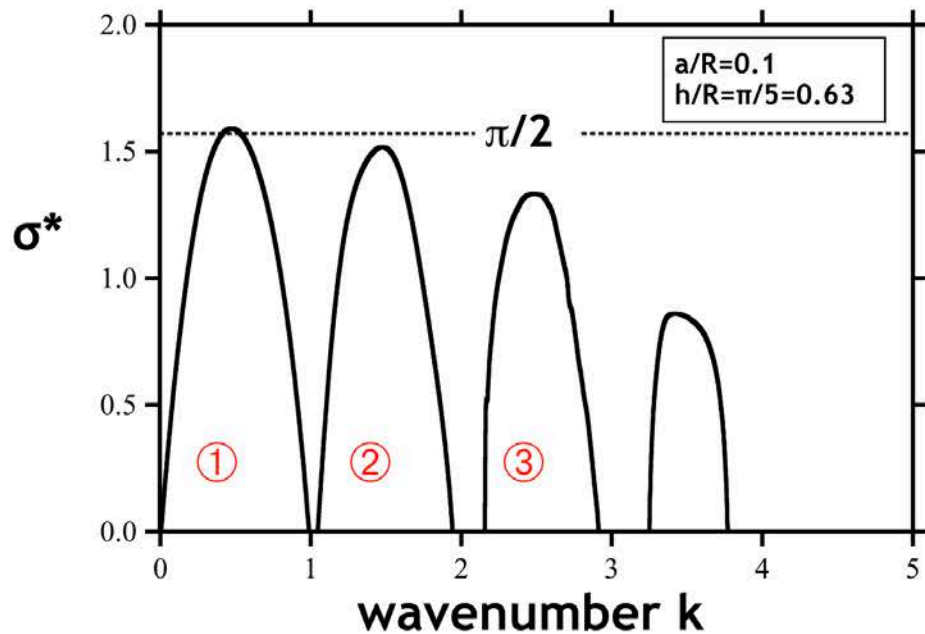
(Widnall 1972, Gupta & Loewy 1974, Fukumoto & Miyazaki 1991)

single helical vortex

$$\sigma^* = f(a/R, h/R, k)$$

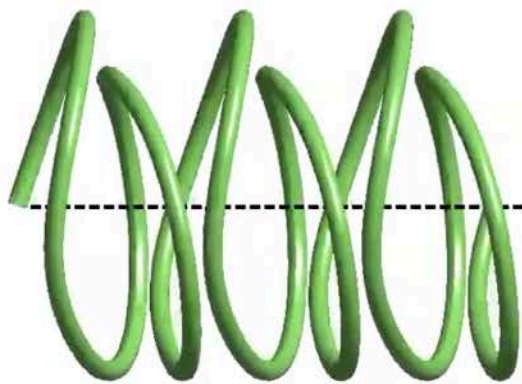
number of waves
in one turn

$$\sigma^* = \sigma \cdot (2h^2/\Gamma)$$



Long-wave instability - theoretical results

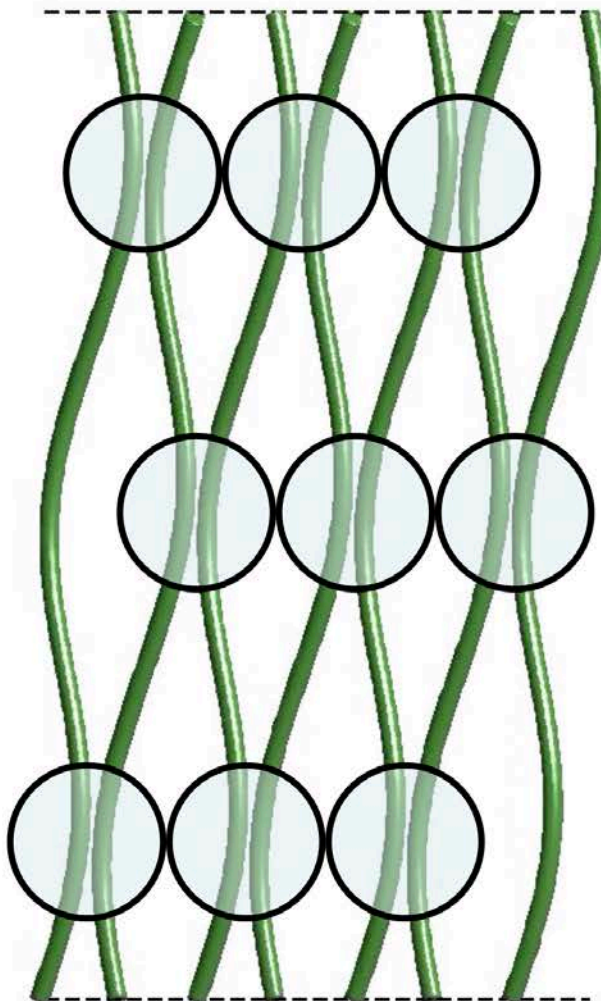
side view



$$k = 3/2$$

$k = m/n$
 m locations of local pairing
in n helix turns

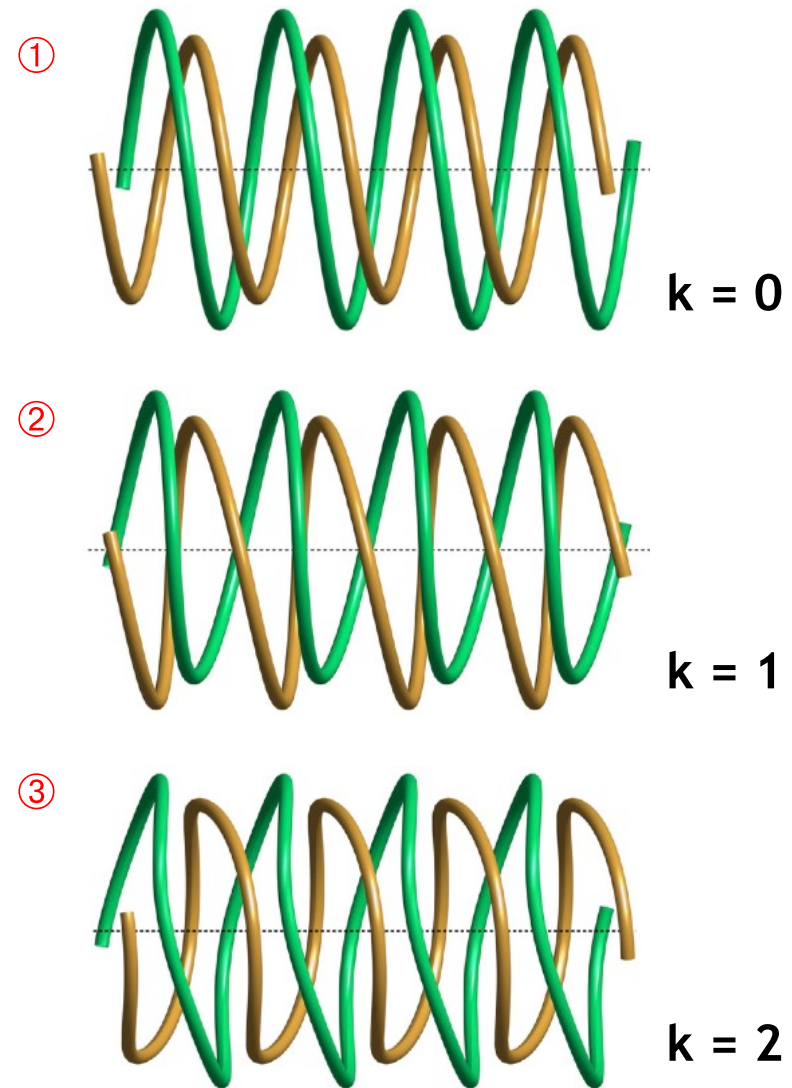
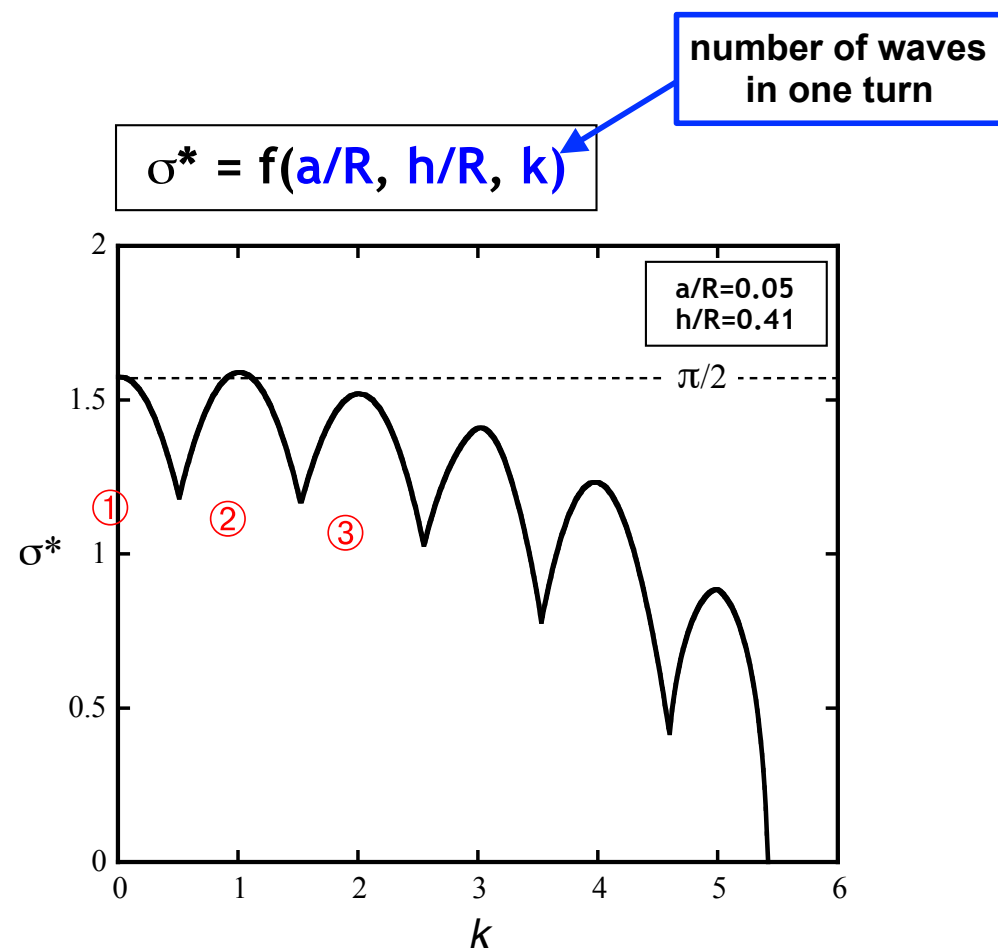
developed plan view



Long-wave instability - theoretical results

(Gupta & Loewy 1974, Okulov & Sørensen 2007)

two interlaced helical vortices

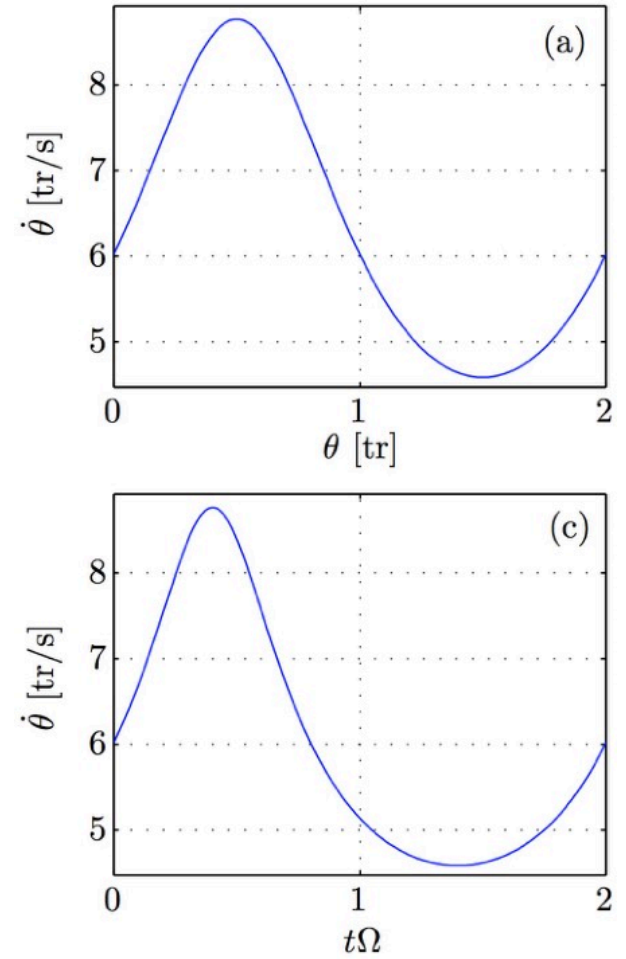
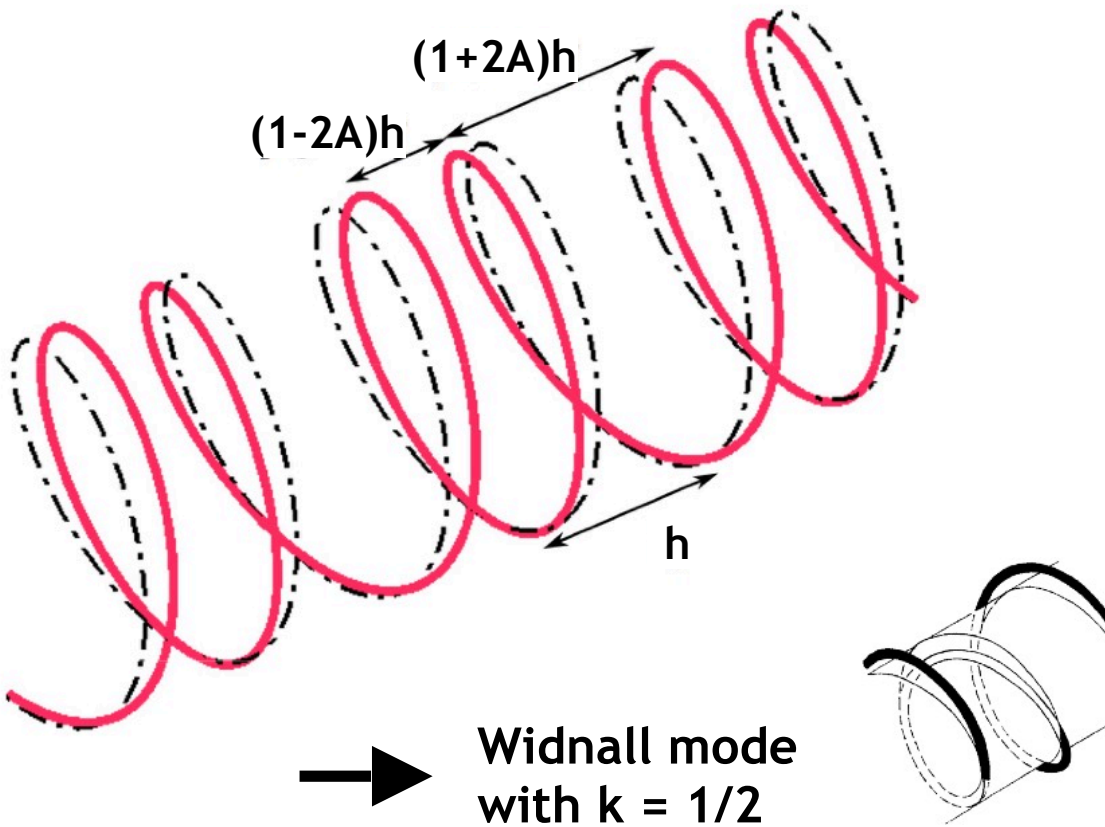


Perturbed flow - single helix

Perturbation of the helix geometry:

$$z/h = \theta/2\pi + A \cos(k\theta)$$

Example: $k = 1/2$ and $A = 0.15$ (for $R/h=2$)



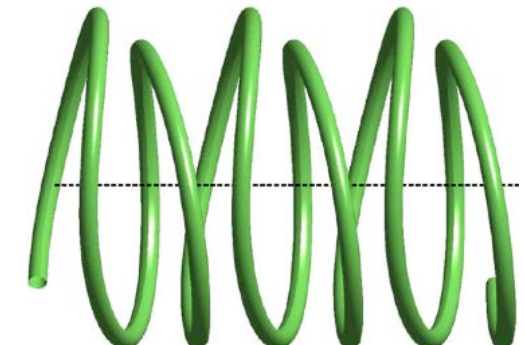
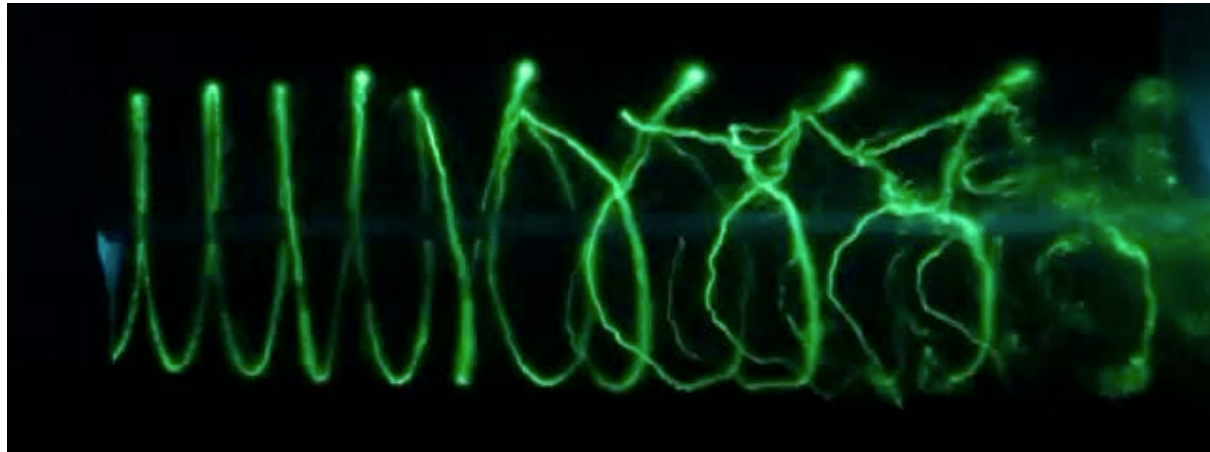
Perturbed flow - single helix

$k = 1/2$ - $A = 0.05$

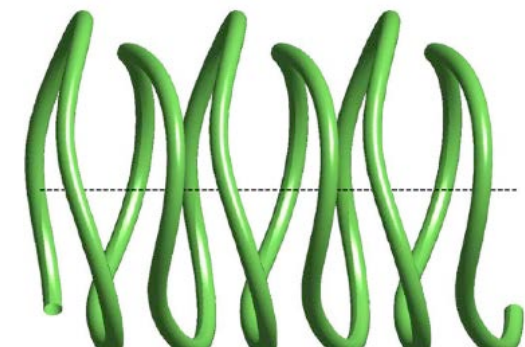
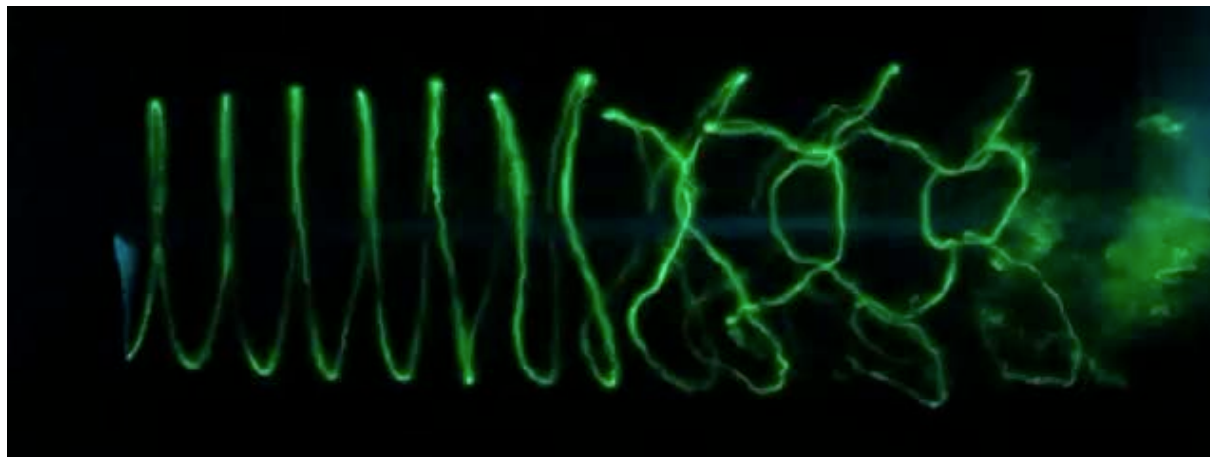


Perturbed flow - single helix

$k = 3/2$ - $A = 0.03$

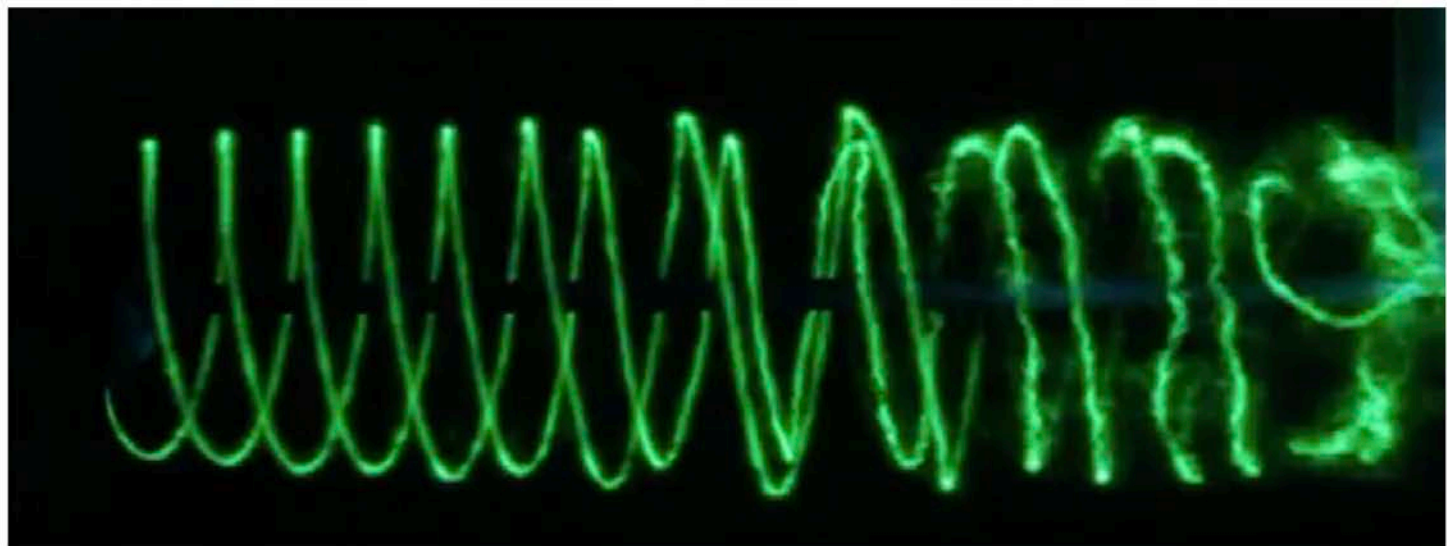


$k = 5/2$ - $A = 0.01$

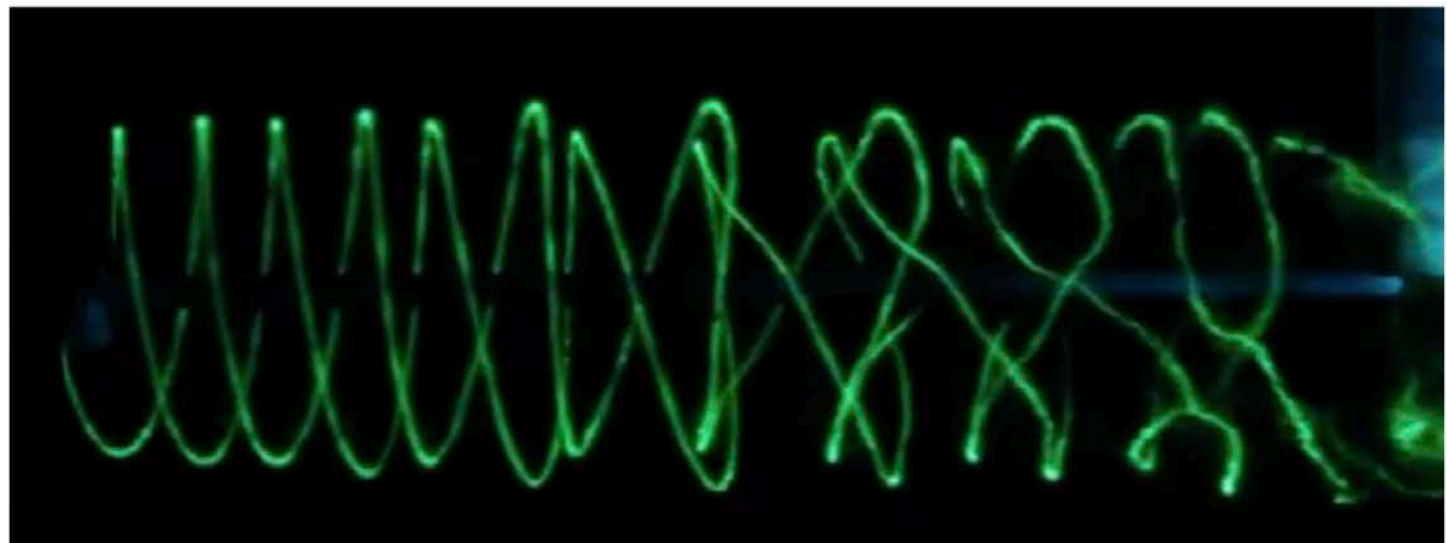


Perturbed flow - double helix

uniform pairing
 $k = 0$

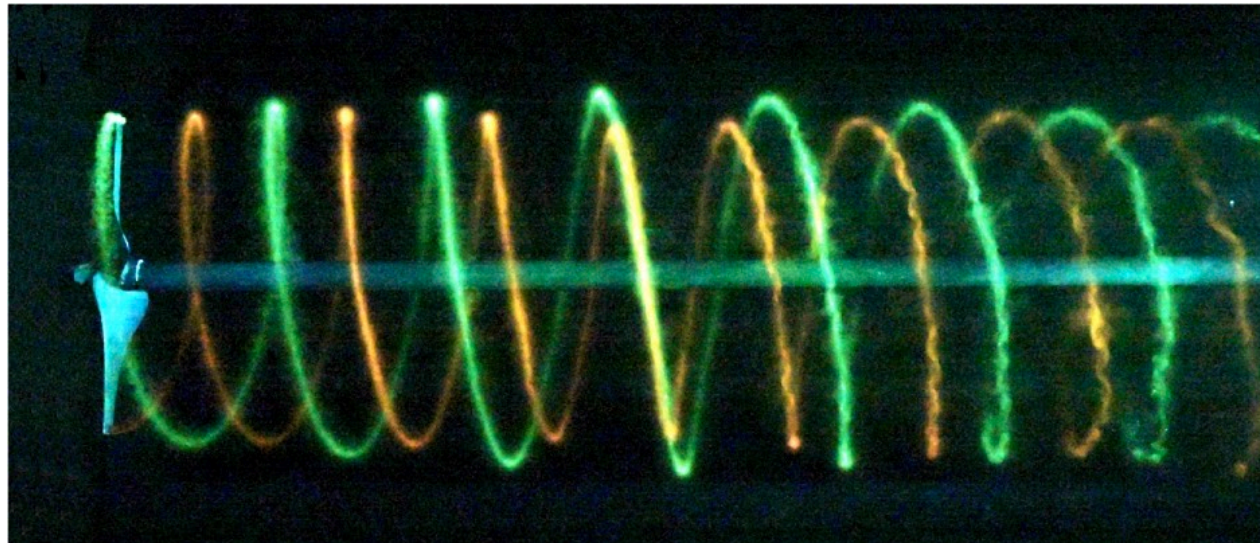


local pairing
 $k = 1$

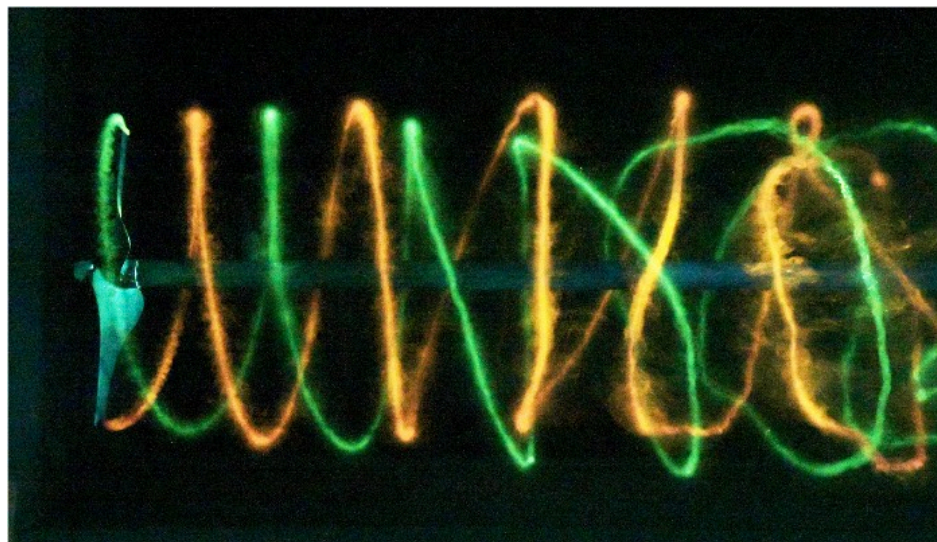


Perturbed flow - double helix

uniform pairing
 $k = 0$



local pairing
 $k = 1$



Growth rate of long-wave instabilities

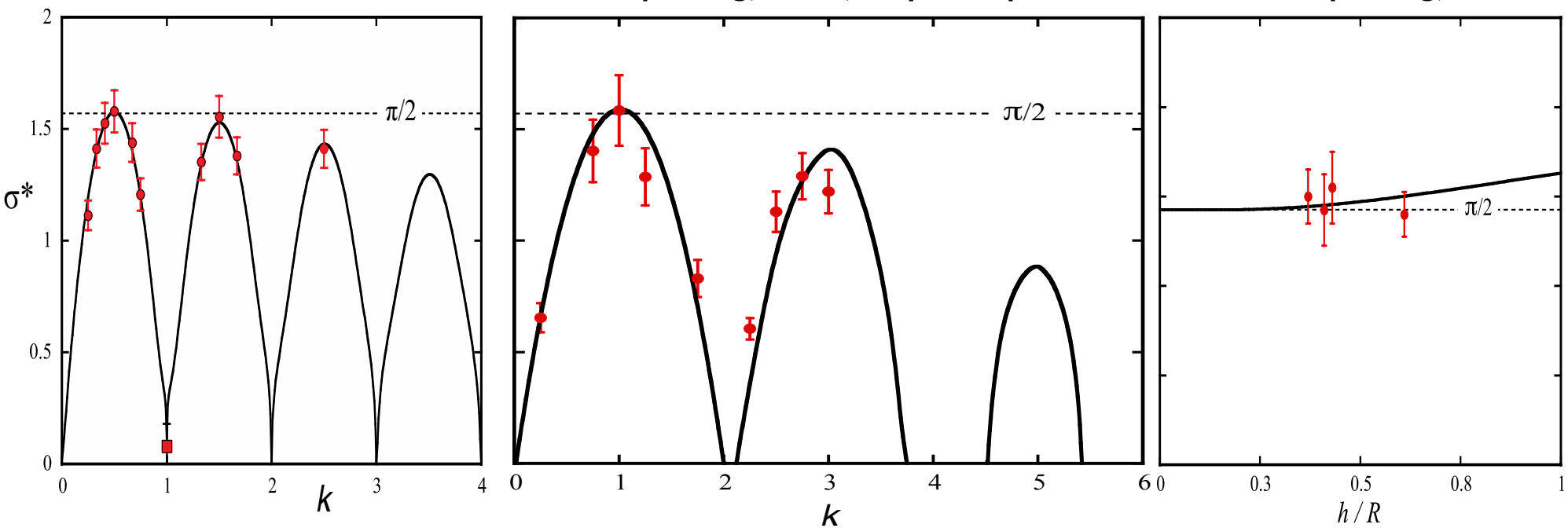
Experiment vs. theory (Gupta & Loewy 1974)

single helix

two helices

local pairing, $k \neq 0$, in-phase pert.

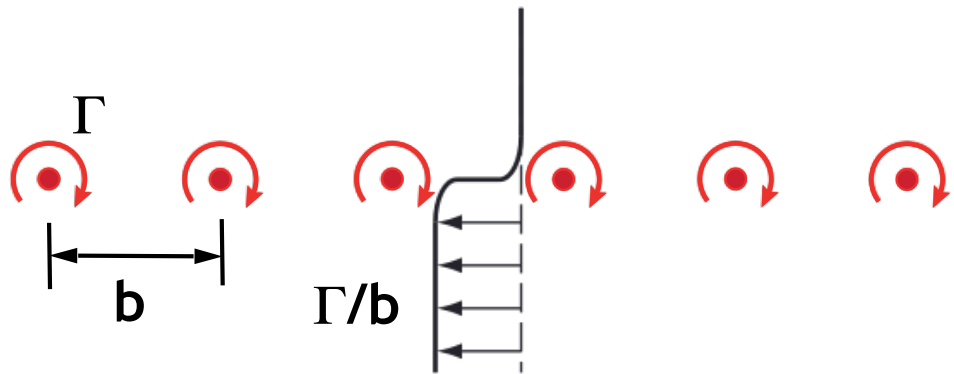
uniform pairing, $k = 0$



Pairing instability

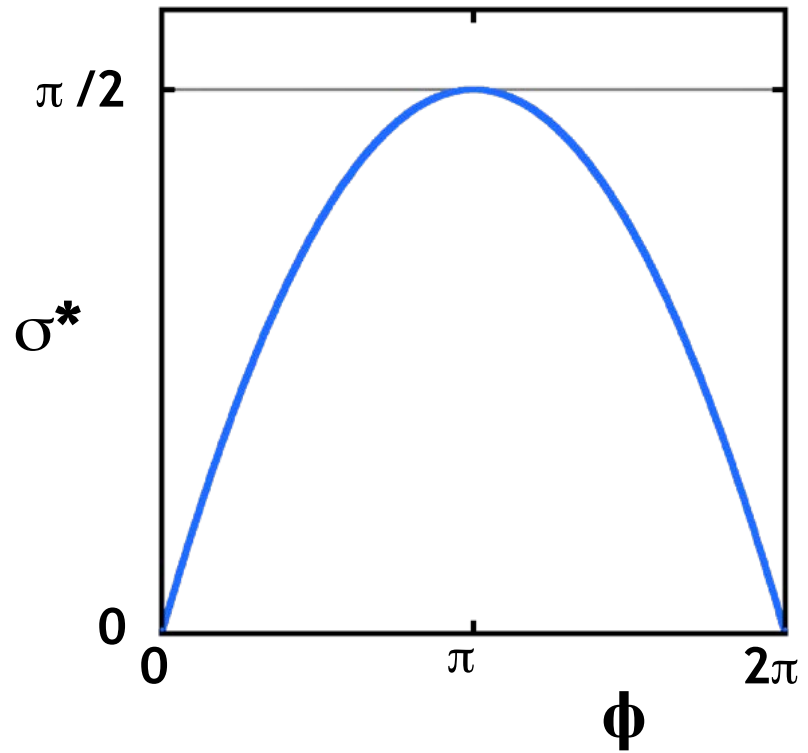
2 dimensions (von Kármán & Rubach 1912, Lamb 1932)

infinite row of point vortices



$$\sigma^* = \sigma \cdot (2b^2/\Gamma)$$

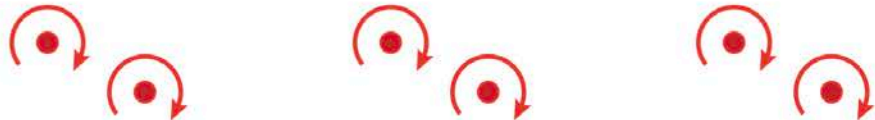
$$\sigma^* = \pi/2 \text{ for } \phi = \pi$$



Pairing instability

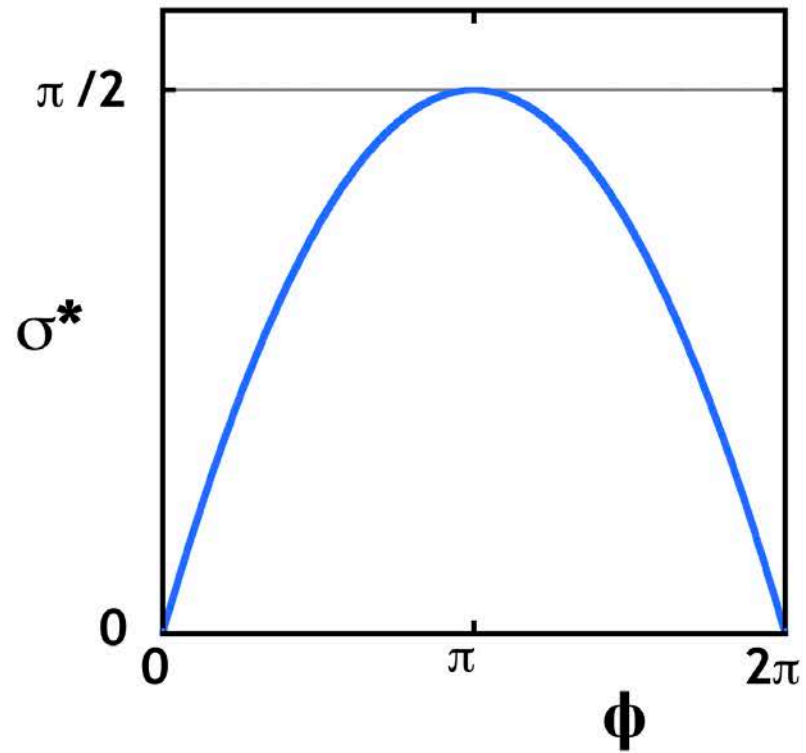
2 dimensions (von Kármán & Rubach 1912, Lamb 1932)

infinite row of point vortices



$$\sigma^* = \sigma \cdot (2b^2/\Gamma)$$

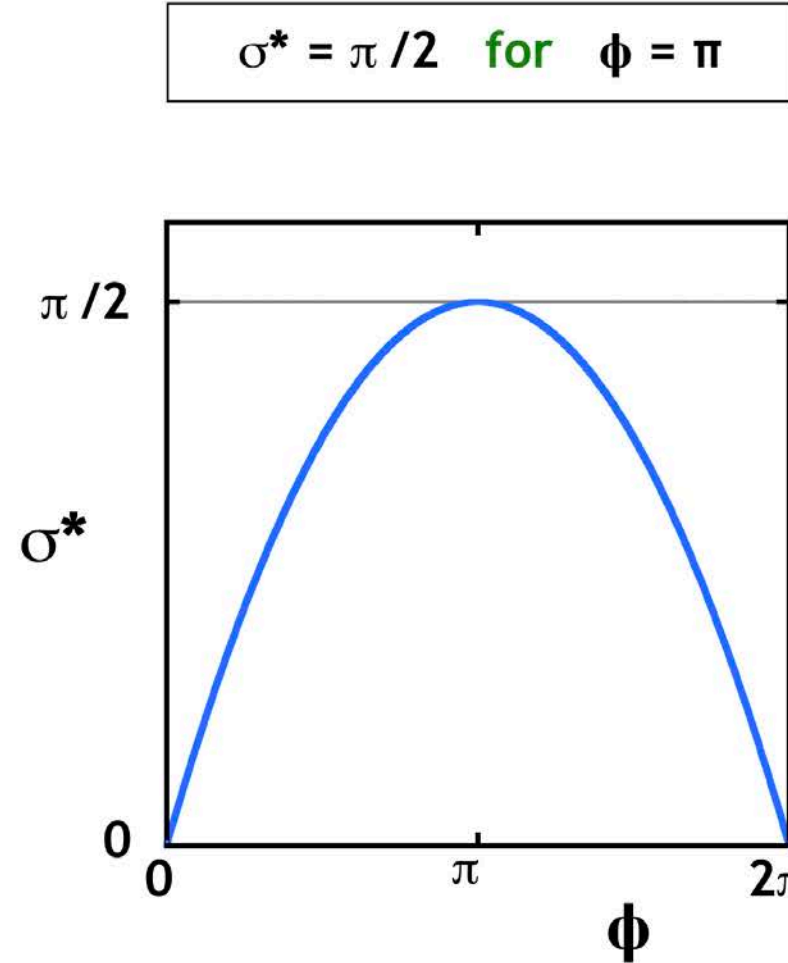
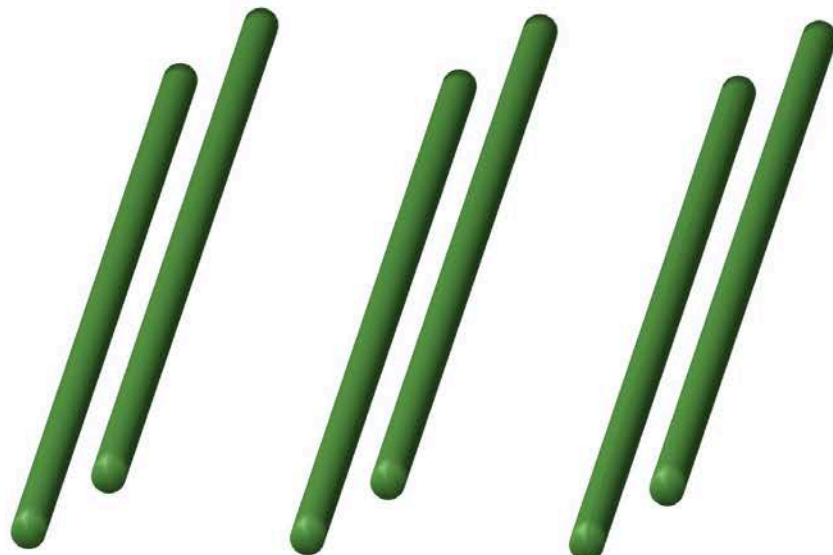
$$\sigma^* = \pi/2 \text{ for } \phi = \pi$$



Pairing instability

2 dimensions (von Kármán & Rubach 1912, Lamb 1932)

infinite array of straight vortices



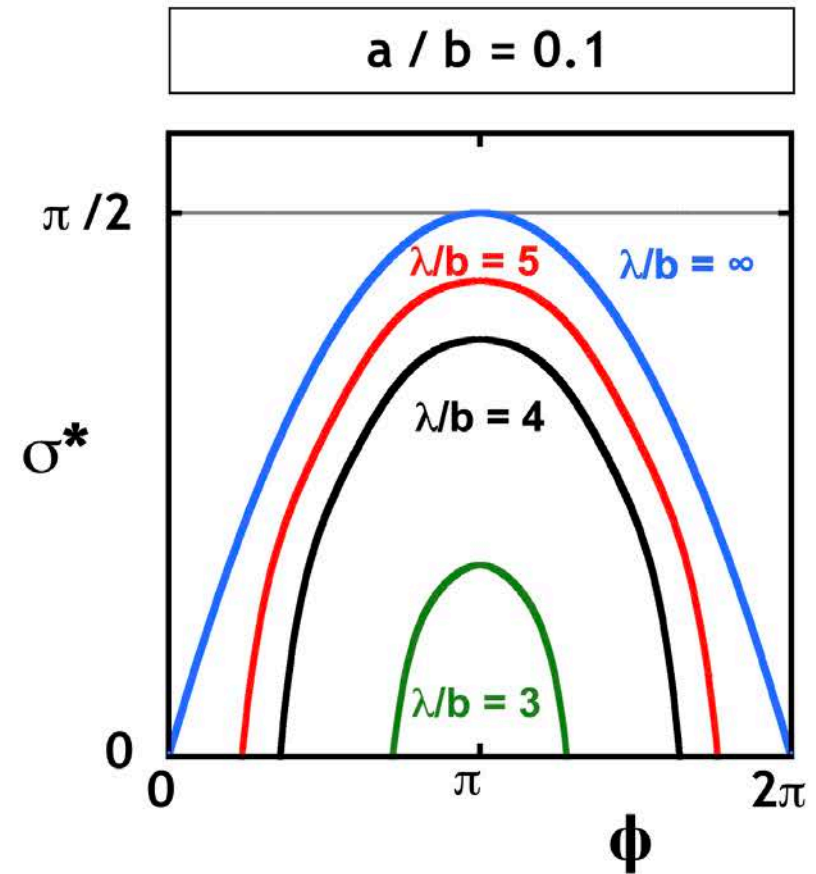
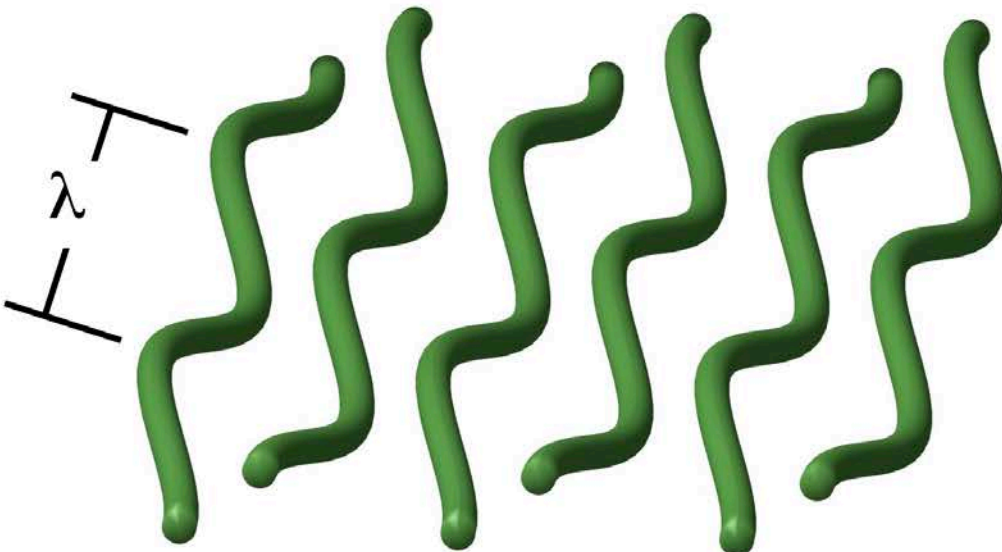
Pairing instability

3 dimensions (Robinson & Saffman 1982)

```
% Robinson & Saffman (1982)
% single row

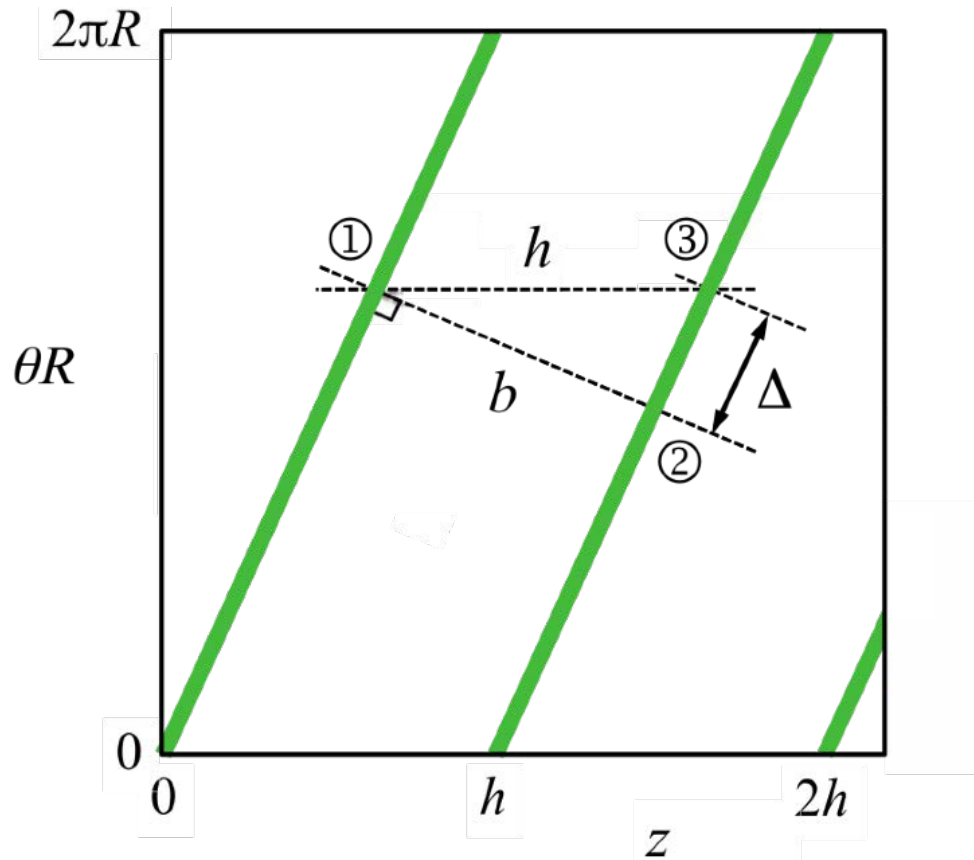
a_sur_l = 0.1; % a/l
l_sur_lambda=1/4;
i=0;
for phi=0:2*pi/100:2*pi;
    i=i+1;
    phi_plot(i)=phi;
    kl = 2*pi*l_sur_lambda;
    eta= kl^2/2*(log(1/(pi*a_sur_l*l_sur_lambda)) ...
        -0.5772+0.25);
    A = pi^2/3;
    At = A;
    for p=1:50;
        A = A - 2*psi_nd(p*kl)/p^2*cos(p*phi);
        At = At - 2*xsi_nd(p*kl)/p^2*cos(p*phi);
    end
    sigma(i) = 1/pi*real(sqrt((A-eta)*(At-eta)));
end
plot(phi_plot,sigma)
```

infinite array of straight vortices



Pairing instability

prediction for helical geometry



Helical vortex
 R, h, k, Γ, a

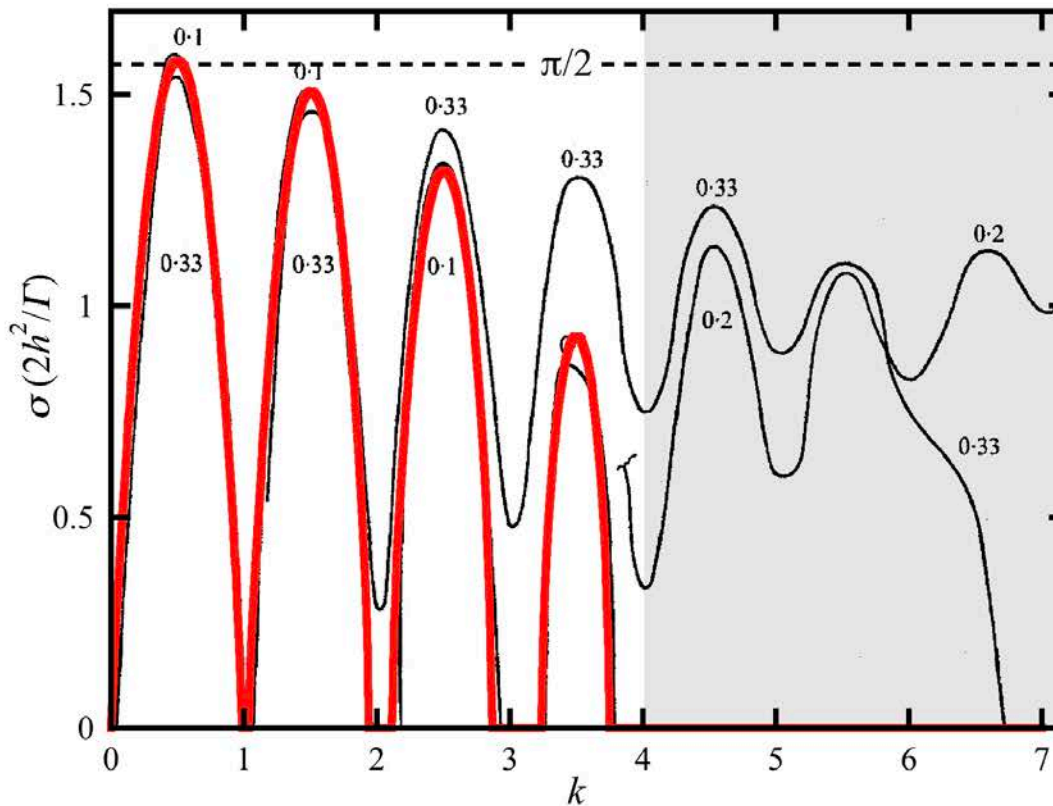
Equivalent array of straight vortices
 $b = f(h, R) \quad \Gamma$
 $\phi = f(k, R, h) \quad a$
 $\lambda = f(k, R, h)$

$$\sigma \cdot (2h^2/\Gamma)$$

Long-wave instability - theoretical results

Growth rate for $h/R = \pi/5 = 0.63$

$a / R = 0.1$

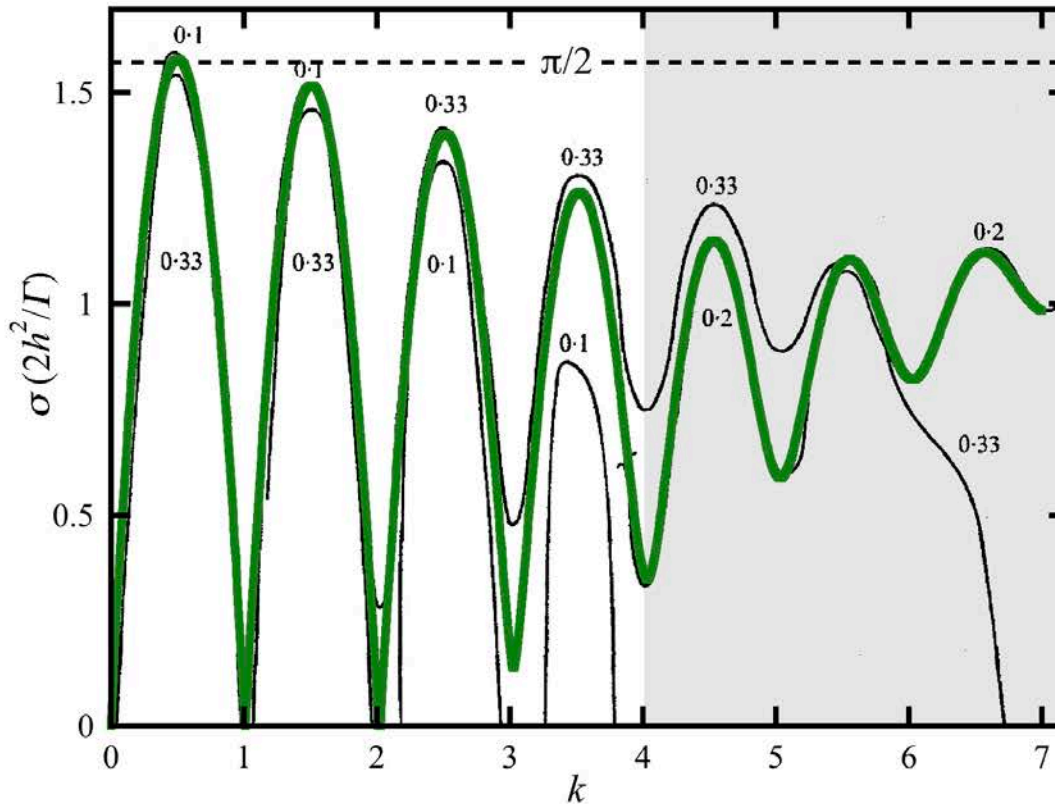


Robinson & Saffman (1982)
applied to helical geometry

Long-wave instability - theoretical results

Growth rate for $h/R = \pi/5 = 0.63$

$a / R = 0.2$

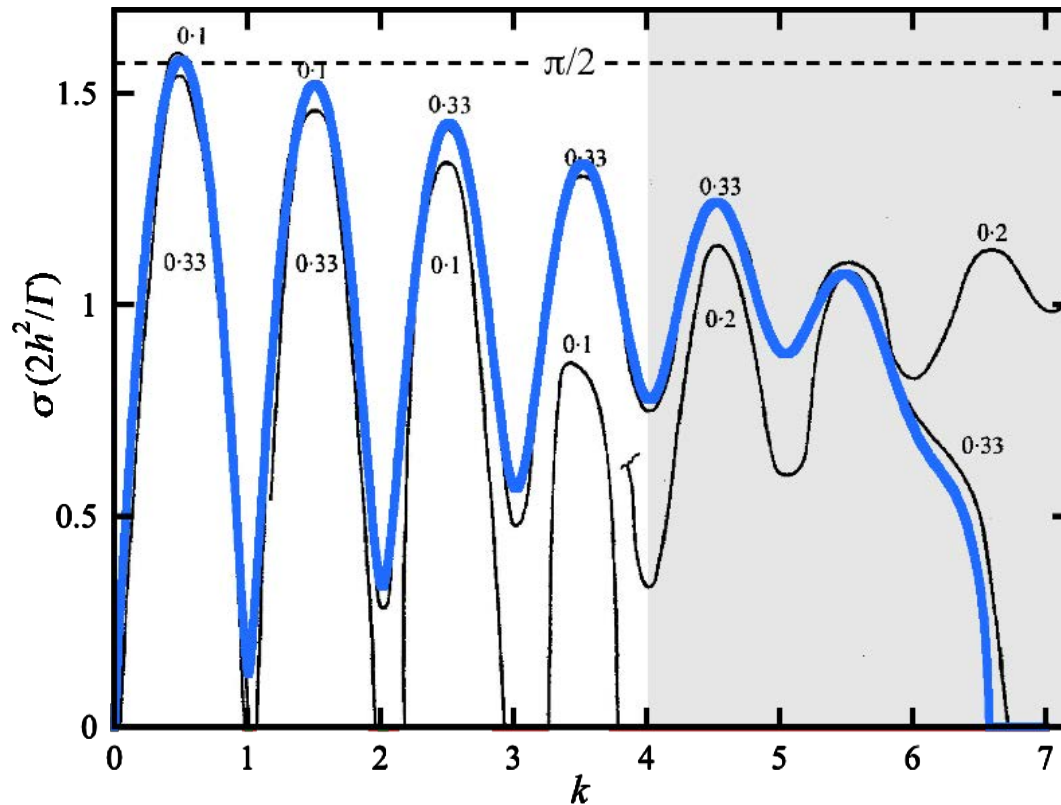


Robinson & Saffman (1982)
applied to helical geometry

Long-wave instability - theoretical results

Growth rate for $h/R = \pi/5 = 0.63$

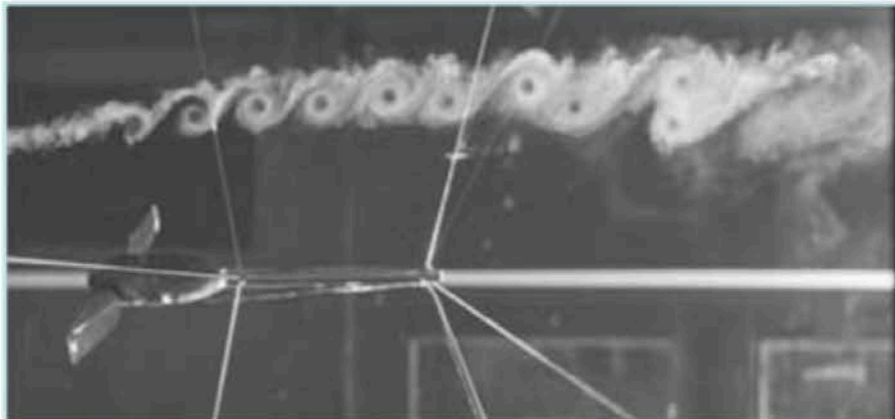
$a / R = 0.23$



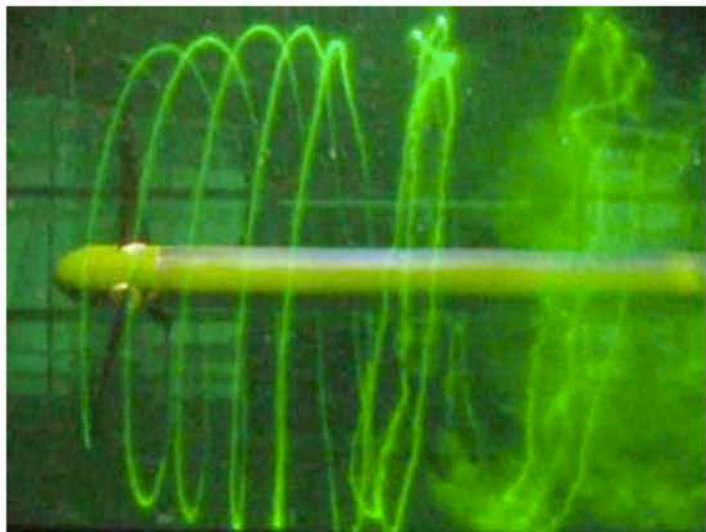
Robinson & Saffman (1982)
applied to helical geometry

Experiments with rotors of more than one blade

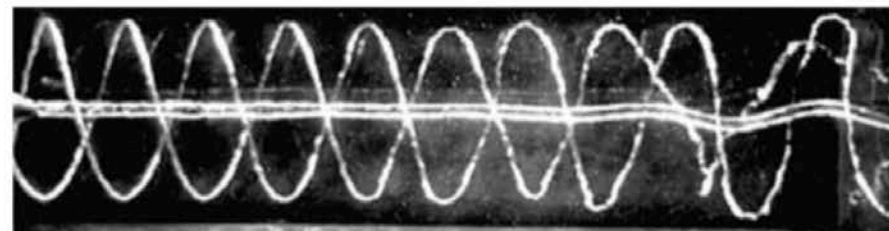
Wind turbine in air (Alfredsson & Dahlberg, 1979)



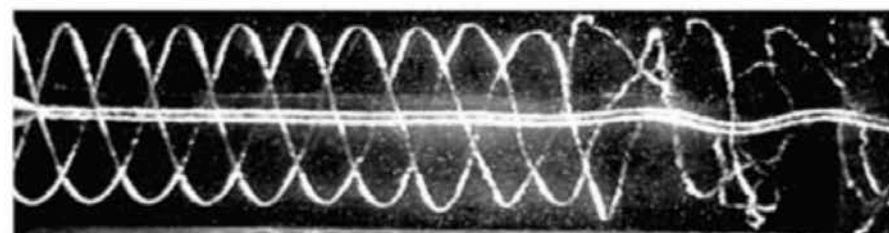
Wind turbine in water (Mikkelsen, 2010)



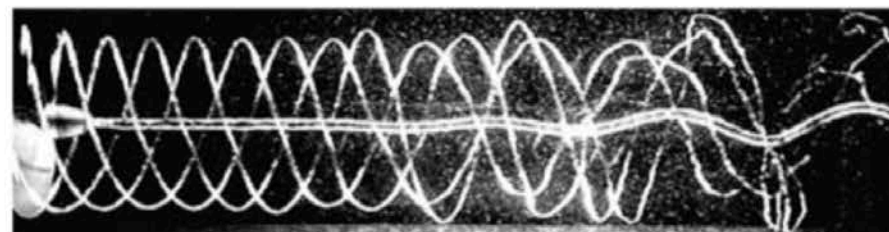
Propeller in water (Felli *et al.*, 2011)



2 blades



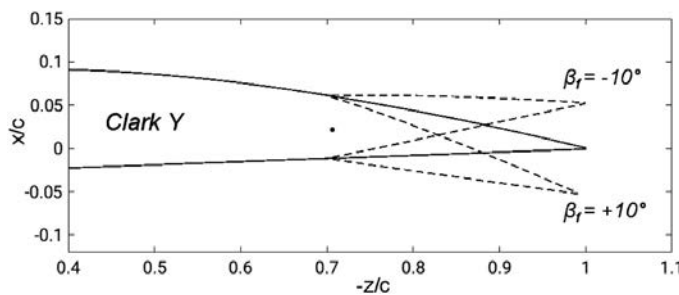
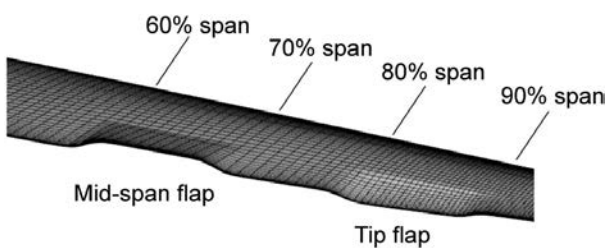
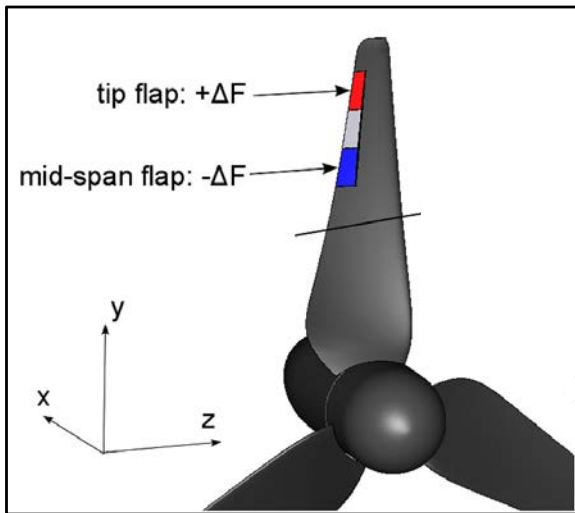
3 blades



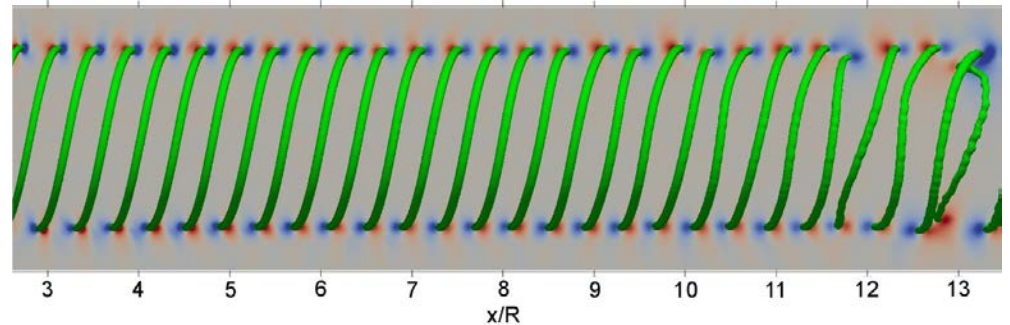
4 blades

Application to wind turbines

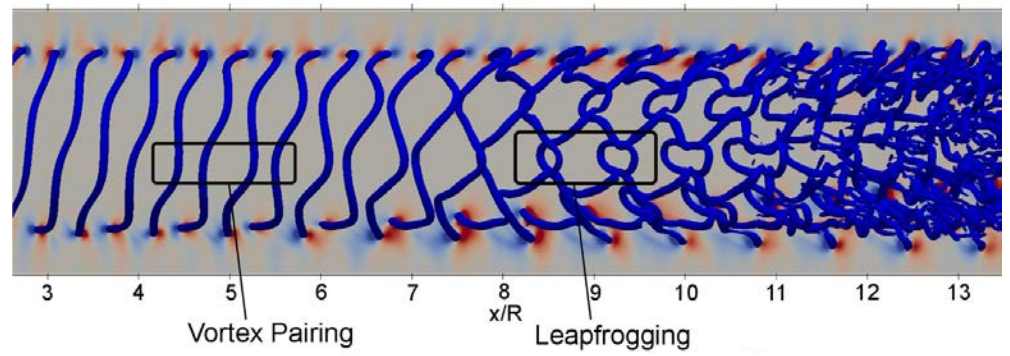
Huang *et al.* (2019)



without flap oscillation



with flap oscillation

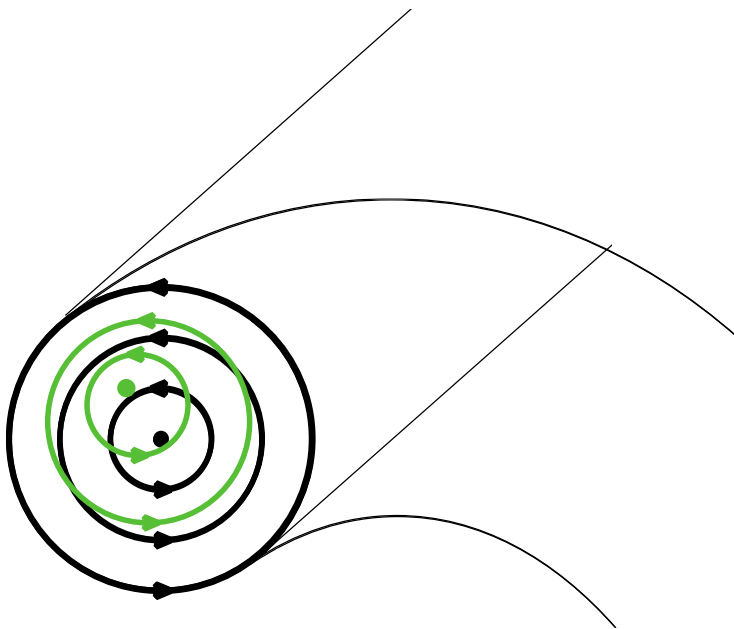


Short-wave instability
Helical vortices

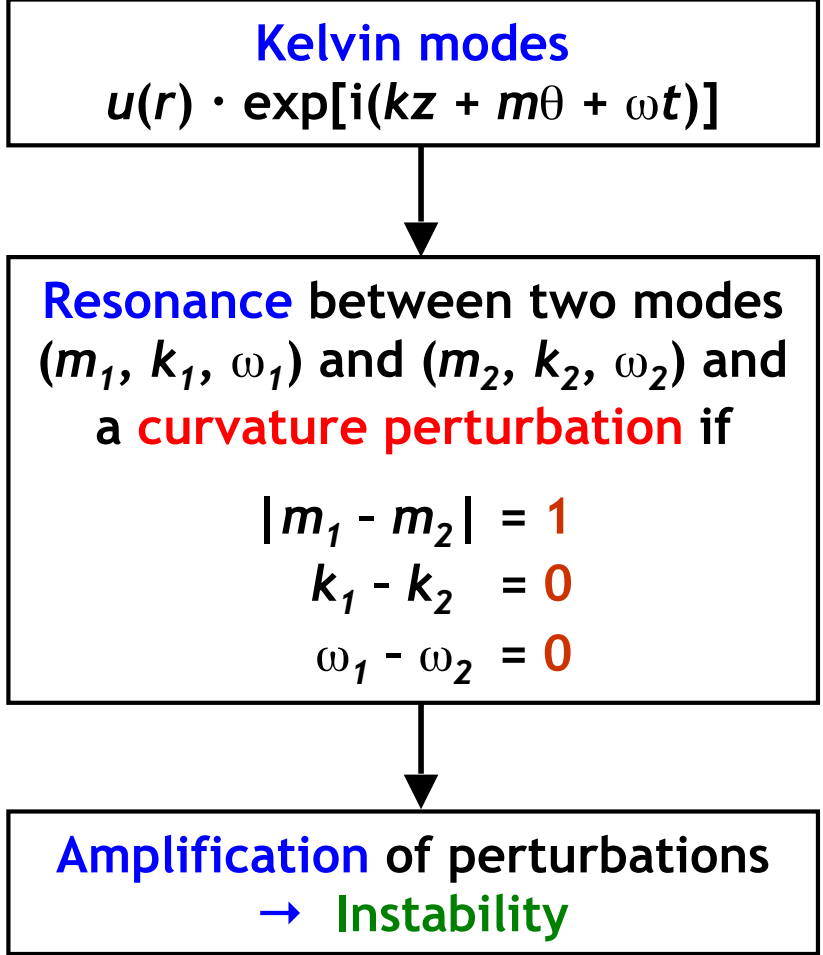
Curvature instability

Short-wave instability mechanism

curved vortex - curvature instability



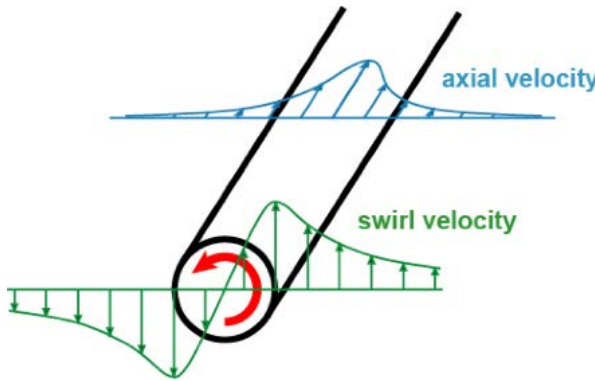
curvature perturbation
 $(m = 1, k = 0)$



Short-wave instability

Theoretical prediction for experimental case

(Blanco-Rodríguez & Le Dizès, 2017)



Gaussian vortex
with axial flow

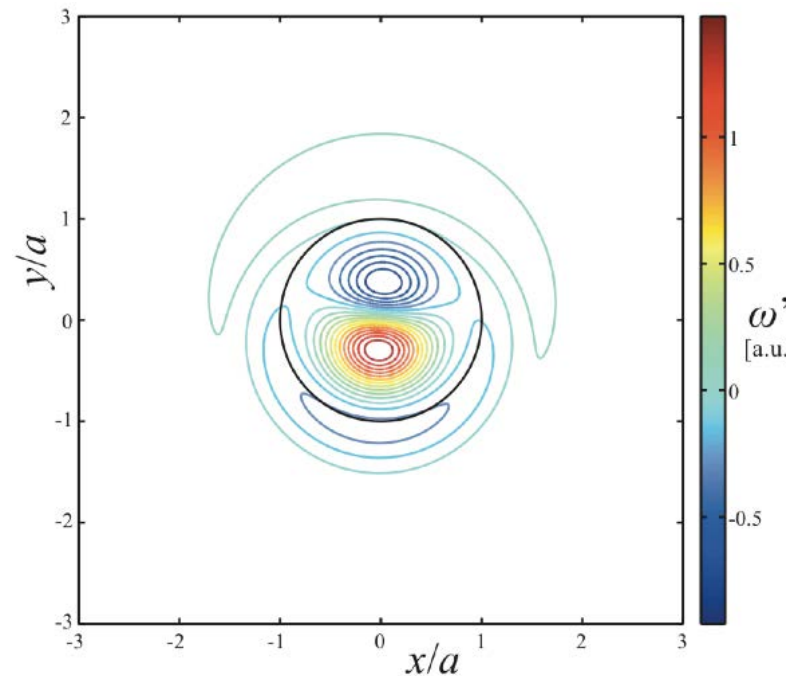
$$h/R = 0.55$$

$$a/R = 0.032$$

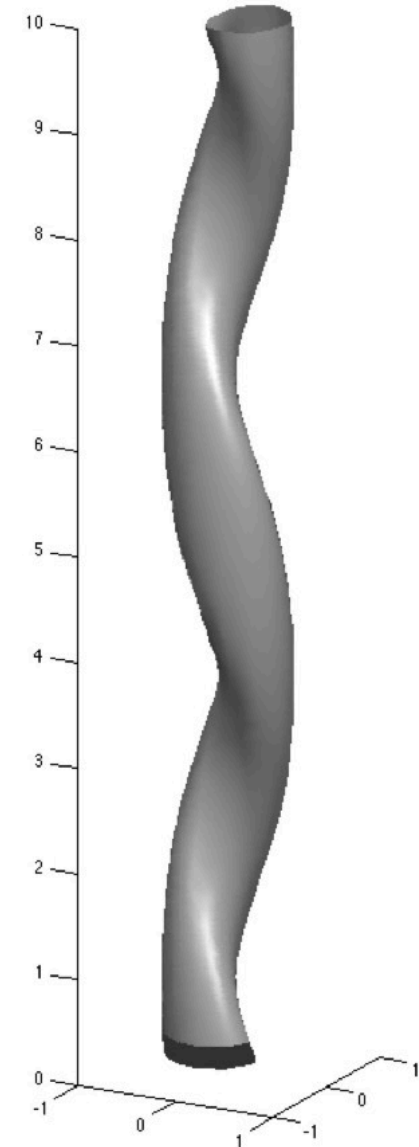
$$V_z \cdot (2\pi a / \Gamma) = 0.51$$

$$Re = 10830$$

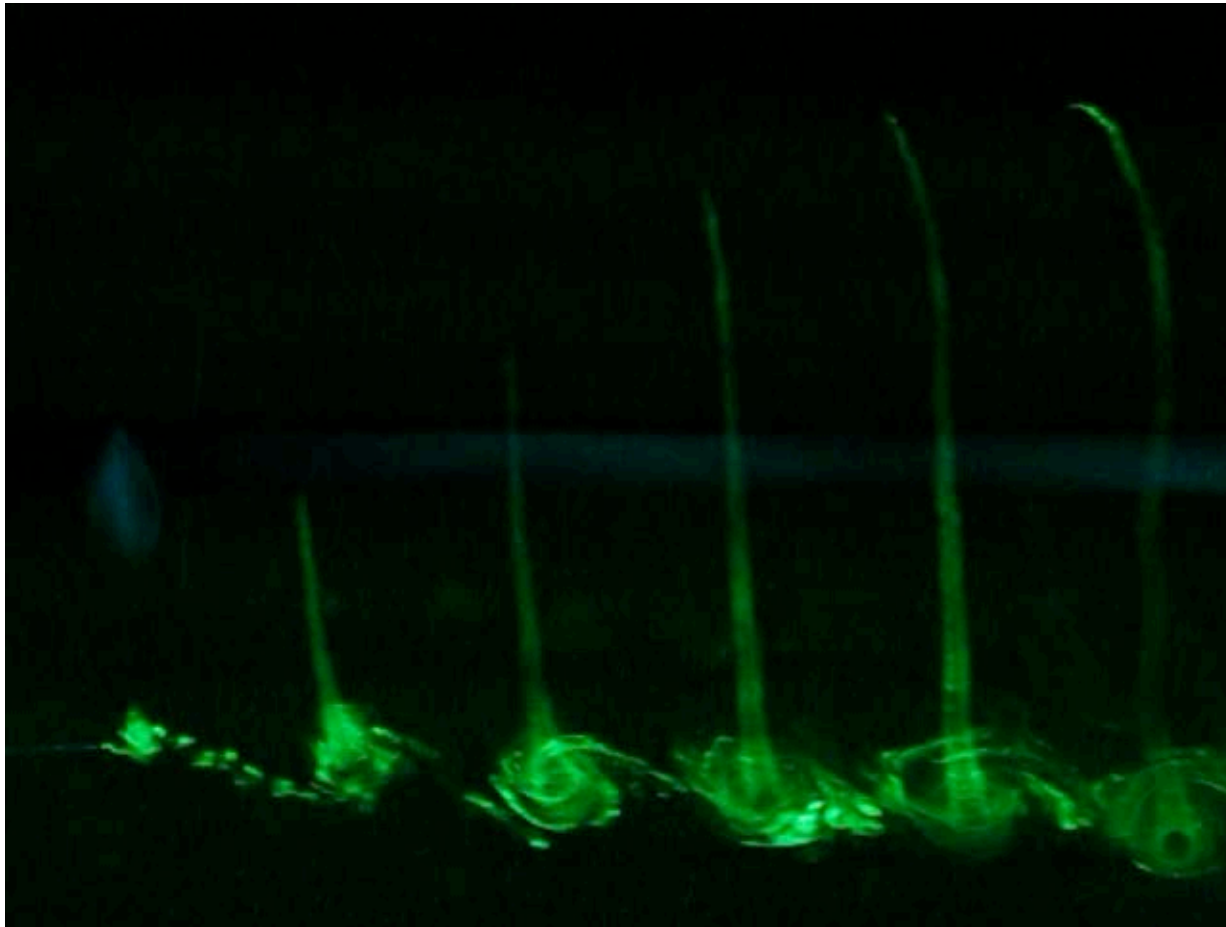
Perturbation vorticity



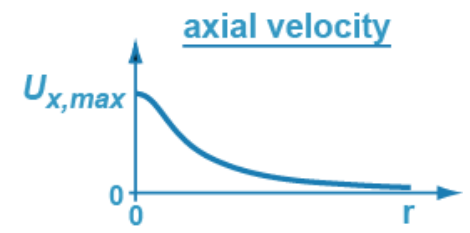
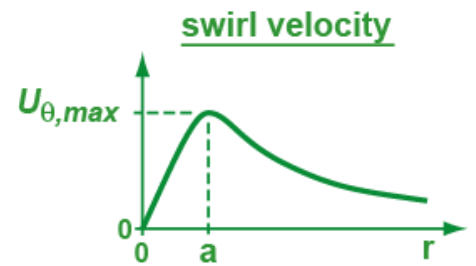
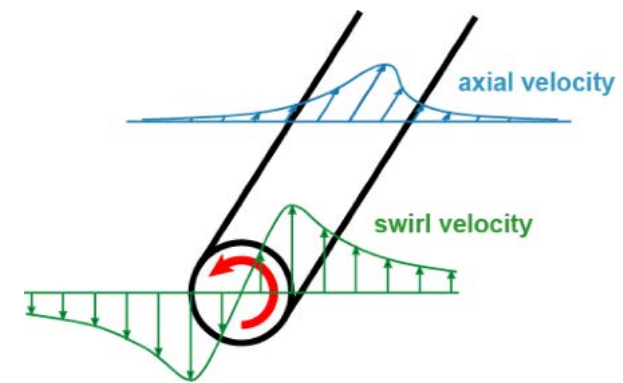
modes
 $m_1=1, m_2=0$



Axial flow in vortex cores

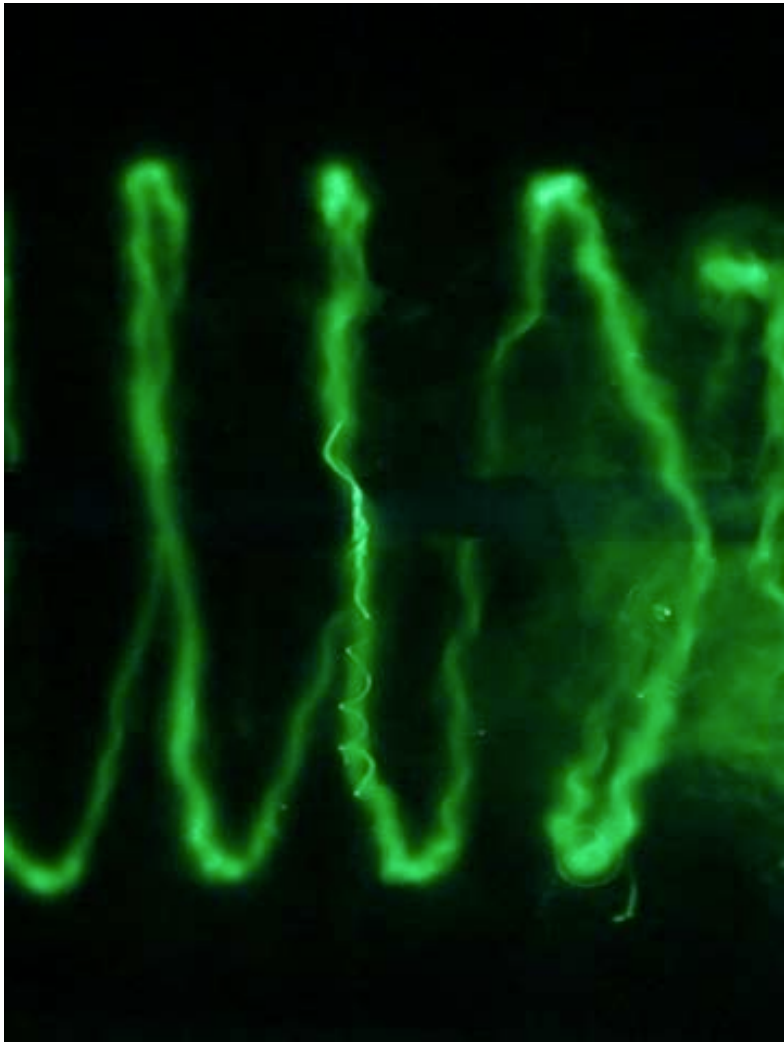


slow motion: real time / 4



Short-wave instability

Experimental observations



slow motion: real time / 8

- wavelength

Experiment: $\lambda \approx 6 a$

Theory: $\lambda = 5.7 a$

- mode shape

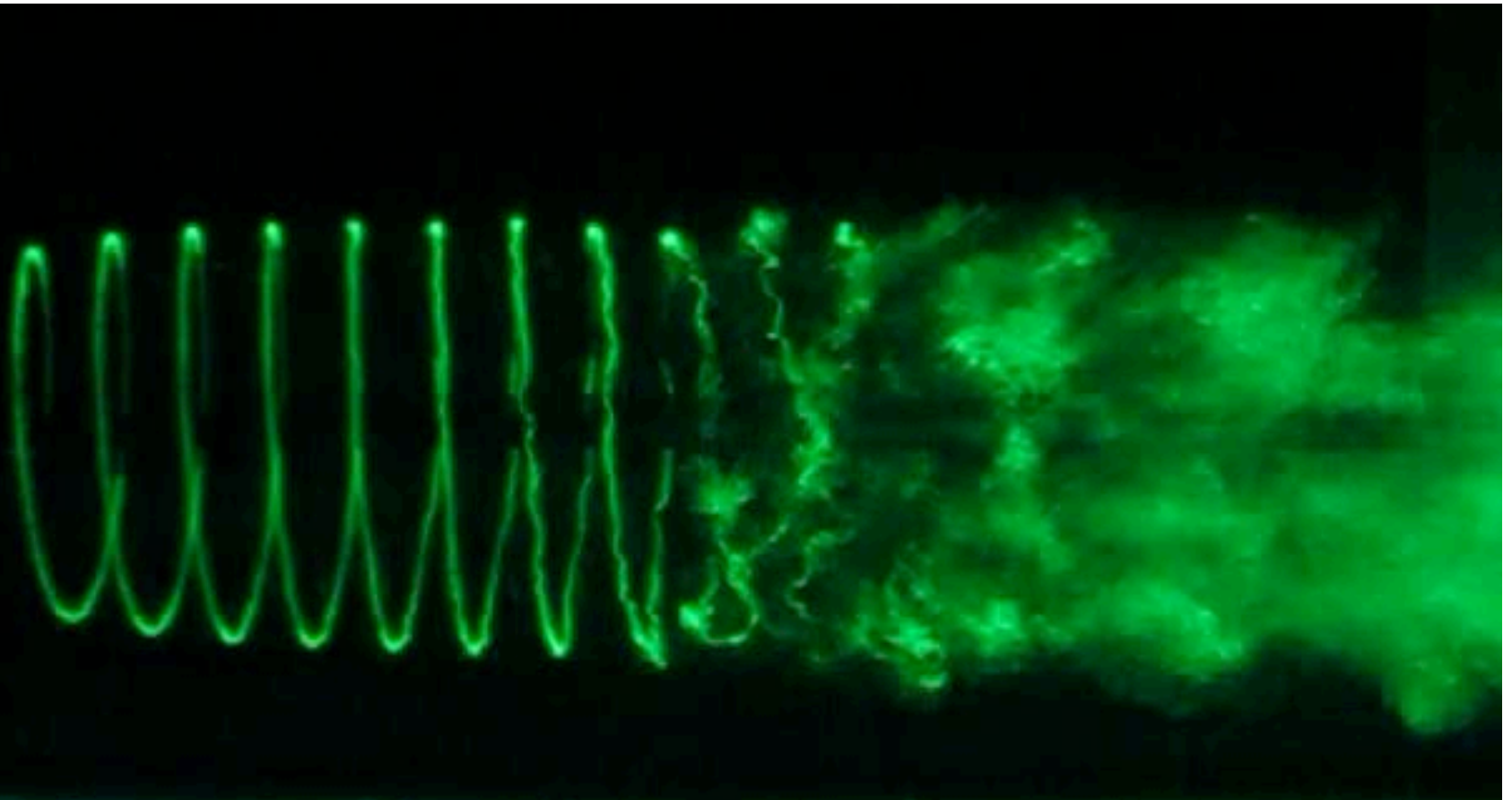
Visualisation compatible
with curvature instability

- growth rate

$$\sigma^* = 0.15$$

Short-wave instability

Experimental observations



slow motion: real time / 4

Takeaways

- **Long-wave instability:** **vortex displacement, wavelength \gg core size**
- **Short-wave instability:** **core deformations, wavelength \approx core size**
- **Vortex pairs**
 - **Long-wave Crow instability**
 - Strain + auto-rotation + mutual induction
 - Counter-rotating pair \rightarrow unstable; co-rotating pair \rightarrow stable
 - **Short-wave elliptic instability**
- **Helical vortices**
 - **Long-wave instability**
 - Pairing of neighbouring helix loops
 - **Short-wave curvature instability**
 - Requires axial core flow

References

- Alfredsson, P. H., Dahlberg, J. A. 1979 A preliminary wind tunnel study of windmill wake dispersion in various flow conditions. The Aeronautical Research Institute of Sweden (FFA), Technical Note AU-1499.
- Blanco-Rodríguez, F., Le Dizès, S. 2017 Curvature instability of a curved Batchelor vortex. *Journal of Fluid Mechanics* **814**, 397-415.
- Crow, S. C. 1970 Stability theory for a pair of trailing vortices. *AIAA Journal* **8**, 2172-2179.
- Crouch, J. D., Miller, G. D., Spalart, P.R. 2001 Active-control system for breakup of airplane trailing vortices. *AIAA Journal* **39**, 2374-2381.
- Fabre, D., Jacquin, L., Loof, A. 2002 Optimal perturbations in a four-vortex aircraft wake in counter-rotating configuration. *Journal of Fluid Mechanics* **451**, 319-328.
- Felli, M., Camussi, R., Di Felice, F. 2011 Mechanisms of evolution of the propeller wake in the transition and far fields. *Journal of Fluid Mechanics* **682**, 5-53.
- Fukumoto, Y., Miyazaki, T. 1991 Three-dimensional distortions of a vortex filament with axial velocity. *Journal of Fluid Mechanics* **222**, 369-416.
- Gupta, B. P., Loewy, R. G. 1974 Theoretical analysis of the aerodynamics stability of multiple, interdigitated helical vortices. *AIAA Journal* **12**, 1381-1387.
- Hand, M. M., Simms, D. A., Fingersh, L. J., Jager, D. W., Cotrell, J. R., Schreck, S., Larwood, S. M. 2001. Unsteady aerodynamics experiment phase VI: Wind tunnel test configurations and available data campaigns. NREL Technical Report NREL/TP-500-29955.
- Huang, X., Alavi Moghadam, S. M., Meysonnat, P. S., Meinke, M., Schröder, W. 2019 Numerical analysis of the effect of flaps on the tip vortex of a wind turbine blade. *International Journal of Heat and Fluid Flow* **77**, 336-351.
- Ivanell, S., Mikkelsen, R., Sørensen, J. N., Henningson, D. 2010 Stability analysis of the tip vortices of a wind turbine. *Wind Energy* **13**, 705-715.
- von Kármán, T., Rubach, H. 1912 Über den Mechanismus des Flüssigkeits- und Luftwiderstandes. *Physikalische Zeitschrift* **13**, 49-59.
- Kelvin (Lord) 1880 On the vibrations of a columnar vortex. *Philosophical Magazine* **10**, 155-168.
- Lamb, H. 1932 *Hydrodynamics*, Cambridge University Press, § 156.
- Leweke, T., Le Dizès, S., Williamson, C. H. K. 2016 Dynamics and instabilities of vortex pairs. *Annual Review of Fluid Mechanics* **48**, 507-541.
- Leweke, T., Williamson, C. H. K. 1998 Cooperative elliptic instability of a vortex pair. *Journal of Fluid Mechanics* **360**, 85-119.
- Leweke, T., Williamson, C. H. K. 2011 Experiments on long-wavelength instability and reconnection of a vortex pair. *Physics of Fluids* **23**, 024101.
- Meijer Drees, I., Hendal, I. 1951 Airflow patterns in the neighbourhood of helicopter rotors. *Aircraft Engineering and Aerospace Technology* **23**, 107-111.
- Okulov, V. L., Sørensen, J. N. 2007 Stability of helical tip vortices in a rotor far wake. *Journal of Fluid Mechanics* **576**, 1-25.
- Ortega, J. M., Bristol, R. L., Savaş, Ö. 2003 Experimental study of the instability of unequal-strength counter-rotating vortex pairs. *Journal of Fluid Mechanics* **474**, 35-84.
- Petz, C., Hege, H.-C., Oberleithner, K., Sieber, M., Nayeri, C. N., Paschereit, C. O., Wygnanski, I., Noack, B. R. 2011 Global modes in a swirling jet undergoing vortex breakdown. *Physics of Fluids* **23**, 091102.
- Quaranta, H. U., Bolnot, H., Leweke, T. 2015 Long-wave instability of a helical vortex. *Journal of Fluid Mechanics* **780**, 687-716.
- Quaranta, H. U., Brynjell-Rahkola, M., Leweke, T., Henningson, D. S. 2015 Local and global pairing instabilities of two interlaced helical vortices. *Journal of Fluid Mechanics* **863**, 927-955.
- Robinson, A. C., Saffman, P. G. 1982 Three-dimensional stability of vortex arrays. *Journal of Fluid Mechanics* **125**, 411–427.
- Walther, J. H., Guénöt, M., Machefaux, E., Rasmussen, J. T., Chatelain, P., Okulov, V., Sørensen, J., N., Bergdorf, M., Koumoutsakos, P. 2007 A numerical study of the stability of helical vortices using vortex methods. *Journal of Physics: Conference Series* **75**, 012034.
- Widnall, S. E. 1972 The stability of a helical vortex filament. *Journal of Fluid Mechanics* **54**, 641-663.
- Widnall, S. E., Bliss, D. B., Zalay, A. 1971 Theoretical and experimental study of the instability of a vortex pair. In *Aircraft Wake Turbulence and Its Detection*, ed. J. H. Olsen, A. Goldburg, M. Rogers, pp. 305–338. Plenum.
- Winckelmans, G., Cocle, R., Dufresne, L., Capart, R. 2005 Vortex methods and their application to trailing wake vortex simulations. *Comptes Rendus Physique* **6**, 467-486.

End of Lecture 4